

**Stem Cells for the Treatment of Corneal Fibrosis**

by

Andrew Joseph Hertsenberg

B.S., Biology, University of Texas at Austin

Submitted to the Graduate Faculty of  
the University of Pittsburgh in partial fulfillment  
of the requirements for the degree of  
Doctor of Philosophy

University of Pittsburgh

2015

UNIVERSITY OF PITTSBURGH

School of Medicine

This dissertation was presented

by

Andrew J. Hertsenberg, PhD

It was defended on

April 23, 2015

and approved by

Neil Hukriede, PhD, Associate Professor, Developmental Biology

Donna Beer Stolz, PhD, Associate Professor, Cell Biology

Hongjun Liu, PhD, Assistant Professor, Ophthalmology

Shivalingappa Swamynathan, PhD, Assistant Professor, Ophthalmology

Dissertation Advisor: James L. Funderburgh, PhD, Professor, Ophthalmology

Copyright © by Andrew J. Hertsenber, PhD

2015

# **STEM CELLS FOR THE TREATMENT OF CORNEAL FIBROSIS**

Andrew J. Hertszenberg, PhD

University of Pittsburgh, 2015

## **ABSTRACT**

The cornea is the optically transparent tissue through which light first enters the eye. Together with the lens, the cornea bends incident light to focus it onto the photosensitive retina. Corneal fibrosis occurs in response to ocular trauma and infection and, by reducing corneal transparency, can impair or completely diminish this function, leading to vision impairment and blindness. Millions of people around the globe suffer from corneal blindness as a result of injury and infection. Fortunately, topical antibiotics and immunosuppressants help to prevent scars from forming. Should a scar develop, corneal transplant is a generally successful procedure that can restore sight to these patients. There are, however, drawbacks and limitations to the procedure in that immunological rejection of the donor graft and a limited supply of donor tissue prevent many patients from sustaining or receiving this treatment. The body of work presented here investigates stem cells as an alternative treatment for vision-impairing fibrotic wounds in the corneal stroma. First, I show that human embryonic stem cells are capable of differentiating to cells with a corneal keratocyte phenotype, a study that may lead to the development of a source of cells to repair damaged corneal tissue. I then show that a population of corneal stromal stem cells can be isolated in a biopsy-like procedure and prevent fibrotic wound healing in the mouse, presenting an autologous source of cells to treat corneal scars. Finally, I investigate a potential mechanism by which these stem cells prevent fibrotic wound healing via

immunomodulation and the suppression of neutrophil infiltration to the wound bed. This work moves toward the development of an alternative to corneal transplantation that will bridge the gap between the supply and demand of donor tissue and provide a treatment option with a significantly reduced risk of failure due to rejection.

## TABLE OF CONTENTS

<b>PREFACE.....</b>	<b>XII</b>
<b>1.0 INTRODUCTION.....</b>	<b>1</b>
<b>1.1 THE CORNEA .....</b>	<b>3</b>
<b>1.1.1 Corneal Development.....</b>	<b>3</b>
<b>1.1.2 Corneal Anatomy and Physiology .....</b>	<b>4</b>
<b>1.1.2.1 The Corneal Epithelium.....</b>	<b>5</b>
<b>1.1.2.2 The Corneal Stroma. ....</b>	<b>6</b>
<b>1.1.2.3 The Corneal Endothelium.....</b>	<b>8</b>
<b>1.2 STEM CELLS IN THE CORNEA .....</b>	<b>9</b>
<b>1.2.1 Limbal Epithelial Stem Cells .....</b>	<b>9</b>
<b>1.2.1.1 Characterization. ....</b>	<b>10</b>
<b>1.2.1.2 Wound healing. ....</b>	<b>11</b>
<b>1.2.2 Corneal Stromal Stem Cells .....</b>	<b>13</b>
<b>1.2.2.1 Characterization. ....</b>	<b>14</b>
<b>1.2.2.2 Niche function of stromal stem cells. ....</b>	<b>14</b>
<b>1.2.2.3 Anti-inflammatory Properties. ....</b>	<b>15</b>
<b>1.2.3 Corneal Endothelial Progenitor/Stem Cells .....</b>	<b>16</b>
<b>1.2.3.1 Characterization. ....</b>	<b>16</b>

1.2.4	Conclusion.....	17
2.0	HUMAN EMBRYONIC STEM CELLS AS AN ALLOGENEIC SOURCE OF CORNEAL KERATOCYTES.....	18
2.1	INTRODUCTION .....	18
2.2	MATERIALS AND METHODS.....	20
2.3	RESULTS.....	25
2.3.1	Selecting Keratocyte Precursor Cells by NGFR Expression.....	25
2.3.2	Isolation and Characterization of hES-derived NC Cells .....	26
2.3.3	Keratocyte Differentiation of hES-derived NGFR+ Cell Population.....	29
2.4	DISCUSSION.....	34
2.5	ACKNOWLEDGEMENTS .....	37
3.0	LIMBAL BIOPSY-DERIVED CORNEAL STROMAL STEM CELLS FOR AUTOLOGOUS TREATMENT OF CORNEAL SCARRING .....	38
3.1	INTRODUCTION .....	38
3.2	MATERIALS AND METHODS.....	40
3.3	RESULTS.....	47
3.3.1	Culture characteristics of limbal biopsy-derived stromal cells.....	47
3.3.2	Stem cell–like properties of LBSCs .....	50
3.3.3	LBSCs differentiate into keratocytes <i>in vitro</i> .....	51
3.3.4	Human LBSCs engraft in murine cornea <i>in vivo</i> .....	53
3.3.5	LBSCs promote regeneration of stromal tissue during wound repair .....	56
3.3.6	LBSC treatment reduced corneal vascularization in mice.....	59
3.4	DISCUSSION.....	60

3.5	ACKNOWLEDGEMENTS .....	64
4.0	NEUTROPHIL REDUCTION PREVENTS CORNEAL LIGHT SCATTER: A POTENTIAL MECHANISM FOR LBSC IN WOUND HEALING .....	65
4.1	INTRODUCTION .....	65
4.2	MATERIALS AND METHODS.....	67
4.3	RESULTS.....	72
4.3.1	LBSC express tsg-6 after TNF $\alpha$ stimulation and during differentiation..	72
4.3.2	LBSC produce TSG-6 in mouse corneal stromal wounds.....	74
4.3.3	LBSC significantly reduce neutrophil infiltration at the wound site via TSG-6. ....	75
4.3.4	LBSC Reduce Corneal Light Scatter After Wounding via TSG-6 Production.....	76
4.3.5	Induction of Neutropenia at the Time of Wounding Prevents Light Scatter 4 Weeks After Wounding. ....	77
4.4	DISCUSSION.....	79
4.5	ACKNOWLEDGEMENTS .....	81
5.0	SUMMARY AND FUTURE DIRECTIONS.....	82
	APPENDIX A .....	86
	BIBLIOGRAPHY .....	89

## LIST OF TABLES

Table 1 Primer sequences used for qPCR.....	23
Table 2 Mouse mRNA expression in isolated cell populations.....	28
Table 3 Area of Colonies Cultured in Different Sera .....	48
Table 4 Target Primers Used for qPCR .....	71

## LIST OF FIGURES

Figure 1 Corneal Development.....	4
Figure 2 The Cornea .....	5
Figure 3 The Corneal Epithelium .....	6
Figure 4 Collagen in the Corneal Stroma .....	7
Figure 5 The Corneal Endothelial Pump Function .....	8
Figure 6 Limbal Stromal Cells Express NGFR Protein.....	26
Figure 7 Co-Culture with PA6 Cells Induces Neural Crest Gene Expression in hES Cells.....	27
Figure 8 Culture and Differentiation of hES Cells .....	27
Figure 9 Magnetic Activated Cell Sorting (MACS) Selects for a Population of NGFR+ Cells.	28
Figure 10 Expression of Neural Crest Genes after PA6 Co-Culture in MACS Sorted NGFR+ Cells .....	29
Figure 11 Expression of Adult Stem Cell Markers After Monolayer Culture.....	30
Figure 12 Upregulation of Keratocyte Specific Gene Expression after Pellet Culture .....	31
Figure 13 Expression Levels of CHST6 and B3GNT7 .....	32
Figure 14 Secretion of Corneal Keratan Sulfate Proteoglycans In Pellet Culture .....	33
Figure 15 Ex Vivo Model of Corneal Limbal Biopsy .....	48
Figure 16 Ex Vivo Expansion and Clonogenicity of Limbal Biopsy Stromal Stem Cells .....	49

Figure 17 Sphere Formation and Stem Cell Gene Expression by LBSC .....	50
Figure 18 Gene Expressio During Ex Vivo Differentiation of LBSC .....	52
Figure 19 Generation of Three-Dimensional Stroma-Like Tissue In Vitro .....	53
Figure 20 Murine Corneal Debridement Model .....	54
Figure 21 LBSC Engraftment and Stromal Matrix Synthesis in Mouse Cornea <i>In Vivo</i> .....	55
Figure 22 LBSC Block Deposition of Fibrotic Matrix in Healing Murine Corneas .....	57
Figure 23 LBSC Treatment Influences Light Transmission Properties of ECM Deposited after Debridement.....	58
Figure 24 Vascularization of Debridement Wounds .....	60
Figure 25 LBSC Express <i>Tsg-6</i> upon TNF-alpha Stimulation and During Differentiation .....	73
Figure 26 LBSC Express TSG-6 In Vivo .....	74
Figure 27 <i>Tsg-6</i> Expression by LBSC Reduces Neutrophil Infiltration to Corneal Wounds .....	75
Figure 28 <i>Tsg-6</i> Knockdown in LBSC Results in Significantly Greater Light Scatter as Measured by OCT Imaging Compared to Unwounded Animals .....	77
Figure 29 Neutrophil Depletion Prevents Light Scatter After Corneal Wounding .....	78

## **PREFACE**

I want to express my sincere gratitude to my thesis advisor, Dr. James L. Funderburgh. His patience and guidance during my time in his laboratory has given me the freedom to develop and test my own hypotheses, collaborate with researchers both locally and internationally, and develop a skill set that has led to my development as a scientist. In addition to being a great mentor, Jim has always been accommodating and understanding on a personal level, a factor that has made my time in pursuing this degree an enjoyable and productive one. Without his support on every level this would not have been possible. I will always be thankful for my time here.

The Department of Ophthalmology and the graduate program in Molecular Genetics and Developmental Biology have been remarkable groups to work with for the past 5 years. The collaborative and friendly atmosphere, administrative and CORE support, and funding opportunities have contributed enormously to my training and research while working here.

I would also like to acknowledge all members of the Funderburgh lab for their support during my time in the lab. I would specifically like to acknowledge Audrey Chan, MD and Sayan Basu, MBBS, with whom I share lead authorship for the work completed in Chapters 2 and 3, respectively. Yiqin Du, MD, PhD has been instrumental in sharing her knowledge of mouse surgery with me, her time and patience are very much appreciated. Martha Funderburgh and Mary Mann have both been wonderful colleagues in the lab and their assistance with

experiments is greatly appreciated. I have to thank Moira Geary for her tireless assistance with animal work. Fatima Syed-Picard, PhD, Michael Burrow, and Adam Sinder have been fantastic colleagues to work next to in the lab and their many contributions are much appreciated. Working with a reliable and enjoyable group of people everyday has truly been a gift throughout this process and for which I will forever be grateful.

I am sincerely thankful for all of the advice and guidance my thesis committee has giving me while completing this work. Their input and critical eyes have been a huge help during this process. In addition to the members listed on page ii, I would like to thank Willi Halfter, PhD, as he was a member on the committee until he relocated to pursue other opportunities.

I cannot thank my family enough for their unconditional love and unyielding support throughout this journey. For always doing their best to incorporate me in birthday celebrations, vacations, and holidays whenever possible; I am indebted to them for including me in those memories, even if from the other end of a telephone. To my parents, for the countless sacrifices they have made without hesitation, their optimism when I embodied pessimism, and their love and encouragement every day. To my siblings, Katie, Michael, Brandy, and Taylor, for their support, understanding, and for never hesitating to keep my ego in check.

Finally, I would like to acknowledge and thank tissue donors and their families, without whom this work could not have been completed. The sacrifice they have made will lead to remarkable advances in science and medicine and their contributions are imperative to that goal.

## 1.0 INTRODUCTION

The cornea is the first tissue through which light enters the eye. It is responsible for two-thirds of the eye's refractive power and is a barrier to environmental insults, trauma from foreign bodies, and infection. As such, it is imperative that its structural and functional integrity be maintained. The three layers of the cornea - the epithelium, stroma, and endothelium - function together to refract light to the photosensitive retina at the back of the eye.

Millions of people around the globe suffer from vision impairment and blindness due to corneal opacities<sup>3,4</sup>. Vision loss dramatically changes an individual's way of living and quality of life. Fortunately, individuals living in parts of the world with reliable access to healthcare rarely develop scarring after injury/infection due to rapid treatment and regular follow-ups with an ophthalmologist. In the event that an individual does develop vision-impairing opacity, corneal transplant is a common procedure with a relatively high success rate. Unfortunately, however, worldwide demand for donor tissue vastly outnumbers available grafts and immunological rejection poses a threat to graft survival.

The goal of this collection of work was to demonstrate that stem cells, both allogeneic and autologous in source, represent alternative therapies for the treatment of corneal fibrosis. To achieve this goal, my colleagues and I have taken cues from corneal development to generate keratocyte-like cells from human embryonic stem cells and worked with clinicians to develop

methods for isolating corneal stem cells in a biopsy treatment to one day use as an autologous method for the treatment of corneal fibrosis.

The human cornea develops from surface ectoderm (corneal epithelium) and the neural crest (corneal stroma and endothelium) starting at 6 weeks gestation and contains all three cellular layers by 11 weeks <sup>5</sup>. The developmental process involves cellular contributions from both the surface ectoderm and neural crest and will be described further in Section 1.1. In most mammals the cornea develops transparency shortly after birth shortly after eyelid opening.

Embryonic development informs the field of regenerative medicine and lends support to hypotheses that aim to differentiate pluripotent stem cells for use in cell therapy and tissue engineering. Indeed, embryonic stem cells are often differentiated *in vitro* toward a desired cell fate by mimicking developmental processes in normal human development, as is demonstrated here in differentiating human embryonic stem cells to a corneal keratocyte-like cell (Chapter 2).

Moreover, stem/progenitor cells have been identified in all three cellular layers of the cornea (Section 1.2), potentially providing a source of cells for autologous cell therapy and undoubtedly enhancing our understanding of corneal cell biology and wound healing. In Chapter 3, I present data demonstrating that a population of corneal stromal stem cells can be isolated in a biopsy-like procedure and prevent fibrotic wound healing in the mouse. Finally, in Chapter 4, I suggest a mechanism by which these stem cells prevent fibrosis in immunomodulation via their interaction with infiltrating neutrophils to the wound bed.

Vision is often taken for granted among the sighted population but is perhaps the sense most vulnerable to impairment and destruction by environmental factors. The current treatment options are generally successful but there is a need for greater demand and higher success rate that must be met – here I suggest that stem cells may lead to such an alternative treatment.

## 1.1 THE CORNEA

### 1.1.1 Corneal Development

Mammalian eye development begins with the formation of the optic vesicle, the morphological result of the evagination of the forebrain. The optic vesicle eventually comes into close proximity with the surface ectoderm wherein inductive signals between the two layers are thought to play a critical role in further ocular development (Figure 1A) <sup>6</sup>. Specifically, the lens placode forms from a region of surface ectoderm that then invaginates to form the lens vesicle (Figure 1B). Importantly, this invagination leads to the formation of the corneal epithelium from the remaining surface ectoderm.

Shortly after the formation of the lens vesicle, the corneal endothelium and stroma form from migrating neural crest cells (Figure 1C). It has been demonstrated in the avian cornea that the formation of the stroma is regulated by chemotactic signals secreted by the lens, with neural crest cells first resting in the periocular mesenchyme (adjacent to the lens) before migrating into the presumptive stroma between the lens and epithelium <sup>7-9</sup>. At birth, the mammalian cornea is not transparent but translucent, but becomes transparent with deturgescence and the expression of corneal crystalline proteins <sup>10,11</sup>. In chapter 2, insights gained from corneal development are used to induce keratocyte differentiation in human embryonic stem cells using a neural crest intermediary step.

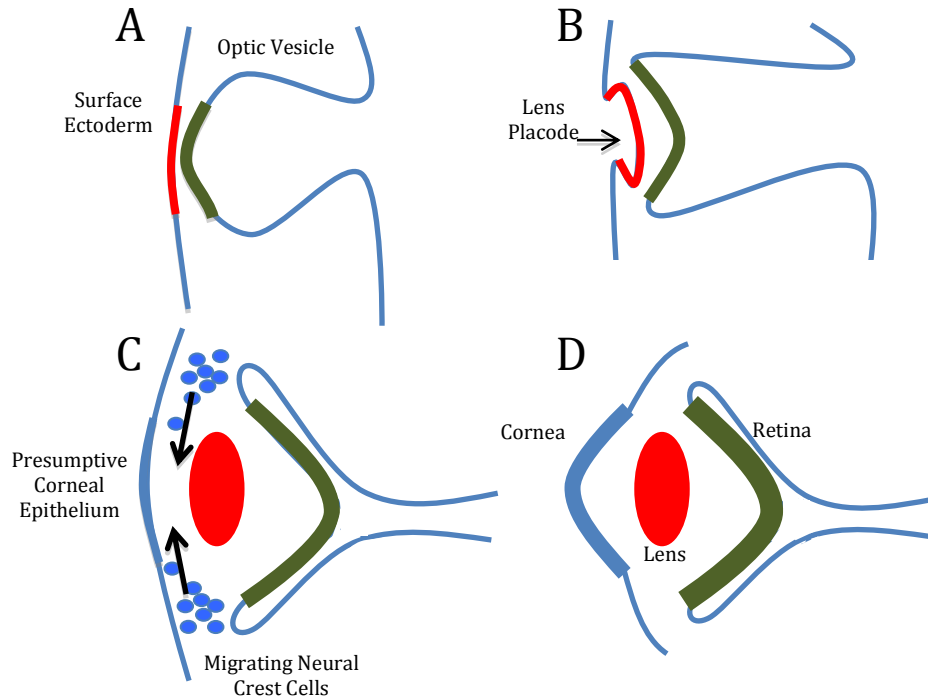


**Figure 1 Corneal Development**

A) Optic Vesicle and Surface Ectoderm interact to initiate the Lens Placode.

B) The Lens Placode (red) results in an invagination of the surface ectoderm and presumptive retina (green).

C) Migrating neural crest cells (blue circles) invade the space between the presumptive corneal epithelium and lens.

D) The cornea, lens, and retina take shape.

### 1.1.2 Corneal Anatomy and Physiology

The cornea is composed of three cellular layers: the corneal epithelium at the anterior, the corneal endothelium at the posterior, and the stroma sandwiched in between (Figure 2). Two basement membranes, the anterior limiting lamina (Bowman's membrane) and posterior limiting lamina (Descemet's membrane) separate the epithelium and corneal endothelium, respectively, from the corneal stroma. While the corneal stroma comprises the bulk of the corneal structure, each layer must function properly in order to maintain transparency required for vision.

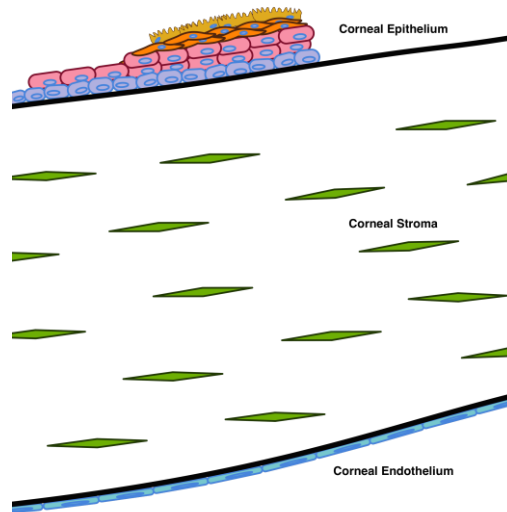


**Figure 2 The Cornea**

The three layers of the cornea: epithelium (shown: epithelial cells), stroma (shown: keratocytes), and endothelium (shown: corneal endothelial cells).

**1.1.2.1 The Corneal Epithelium.** Corneal epithelium is regularly renewed due to continuous environmental insults and desquamation. A steady movement of epithelial cells from the peripheral limbal region of the cornea (an anatomical marker between the cornea and sclera) toward the central cornea has been documented in a number of studies <sup>12-15</sup>. For this reason, corneal abrasions limited to the epithelium are generally well tolerated (though painful) and do not lead to vision impairment or blindness. However, in rare instances, corneal epithelial abrasions do not heal properly and lead to corneal edema and irregularity of the epithelial surface, both of which cause vision impairment. Normally smooth, a rough epithelial surface leads to impairment in light refraction by the cornea that results in visual impairment <sup>16,17</sup>.

Fortunately, limbal epithelial cell transplant may restore epithelial integrity and the smooth surface necessary for transparency.

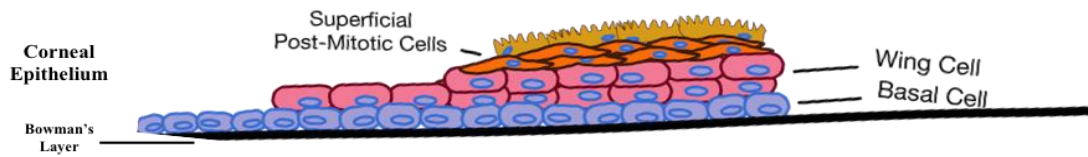


**Figure 3 The Corneal Epithelium**

Immediately posterior to the corneal epithelium is the Anterior Limiting Lamina, or Bowman's Membrane (BM). Approximately 12  $\mu\text{m}$  thick, BM is composed of collagen fibrils that contribute to a smooth anterior surface and merge posteriorly with stromal collagen<sup>18</sup>. There are multiple hypotheses suggesting a function for BM, namely that it serves as a protective barrier to the stroma, a biological barrier preventing infectious agent infiltration to the stroma, and as a facilitator of rapid stromal wound healing after corneal injury<sup>19,20</sup>. Importantly, BM does not regenerate after wounding and may contribute to scar formation, though more studies are needed to demonstrate its function in wound healing<sup>21</sup>.

**1.1.2.2 The Corneal Stroma.** The corneal stroma is a tough, collagenous tissue that comprises about 90% of the cornea. Corneal collagen is arranged in sheets of fibrils called lamellae that are arranged orthogonally throughout the stroma. The precise spacing and arrangement of the fibrils and lamellae is essential to stromal transparency<sup>22</sup>. The stroma is sparsely populated with quiescent, mesenchymal cells, called keratocytes, which are responsible for collagen production and turnover. The quiescent stroma is avascular and optically transparent, ensuring visual acuity.

The stroma is composed of tightly packed and regularly spaced collagen, primarily types I and V<sup>23</sup>. Due to the physiological requirement that the cornea be transparent for acute vision and the unique arrangement of corneal collagens not seen in opaque collagenous tissues in the

body (e.g. skin), investigators concluded that there may be a role for collagen arrangement in stromal transparency<sup>24,25</sup>. Indeed, the collagen fibrils and their interactions with proteoglycans/glycosaminoglycans in the stroma, as well as the arrangement of fibers into lamellae are key to stromal transparency<sup>26</sup>. Collagen fibrils are connected and their growth and arrangement thought to be regulated by proteoglycans, heavily glycosylated proteins with covalently attached glycosaminoglycans (Figure 4)<sup>27-29</sup>. Since collagen arrangement and fibril spacing is thought to be important to stromal transparency, it stands to reason that abnormalities in stromal ECM and collagen arrangement would lead to corneal opacity. Fibrotic wound healing after injury often leads to the deposition of extracellular matrix that lacks this organization, preventing stromal transparency.

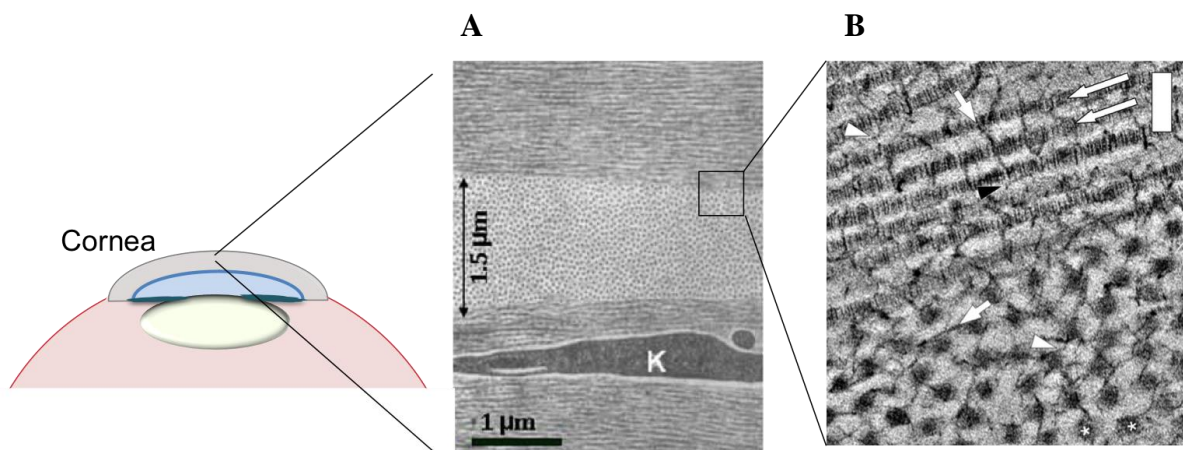


**Figure 4 Collagen in the Corneal Stroma**

Transmission Electron Microscopy (TEM) images of the corneal stroma. **A)** TEM of the corneal stroma reveals orthogonally organized collagen lamellae; K, Keratocyte. **B)** TEM at the lamellar border shows fibril bands longitudinally and in cross section. Arrowheads show proteoglycans. Scale bar: 100 nm.

Reprinted with permission: (A) Ambekar et. al.<sup>1</sup> (B) Lewis et. al.<sup>2</sup>

Upon wounding, the normally quiescent keratocytes adjacent to the damaged area become mitotically active fibroblasts and migrate to the healing area, subsequently differentiating to myofibroblasts. These cells are responsible for the production of matrix

metalloproteinases and of fibrotic extracellular matrix components that contribute to light scatter by stromal scarring<sup>30-34</sup>. Fibronectin, tenascin-C, laminin, collagens III, IV, VII, and hyaluronan production is markedly upregulated within 10 days after wounding, contributing to disorganized, opaque extracellular matrix inconsistent with transparency<sup>35</sup>.

Collagen turnover in the healing cornea eventually results in normal collagen production and, with time, the newly synthesized lamellae join with the lamellae at the wound edge<sup>36</sup>. It has been shown in rabbits that in 12-18 months this remodeling process results in transparent stromal tissue from opaque scar tissue<sup>37,38</sup>. Unfortunately, scar resolution in humans varies enormously between individuals and causes such decline in quality of life that corneal transplant is recommended.

**1.1.2.3 The Corneal Endothelium.** Immediately subjacent to the corneal stroma lies the posterior limiting lamina, or Descemet's Membrane (DM), and the corneal endothelium. Descemet's Membrane consists of collagens type IV and VIII and is 8-10  $\mu\text{m}$  thick in adults<sup>39,40</sup>. Damaged DM often requires transplant surgery, as the membrane is required for corneal

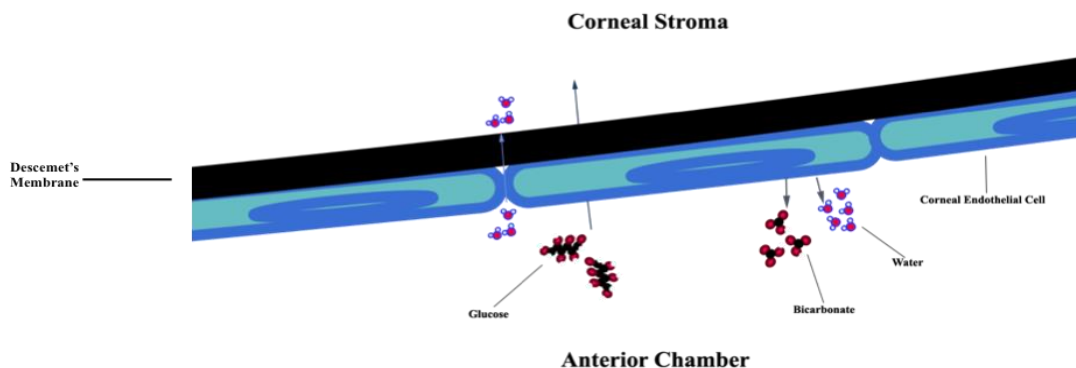


**Figure 5 The Corneal Endothelial Pump Function**

The corneal endothelial allows passive transport of water molecules into the stroma and actively transports glucose into the stroma. To maintain corneal deturgescence, water is actively transported from the stroma into the anterior chamber via a chemical gradient (e.g. by transporting bicarbonate into the anterior chamber and allowing water to follow).

endothelial cell function, which is critical to corneal transparency.

The corneal endothelium (CE) is a single layer of epithelial cells that lie on the DM facing the anterior chamber. This layer plays a critical role in stromal transparency by helping to maintain corneal deturgescence. Corneal endothelial cells have a pump function that effluxes water from the stroma via a chemical gradient made of solutes like sodium bicarbonate (Figure 5). Because water is able to passively diffuse into the stroma from the anterior chamber, the steady pump function is necessary to keep the stroma in a relative state of dehydration that maintains collagen arrangement and spacing in so as to maintain transparency. Additionally, the CE transports nutrients such as glucose across DM and into the stroma for cell metabolism and tissue function.

## **1.2 STEM CELLS IN THE CORNEA**

### **1.2.1 Limbal Epithelial Stem Cells**

A remarkably important tissue for both corneal and ocular health, the corneal epithelium (with the tear film) is the first line of defense against foreign bodies and pathogenic microorganisms. The corneal epithelium is constantly undergoing desquamation and regeneration as a normal physiological process. It is imperative that the corneal epithelium remains intact to protect the eye and ensure the refractive power of the cornea. Investigators have long been studying the mechanism by which epithelial turnover occurs. Based on a collection of studies comparing differentiation markers, proliferation capacity, and wound healing capability, it is now widely

accepted that there exists a population of stem cells in the epithelium of the corneal limbus, the border between the cornea and sclera.

**1.2.1.1 Characterization.** In the search for a corneal epithelial stem cell population responsible for the regeneration of desquamating corneal epithelium, investigators have characterized differences in cell cycle dynamics and protein expression between mature corneal epithelium and that of the corneal limbus. DNA labeling using tritiated thymidine of basal cells in the limbal region revealed a population of “slow cycling” cells, a characteristic of stem cells. Basal epithelial cells in the limbus were revealed show differences in protein expression when compared to basal cells of the central epithelium <sup>41</sup>. Keratin expression is notably different in the limbal basal cells, with a lack of cytokeratins (CK) 3 (a marker of differentiated corneal epithelial cells) and 12 but positive staining for CK14 and CK5, two markers associated with epithelial stem cells in the skin <sup>42-48</sup>. Additionally, basal limbal cells grow clonally as holoclones and show greater proliferative capacity, whereas clones from epithelial cells isolated from the central cornea are rare and do not proliferate extensively <sup>49,50</sup>. Taken together, the finding of a label-retaining cell population with an inverse expression of known differentiation/stem makers as well as a difference in proliferation capacity when compared to known mature epithelium, these studies strongly support the existence of a stem cell population in the basal layer of the corneal limbal epithelium.

The adult stem cell marker ATP-Binding Casette Sub-Family G Member 2 (ABCG2) has proven remarkably useful in the identification and isolation of stem cells, namely mesenchymal stem cells derived from bone marrow, due to its ability to efflux Hoechst 33342, a fluorescent dye that binds DNA. Expression of ABCG2 alters cellular fluorescence in the presence of Hoechst, allowing sorting of a cell population called the ‘side population’ via FACS, separating

the ABCG2<sup>+</sup> cells (stem cells) from a heterogeneous population. Side population sorting of the limbal epithelium has indeed isolated a population of ABCG2<sup>+</sup> stem cells that have greater colony-forming efficiency and reduced CK3/CK12 expression compared to central corneal epithelium<sup>51,52</sup>. ABCB5, another member of the ATP binding cassette family of proteins, has also been identified as a definitive limbal epithelial stem cell (LESC) marker. Experiments in both mouse and human revealed that the ABCB5<sup>+</sup> limbal epithelium is necessary for proper wound healing, corneal development, and epithelial homeostasis<sup>53</sup>. Additional stem cells genes are expressed by LESCs, notable among them are C/EBP-delta and Notch1, proteins known to regulate stem cell self-renewal and differentiation<sup>54,55</sup>.

**1.2.1.2 Wound healing.** In self-renewing epithelia, stem cells are essential for normal tissue maintenance because they can regenerate tissue that has been damaged or lost<sup>56-58</sup>. Additional *in vivo* studies support the importance of LESCs after epithelial debridement, concluding that limbal epithelial cells are necessary for the rapid healing of the epithelium<sup>59,60</sup>. Importantly, it has been shown that when the basal limbal epithelium is completely removed before corneal wounding, vascularization and conjunctivalization result<sup>61</sup>. When the limbal cells were in place, however, wounds healed without vascularization and cells from the limbal region migrated into the central cornea to reform the epithelium<sup>61</sup>. In addition to replenishing the mitotic basal cells of the central epithelium, cells in the limbal epithelium appear to provide a biological barrier preventing conjunctivalization and vascularization of the corneal epithelium after wounding<sup>62,63</sup>.

Expansion of limbal cells *in vitro* and their subsequent transplantation to central cornea can restore epithelial function for more than 10 years in human eyes<sup>64</sup>. In these corneas there is no direct evidence that stem cells have repopulated a limbal niche, leaving open the question as to whether this tissue, like skin, can be supported by a distributed population of stem cells. The

idea is supported by a study of destrin knockout mice, which show limited or no migration of epithelial cells <sup>65</sup>. Indeed, human eyes with limbal damage contain patches of normal epithelium in the central cornea, suggesting maintenance by local stem cells <sup>66</sup>. In a 2008 study, limbal tissue expressing beta-galactosidase ( $\beta$ Gal) was transplanted into normal mouse eyes but showed no centripetal migration of the labeled cells unless the central epithelium was wounded <sup>67</sup>. Both this and a more recent study found that cells from the central epithelium are capable of growing as holoclones <sup>67,68</sup>. These studies suggest that rare stem cells may occur in the central epithelium and that, where they do occur, they can maintain a stable column of epithelium in a manner similar to that of epidermis. A more recent study reconfirmed limbal stem cell driven migration using lineage-tracing expression of fluorescent proteins driven by the promoter for the stem cell specific protein cytokeratin 14. This gene is limited to stem and progenitor cells in the limbus, thus all fluorescent cells after induction will represent descendants of those progenitors. After induction, fluorescent cells were observed in radial streaks of cells moving toward the central cornea at about 11  $\mu$ m/day in normal, unwounded eyes <sup>69</sup>. These experiments confirm the centripetal migration of cells observed in many earlier studies and support the idea that these descend from limbal stem cells. The current state of our understanding leaves open the question as to whether stem cells in the central cornea can and do contribute to epithelial homeostasis on a long-term basis and whether the centripetal movement of progenitor-derived cells is a requirement for maintenance of healthy and stable corneal epithelium.

In spite of these unresolved questions there remains no doubt in the clinical importance of LESC. This is manifest in the condition known as Limbal Stem Cell Deficiency (LSCD). In this relatively rare condition, loss of limbal cells, typically as a result of genetic disease or chemical burns, results in conjunctivalization of the cornea, inflammation, neovascularization, pain, and

corneal opacity<sup>70</sup>. Standard penetrating keratoplasty involves only central cornea and allogenic tissue grafts that do not include limbal tissue experience an increased rate of failure<sup>71-73</sup>. In unilateral LSCD, limbal tissue can be harvested from the healthy eye without significant damage and cells transplanted on the affected cornea either directly or after expansion in culture<sup>74-76</sup>. Use of autologous LESC provides long-term stable epithelium to 50-70% of recipient eyes and regrafting can improve that result<sup>77,78</sup>. LESC allografts from cadaver eyes often fail<sup>79</sup>; however, use of biopsy tissue from living relatives and systemic anti-rejection drug therapy has led to survival rates for allogenic grafts similar to that of autologous tissue<sup>80</sup>. LESC treatment has been carried out on >1000 individuals, becoming the most common and successful of non-hematopoietic stem cell transplantation procedures, restoring vision to individuals with no alternative.

### **1.2.2 Corneal Stromal Stem Cells**

Loss of visual acuity due to stromal opacity affects more than 23 million individuals worldwide and 4.6 million are estimated to suffer bilateral corneal blindness<sup>3</sup>. Although comprehensive data are limited, stromal opacity is the source of most corneal blindness, greatly exceeding the numbers of individuals affected by LSCD<sup>81-83</sup>. Although fully prosthetic corneal replacements are in limited use and acellular prosthetic tissue replacements are in clinical trials, replacement of scarred stromal tissue with cadaveric human stromal tissue via corneal transplant (penetrating keratoplasty) is the current clinical method of choice<sup>84,85</sup>. While transplant is widely successful and frequently performed, immune-rejection and available donor tissue are significant limitations to the procedure. Indeed, graft survival is only 60% 10 years after surgery, and is progressively worse with repeated transplant procedures<sup>86</sup>.

**1.2.2.1 Characterization.** Over the past 15-20 years a large number of reports have identified and characterized stem cells from various mesenchymal tissues, namely bone marrow mesenchyme, adipose tissue, and dental pulp. These stem cell populations are identified by self-renewal ability, differentiation into multiple cell types, and their ability to grow clonally. In an initial study, a small population of cells exhibiting clonal growth from bovine corneal stroma was found to express genes associated with mesenchymal stem cells <sup>87</sup>. Successful stem cell isolation from the bovine cornea led to investigation of human corneal tissue for a similar population. To achieve this, the well-documented adult stem cell marker ABCG2 was used <sup>88</sup>. ABCG2 is an ABC cassette membrane transporter which has the ability to efflux the DNA binding dye Hoechst 33342, allowing the ABCG2<sup>(+)</sup> cells to be sorted via fluorescence activated cell sorting (FACS). ABCG2<sup>+</sup> cells from the limbal region of human cornea were found to represent less than 1% of the total cell population. These side population (SP) cells were shown to grow clonally and exhibited a multipotent differentiation potential, unlike ABCG2<sup>(-)</sup> cells isolated from the same region <sup>89</sup>. When cultured in serum-free medium supplemented with ascorbic acid and insulin, the human corneal SP cells up-regulated keratocyte specific markers, including the corneal stroma specific proteoglycan keratocan <sup>89</sup>. Since the original report, cells isolated from corneal stroma with characteristics of mesenchymal stem cells have been described in a number of publications <sup>90-97</sup>. Similar properties and the location of these reported stem cells support the idea that each study is describing a the same population of mesenchymal stem cells largely localized to the anterior limbal stroma <sup>98</sup>.

**1.2.2.2 Niche function of stromal stem cells.** Several studies have shown limbal mesenchymal cells with stem cell properties to be closely associated in vivo with limbal epithelial cells <sup>94,96,98-103</sup>. The two cell types are also co-isolated in collagenase digests of the limbal tissue <sup>96,99</sup>. In

vivo and ex vivo, the two associated cell types exhibit different protein phenotypes, and both express stem cell genes <sup>96,99</sup>. A recent three- dimensional electron microscopic analysis of the limbal region found the epithelial basement membrane to be fenestrated, providing direct cell-cell contact between basal epithelial cells and elongated stromal cells in the limbus <sup>103</sup>. Melanocytes were also associated with the niche complex. Both LESC and the limbal mesenchymal stem cell express N-cadherin, suggesting this cell-cell junction protein provides interaction between these cell populations <sup>94,100,104,105</sup>. In vitro, co-culture of LESC with co-isolated stromal stem cells improved LESC expansion and clonogenicity <sup>94</sup>. Similarly, culture of limbal epithelial cells shows improved expansion if it is carried out in the presence of limbal mesenchymal cells but less so in the presence of mesenchymal cells from the central stroma<sup>99</sup>. These findings lend credence to the idea that some or all of the mesenchymal stem cells in the stroma exist in vivo as a part of a multicellular limbal niche complex, and their presence supports the stem cell character of the LESC population.

**1.2.2.3 Anti-inflammatory Properties.** In addition to their ability to generate corneal tissues in vitro, Human Corneal Stromal Stem Cells (hCSSC) like many mesenchymal stem cells, exhibit a potential to mediate immune response. In the lumican knockout mouse model of corneal haze, hCSSC were shown to restore transparency after being injected directly into the stroma <sup>106</sup>. Even more striking, hCSSC were shown to completely prevent stromal scarring in a mouse wound model <sup>107</sup>. Prevention of scarring appears to be the result of paracrine signaling, as tissue regeneration occurs both in the anterior stroma where the cells were present as well as the posterior where no cells were seen <sup>107</sup>. Importantly, in neither *in vivo* study was T-cell mediated tissue rejection observed. This points to both the immune-privilege and immunomodulatory characteristics of hCSSC.

### 1.2.3 Corneal Endothelial Progenitor/Stem Cells

The corneal endothelium of many mammals is notable for its lack of mitotic activity in adults and inability to regenerate after damage <sup>108</sup>. Upon corneal endothelial cell loss during aging, surrounding cells spread out and change shape. If enough cells are lost, the pump function is compromised and the cornea becomes edematous and cloudy. Perhaps the most common disorder of this nature is Fuch's Dystrophy, leading to the thickening of Descemet's membrane and corneal edema causing corneal haze. Currently the only treatment option to restore vision requires transplantation of donor tissue. While this is largely successful, it does not avoid the problems often encountered with transplant operations, namely immune rejection and the declining availability of donor tissue.

**1.2.3.1 Characterization.** Many laboratories are searching for corneal endothelial stem cells for their potential in regenerative medicine. It has been shown that cells with clonogenic potential exist in the normal adult corneal endothelium by sphere-formation <sup>109</sup>. While these cells did not express markers that would be indicative of a stem cell population, clonogenic sphere formation and their ability to form a hexagonal monolayer of cells with pump function may indicate that they are corneal endothelial progenitor cells <sup>91</sup>. As is seen in other ocular tissues, notably the corneal epithelium, stroma, and retina, proposed stem cell niches are often found at the periphery of the tissue <sup>49,89,110,111</sup>. Further characterization of the sphere forming corneal endothelial cells revealed that the cells at the periphery of the endothelium have a greater propensity to form spheres than do those in the center, as has previously been described in rabbits <sup>112,113</sup>.

Recently a progenitor cell population in human corneal endothelium was identified using the established stem cell marker Leucine-Rich Repeat-Containing G-protein Coupled Receptor 5

(LGR5)<sup>114</sup>. LGR5<sup>+</sup> endothelial cells were shown to have greater proliferation capacity than LGR5<sup>-</sup> cells and were located at the periphery of the cornea, both expected characteristics of a stem/progenitor cell population. Another laboratory identified a progenitor cell population based on expression of the neural crest cell markers p75, SOX9, and FOXC2<sup>115</sup>. It was further shown that the progenitor cells had high proliferative capacity and demonstrated pump function. While there was no statistical difference between the number of p75<sup>+</sup> cells between the periphery and central corneal endothelium, the cells in the center were dispersed and those at the periphery much more concentrated, suggesting the presence of a niche.

#### **1.2.4 Conclusion**

Corneal wounding and disease often have the devastating consequence of visual impairment or blindness. While there are treatment options available when this occurs, tissue rejection and graft availability limit the ability to treat the numerous patients in need. Stem cells isolated from the cornea may offer an alternative to the current treatment options in that they can be used in an autologous fashion. This is already being used for trauma and corneal epithelial disorders such as Limbal Stem Cell Deficiency (LSCD) and is widely successful<sup>78,116</sup>. Corneal stromal stem cells have successfully been isolated from human tissue and animal studies show encouraging results that these cells may soon be used to treat stromal scarring. The corneal endothelium appears to have a progenitor population that may provide a source of cells for regeneration, though more studies need to be completed to demonstrate this. Taken together, the progress made thus far in the isolation and use of corneal stem cells for use in the clinic is promising. Though much work still needs to be done, an alternative, cell-based treatment for corneal pathologies is achievable.

## **2.0 HUMAN EMBRYONIC STEM CELLS AS AN ALLOGENEIC SOURCE OF CORNEAL KERATOCYTES**

### **2.1 INTRODUCTION**

The cornea is an optically clear, multi-laminar tissue that functions to transmit and focus light on the retina. Connective tissue of the corneal stroma constitutes 95% of the cornea's thickness and strength <sup>117</sup>. The transparency of the cornea to light depends on the unique molecular composition and organization of the extracellular matrix of the stroma, a product of keratocytes, specialized neural crest (NC) -derived mesenchymal cells. The stroma is composed of collagen fibrils stretching from limbus to limbus in parallel lamellar sheets, forming an organized, regularly spaced lattice arrangement that transmits visible light to the interior of the eye. Loss of collagen fibril organization, as occurs after trauma or infection, results in scarring and decreased transparency, sometimes leading to permanent blindness.

Currently, the only treatment for many corneal opacities is transplantation of corneal allografts. Though this therapy is highly successful, corneal transplants are limited due to a worldwide shortage and decreasing availability of donor corneal tissue. A potential approach to address these issues is development of material suitable for stromal replacement. Currently, several models of tissue-engineered collagen-based corneal substitutes are being developed in which scaffolds are made for human keratocytes to populate <sup>118-120</sup>. Keratocytes, however, lose

the ability to secrete and organize stromal connective tissue after expansion in vitro <sup>121</sup>. Therefore, there is a need for a renewable source of keratocytes, able to integrate into the scaffold and produce stromal connective tissue. Stem cells offer such a potential source for construction of biosynthetic corneal tissue <sup>98</sup>. Stem cells from adult tissues exhibit a limited repertoire of differentiation and typically a limited replicative lifespan in vitro, whereas stem cells derived from early embryos appear to have an unlimited lifespan and potential for differentiation to any somatic cell type. Pluripotent stem cells, therefore, offer a consistent and abundant cell source for development of bioengineering models.

Human embryonic stem (hES) cells readily differentiate into cells of neural lineage when co-cultured with the mouse fibroblast line PA6 <sup>122</sup>. Recently it has been shown that, during the three-week course of neural differentiation, hES cells transiently express a NC phenotype <sup>123-125</sup>. In the first week of co-culture the hES cells express low-affinity nerve growth factor receptor, NGFR (also known as CD271 and p75NTR) <sup>125</sup>. Expression of this protein is observed on migrating neural crest populations during development and is also detected on adult stem cells with NC properties <sup>126-128</sup>. Separation of NGFR-expressing cells before full neural differentiation isolated a population of cells with genetic, phenotypic and functional characteristics of embryonic NC cells <sup>125</sup>.

Corneal stroma and endothelium are both tissues of NC lineage. We therefore hypothesized that differentiation of hES cells to stromal keratocytes could be effected using hES cells that have adopted a NC phenotype. In the current study we captured hES in the NC phase of their neural differentiation and induced keratocyte phenotype in pellet culture after a week-long expansion in monolayer culture. We found this sequence of culture environments to markedly

upregulate expression of mRNAs characteristic of differentiated keratocytes. Furthermore the pellet-cultured cells secreted corneal-specific keratan sulfate proteoglycan.

## 2.2 MATERIALS AND METHODS

### **hES Cell and PA6 Co-Culture**

The murine stromal PA6 cell line (Riken Bioresource Center Cell Bank, Japan) was cultured on 0.1% gelatin-coated plates in 90% MEM-alpha (Life Technologies, Carlsbad, CA) containing 10% fetal bovine serum (FBS). The hES cell line WA01 (H1) was obtained from the University of Pittsburgh Stem Cell Core under license from WiCell (Madison, WI), and its use was approved by the University of Pittsburgh Human Stem Cell Research Oversight Committee. The hES cells were grown on Matrigel (BD Biosciences, Franklin Lakes, NJ) in mTeSR-1 basal medium (Stemcell Technologies, Canada) and maintained as described in previous protocols<sup>129</sup>. Differentiation of the hES cells into NC cells during PA6 co-culture was carried out as previously described<sup>122</sup> with minor modifications. Overgrown and differentiated hES colonies were identified and individually scraped off and removed from culture plates with a glass pipette. Remaining undifferentiated hES colonies were manually collected and sectioned using a StemPro EZPassage tool (Life Technologies). Remaining segmented colonies were mechanically dislodged and collected in 50 mL conical tubes, then washed and resuspended in Induction Medium (90% BHK21-medium/Glasgow modified Eagle's medium, 2 mM glutamine, 10% knockout serum replacement, 1 mM pyruvate, 0.1 mM nonessential amino acid solution, 0.1 mM  $\beta$ -mercaptoethanol, 100 IU/mL penicillin, 100  $\mu$ g/mL streptomycin) (all from Life Technologies)<sup>125</sup>. The hES colonies suspended in medium were added in a drop-wise fashion to 95% confluent

PA6-cultures. The density of plating was approximately 9,000 colonies per 10 cm plate. The co-cultured plate was incubated at 37°C for 6 days without media changes.

### **Immunostaining**

Immunostaining was carried out on 8 µm cryostat sections of donor human corneas fixed in 3.2% paraformaldehyde overnight. Nonspecific binding was blocked with 10% heat-inactivated goat serum in phosphate buffered saline (PBS). Sections were incubated 2 hr at room temperature with 1 µg/ml primary antibodies against NGFR (Clone ME20.4, Biolegend, San Diego, CA) in 1% bovine serum albumin. After three PBS washes, anti-mouse Alexa-546 secondary antibodies and nuclear dye DAPI were added and incubated for 2 hr at ambient temperature. Samples were imaged using a confocal microscope (Olympus) with a 20× oil objective.

### **Cell Isolation**

Human keratocytes were isolated from central stroma of fresh human donor corneas (<48 hr from TOD) as previously described <sup>89</sup>. Briefly, the central cornea was excised, rinsed and incubated in 2.4 U/ml Dispase II (Roche Diagnostics, Pleasanton, CA) overnight at 4°C. Epithelial and endothelial cells were removed by dissection and debridement, and the stroma was minced into 2-mm cubes. Stroma was digested up to 3 hours at 37°C in Dulbecco's modified Eagle's medium (DMEM) containing 1 mg/ml collagenase type L (Sigma-Aldrich) and 0.2 mg/ml testicular hyaluronidase (Sigma-Aldrich). Cells were harvested by centrifugation and immediately lysed for RNA as described below.

### **Quantitative Reverse Transcription-polymerase Chain Reaction (qPCR)**

hES cell samples were collected at days 2, 4, 6, and 8 of PA6 co-culture and lysed in 0.35 ml RLT buffer for RNA isolation using the RNeasy mini kit (Qiagen, Valencia, CA). The RNA was

treated with DNase I and concentrated by ethanol precipitation. First strand cDNA was prepared from 400 ng RNA by reverse transcription using Super Script First Strand Synthesis System for RT-PCR (Life Technologies) as described<sup>87</sup>. Quantitative RT-PCR (qPCR) was performed using SYBR Green reagents (Fisher Scientific Inc.) with the primers listed (Table 1) or with previously reported primers for adult human corneal stem cells and keratocytes<sup>89,130</sup>. Sequences of primers for the human NC genes were compared to their mouse homologues in the NCBI mouse RefSeq mRNA library with BLAST (<http://blast.ncbi.nlm.nih.gov/>) to rule out amplification of mouse cDNA by these primers. qPCR with these primers on cDNA from PA6 cells confirmed their non-reactivity with murine RNA. Amplification was 40 cycles of 15 sec at 95°C and 1 min at 60°C after initial incubation at 95°C for 10 min. Total reaction volume was 20 µL, including Maxima SYBR Green qPCR Master Mix (containing Maxima Hot Start Tac DNA polymerase, ROX, MgCl<sub>2</sub>, and nucleotides, Fermentas, Fisher Scientific) with cDNA transcribed from 20 ng of RNA and 0.2 µM forward and reverse primers. The StepOne Real-Time PCR System (Applied Biosystems) was used to generate a dissociation curve for each reaction. Mean threshold cycle number (Ct) of triplicate reactions was determined by StepOne Software v2.2.2 and compared to the mean Ct value for 18S for the same cDNA and expressed as a power of 2 to calculate relative cDNA abundance.

## Isolation of NGFR+ Cell

On day 7 of PA6 co-culture, the hES colonies were dislodged with Accutase (Life Technologies) and triturated by pipetting into a single-cell suspension. After rinsing twice, the cells were filtered through a 70  $\mu\text{m}$  cell strainer to remove any clumps and counted. The cells were washed twice in PBS containing 0.5% bovine serum albumin and ethylene-diamine-tetraacetic acid, 0.1 mM, then resuspended in 0.1 mL of the same buffer. After adding Fc blocking reagent (Miltenyi Biotec, Auburn, CA), the cells were fluorescently labeled by incubating with APC-labeled anti-NGFR antibody, washed, and incubated with magnetic beads covalently linked to anti-APC antibodies (Miltenyi Biotec). The MACS Cell Separation system (Miltenyi Biotec) was then used to separate NGFR+ magnetically labeled cells according to the manufacturer's instructions.

**Flow-through** and **Bound** cell populations were collected from the MACS columns and analyzed as to NGFR by flow cytometry and for NC gene expression by qPCR. For flow cytometry,  $10^5$  cells in 0.1 ml PBS were incubated with 2  $\mu\text{g}$  APC-labeled antibody to NGFR (Miltenyi Biotec) or with APC-labeled nonspecific isotype control antibody along with Fixable Violet Live/Dead stain (Life Technologies) for 30 min on ice. Cells were rinsed by centrifugation and then fixed in 2% paraformaldehyde in PBS. Staining was determined by flow cytometry on a BD Biosciences FACS Aria III flow cytometer.

Gene (GenBank mRNA)	Forward Primer	Reverse Primer
GAPDH (NM_002046)	TGTTGCCATCAATGACCCCTT	CTCCACGACGTACTCAGCG
NGFR (NM_002507)	CCTACGGCTACTACCAGGATG	CACACGGTGTCTGCTTGTC
NTRK3 (NM_001007156)	TCCGTCAGGGACACAACCTG	GCACACTCCATAGAAGCTTGACA
SOX9 (NM_000346)	GCCAGGTGCTCAAAGGCTA	TCTCGTTCAGAAGTCTCCAGAG
SNAI1 (NM_005985)	AATCGGAAGCCTAACTACAGCG	GTCCCAGATGAGCATTGGCA
SLUG (NM_003068)	AAGCATTTCAACGCCTCCAAA	AGGATCTCTGGTTGTGGTATGAC
MSX1 (NM_002448)	CTCCGCAAACACAAGACGAAC	CACATGGGCCGTGTAGAGTC
Mouse Tbp1 (NM_013684)	AGAACAACAGCCTTCCACCTTATG	CAAGTTTACAGCCAAGATTCACGG

**Table 1 Primer sequences used for qPCR**

## Cell Expansion and Pellet Culture

NGFR+(Bound) cells were cultured as monolayers in 10 cm tissue culture dishes coated with FNC (AthenaES, Baltimore, MD) in MEM-alpha with 10% FBS or alternately on plates coated with poly-L-ornithine/laminin/fibronectin<sup>123</sup> in N2 Medium [DME/F12 medium (Sigma) with N2 supplement (Life Technologies), 10 ng/ml FGF2 (Sigma) and 10 ng/ml EGF (Sigma)].

Because of the presence of abundant PA6 cells, flow-through cells were not further cultured.

After 7 days, the cultured Bound cells were collected for qPCR analysis and also transferred to pellet culture to induce keratocyte-differentiation<sup>130</sup>. Briefly,  $1.8 \times 10^5$  cells were collected in 15-mL conical tubes and centrifuged at 1500 rpm for 5 minutes to form pellets. The pellets were cultured 2% FBS in DME-F12 medium and after 2 days transferred to keratocyte differentiation medium (KDM): Advanced DMEM with 10 ng/mL FGF2, and 0.1 mM ascorbic acid-2-phosphate<sup>130</sup>. Although cells in pellets maintained viability based on staining with Calcein AM, the pellets were difficult to disperse and were not passaged.

For protein expression analysis, NGFR+ cells were cultured for two weeks as pellets in DMEM/F-12, with 1 mM ascorbate-2-phosphate, ITS (Gibco), 0.1 mM non-essential amino acids, 10 ng/mL FGF2, and antibiotics as above. Proteoglycans were isolated from conditioned media by ion exchange chromatography as described previously<sup>31</sup>, dialyzed, dried, and biotin labeled using sulfosuccinimidyl-6-(biotinamido) hexanoate (Sulfo-NHS-LC-Biotin, Fisher Scientific) at 2 mg/ml in 0.1 M NaHCO<sub>3</sub>, 1 hr at room temperature. Cornea-specific keratan sulfate proteoglycans were immune precipitated with a polyclonal antibody to keratocan<sup>31,121</sup> or a monoclonal antibody to keratan sulfate, J19<sup>131</sup>, bound to protein G-magnetic beads (Dynabeads, Life Technologies). Keratan sulfate on half of each sample was digested with endo-

beta-galactosidase<sup>121</sup> (QA-Bio, Palm Desert, CA) 0.05 U/ml, 2 hr at 37°C. Digested and undigested samples were separated by electrophoresis on 4%–20% SDS-PAGE gel and transferred to a PVDF membrane. Membranes were probed with streptavidin-IR700 dye and imaged on a LiCor Odyssey Imaging System<sup>132</sup>.

## 2.3 RESULTS

### 2.3.1 Selecting Keratocyte Precursor Cells by NGFR Expression

We and others have shown that the limbal (peripheral) region of the corneal stroma contains mesenchymal cells with stem cell properties<sup>98</sup>. These cells have the ability to differentiate to keratocytes in vitro and in vivo<sup>106,130,133</sup>. Consistent with the neural crest origin of the stroma, limbal stromal cells express several proteins characteristic of neural precursor and neural crest cells including nestin and Six2<sup>130</sup>. The cell surface low affinity nerve growth receptor (NGFR) is expressed on migrating embryonic neural crest cells as well as a number of adult stem cells, particularly those with neural crest character<sup>126,128,134</sup>. NGFR has also been detected in limbal epithelial and stromal cells of human cornea<sup>135,136</sup>. Immunohistochemistry confirmed the observation that cells in the limbal stroma express NGFR (Figure 6A) and found that few or no cells in the central stroma stained for NGFR (Figure 6B). Because hES cells exhibit transient expression of NGFR when induced to differentiate to the neural lineage<sup>125</sup>, we adopted the rationale that isolation of hES cells expressing NGFR might provide a source of cells with the potential to differentiate to keratocytes.

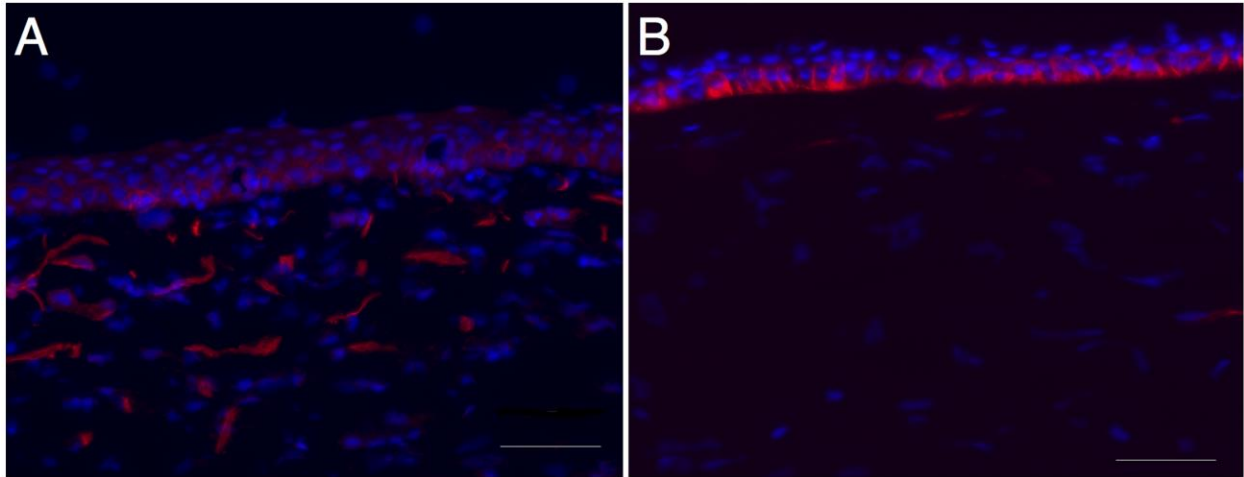


**Figure 6 Limbal Stromal Cells Express NGFR Protein**

Cryosections of cornea from a 34 yr old donor were immunostained with antibody to NGFR (p75<sup>ntr</sup>) protein (red) and counterstained with DAPI (blue). (A) Shows anterior stroma and epithelium at the limbus. (B) Shows central cornea. Bars in the images indicate 50  $\mu$ m.

Chan, Hertszenberg et. al. doi:10.1371/journal.pone.0056831.g001

### 2.3.2 Isolation and Characterization of hES-derived NC Cells

When hES cells are co-cultured with mouse embryonic fibroblast PA6 cells (Figure 7A) they differentiate to neural cells. Early in this process the hES cells transiently express a NC phenotype<sup>125</sup>. We found that expression of several characteristic NC genes (NGFR, SNAI1, NTRK3, SOX9, and MSX1) was upregulated after two days of the co-culture (Figure 8). Consistent with previous reports, expression of these NC genes plateaued at days 6–8, after which the cells transitioned into neural cell phenotypes<sup>89,118,120</sup>.

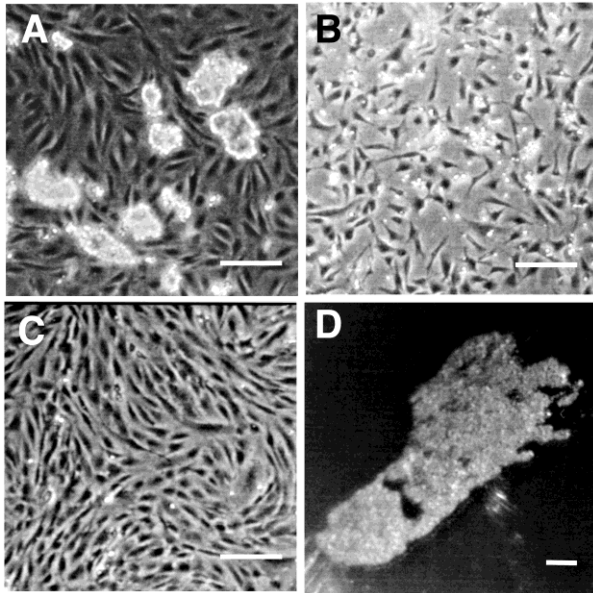


**Figure 7 Culture and Differentiation of hES Cells**

A) Shows colonies of hES cells cultured on monolayers of PA6 mouse cells to induce neural differentiation. (B) NGFR+ derived hES cells after 6 days of co-culture were cultured as monolayers in serum-free N2 medium. The cells remain small and exhibit polygonal morphology. (C) NGFR+ derived hES cells are cultured as a monolayer in serum-containing alpha-MEM medium. The cells form aligned, spindle-shaped confluent monolayers. (D) Pellet from alpha-MEM cultured cells after 2-week culture. Cells are small, tightly packed and difficult to disperse. Bars show 200 µm. Chan, Hertsensberg et. al. doi:10.1371/journal.pone.0056831.g002

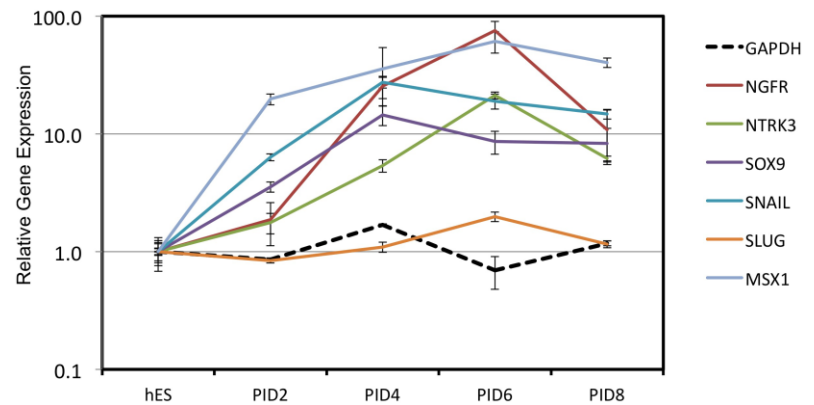


**Figure 8 Co-Culture with PA6 Cells Induces Neural Crest Gene Expression in hES Cells**

hES cells were co-cultured with PA6 cells. RNA was isolated at post-induction days (PID) 2, 4, 6, and 8. Expression of characteristic neural crest (NC) marker genes was determined by qPCR using human-specific primers. Expression levels are calculated relative to untreated hES cells (hES = 1). Error bars show the standard deviation (S.D.) of triplicate analyses. Chan, Hertsensberg et. al. doi:10.1371/journal.pone.0056831.g003

From 6-day induced hES cells, a population of cells expressing the cell surface NC protein NGFR was selected using magnetic beads attached to anti-NGFR antibody (Bound Cells). Cells expressing lower levels of NGFR (Flow Through) were also collected. Flow cytometry of these populations (Figure 9) showed that the affinity procedure enriched for cells with the NGFR cell surface marker, increasing its abundance 4-fold in the Bound-cell population compared to starting material.  $4.9 \times 10^6$  cells were recovered from a starting population of  $7.8 \times 10^7$  total (hES+PA6) cells representing about 6% of the total cells. Viability of the Bound cells was >95%.

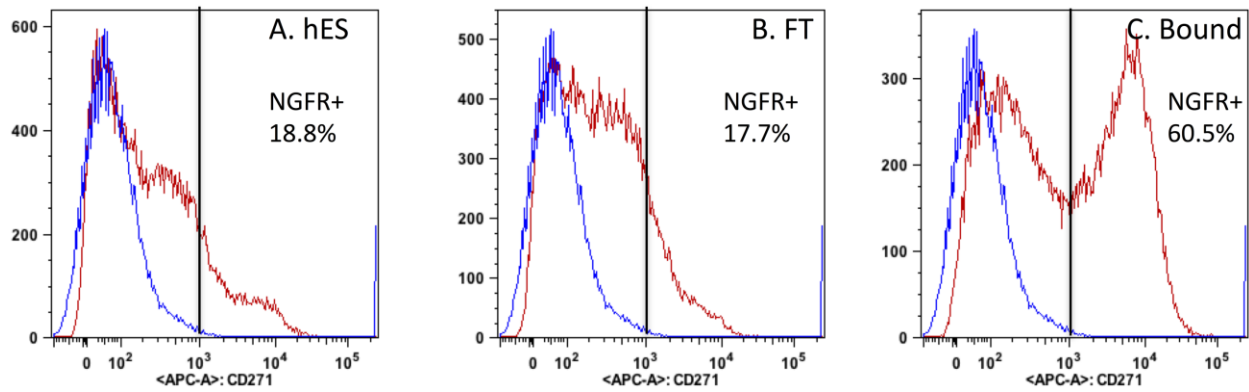


**Figure 9 Magnetic Activated Cell Sorting (MACS) Selects for a Population of NGFR+ Cells**

Single cell suspensions of hES cells after 6 days of co-culture with PA6 cells were stained with APC-labeled NGFR antibody and analyzed by flow cytometry either before or after separation of NGFR-positive cells by MACS columns as describe in Methods. The blue trace shows the cells stained with non-specific isotype-matched control antibody. (A) Unfractionated hES+PA6 co-culture. (B) Flow-through, cells not bound to the NGFR MACS column. (C) NGFR+ cells bound and released from MACS column. The vertical bar marks the population containing <0.1% non-specific control cells (blue trace). The calculated percentages of the population (red trace) with positive staining are listed on the graph.

Chan, Hertsenber, et. al. doi:10.1371/journal.pone.0056831.g004

Because the cells introduced to the MACS columns represented a mixture of hES and murine PA6 feeder layer cells, it was important to verify that PA6 cells were not collected in the NGFR+ fraction. Presence of mRNA for a constitutively expressed mouse gene *TBP1*<sup>137</sup> was compared using qPCR from the starting cells and the cells after isolation. The expression relative to the pure PA6 line is shown (Table 2). By this measure, the recovered NGFR+ cells were found to be >99.99% human, similar to the pure hES cell cultures. This proportion remained after expansion and passage of these cells. Therefore, magnetic-activated cell sorting is an effective way of isolating a NGFR+ population of cells from PA6 co-cultured treated hES cell culture without contamination from the murine feeder layer.

**Table 2 Mouse mRNA expression in isolated cell populations.**

Cells	Mouse Tbp1
PA6 (mouse cells)	100
hES (human cells)	0.002
NGFR+ MEM-FBS p0	0.001
NGFR+ MEM-FBS p1	0.0005
NGRF+ N2 p0	0.002

Chan, Hertsenber, et. al.  
doi:10.1371/journal.pone.0056831.t002

Quantification of NC gene expression in the isolated (Bound) cell population (Figure 10) found NGFR expression to be enriched 6-fold compared to Flow-through cells. Expression of other NC marker genes (NTRK3, SNAI1, and SLUG) was significantly enriched in the NGFR+ cells, but two NC markers (SOX9 and MSX1) did not appear to be specifically associated with the NGFR+ cell population.

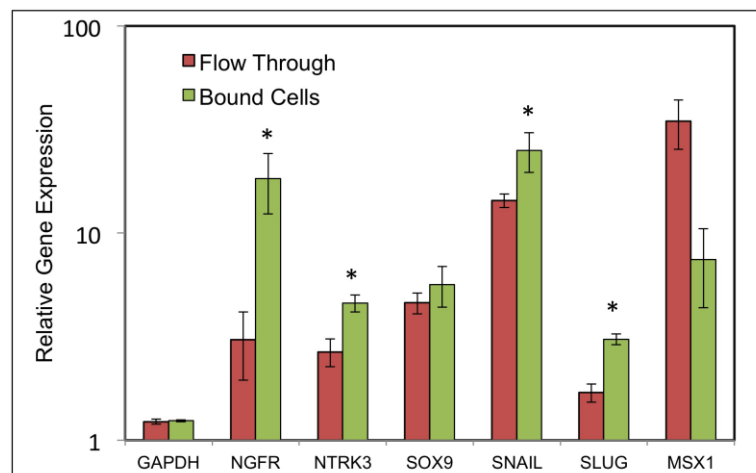


**Figure 10 Expression of Neural Crest Genes after PA6 Co-Culture in MACS Sorted NGFR+ Cells**

Expression of human NGFR, NTRK3, SOX9, SNAI1, SLUG and MSX1 was determined in 6-day PA6-cocultured hES cells after separation of NGFR+ (Bound) and NGFR- (Flow through) by MACS columns as described under [Methods](#). Expression levels were calculated by qPCR relative to hES cells (hES expression = 1). Error bars show S.D. of triplicate analyses. Asterisks show significantly ( $p < 0.05$ ) increased expression in bound cells as determined by Student's t-test.

Chan, Hertsberg, et. al. doi:10.1371/journal.pone.0056831.g005

### 2.3.3 Keratocyte Differentiation of hES-derived NGFR+ Cell Population

Adult stem cells isolated from the human corneal stroma exhibit a phenotype different from differentiated keratocytes, but with similarities to mesenchymal stem cells from bone marrow<sup>87,89,130</sup>. These cells can be distinguished from keratocytes by expression of several stem cell-associated genes, and will differentiate into keratocytes when cultured as substratum-free

floating pellets in serum-free medium containing ascorbic acid-2-phosphate and FGF2<sup>130</sup>. Our initial attempts to maintain the isolated NGFR+ cells directly in pellet cultures led to cell death, but we found that expansion of these cells in monolayer culture (as shown in Figure 7B and C) maintained their viability. We compared isolated NGFR+ cells and the subsequent monolayer cultures for expression of six genes (Figure 11) previously identified as abundant in human corneal stromal stem cells, (Pax6, Nestin, Kit, Notch1, Six2, BMI1)<sup>130</sup>. All six genes were expressed in the NGFR+ cells and in culture, expression was maintained for all but PAX6 which was decreased by >90% in the cultured cells. Expansion in serum-free conditions in the presence of EGF, FGF2 and N2 supplement (N2 medium, Figure 7B) was marginally better at maintaining stem cell gene expression than culture in 10% fetal bovine serum in MEM-alpha medium (MEM-FBS, Fig. 5C). Passage in MEM-FBS reduced the adult stem cell expression even further (not shown).

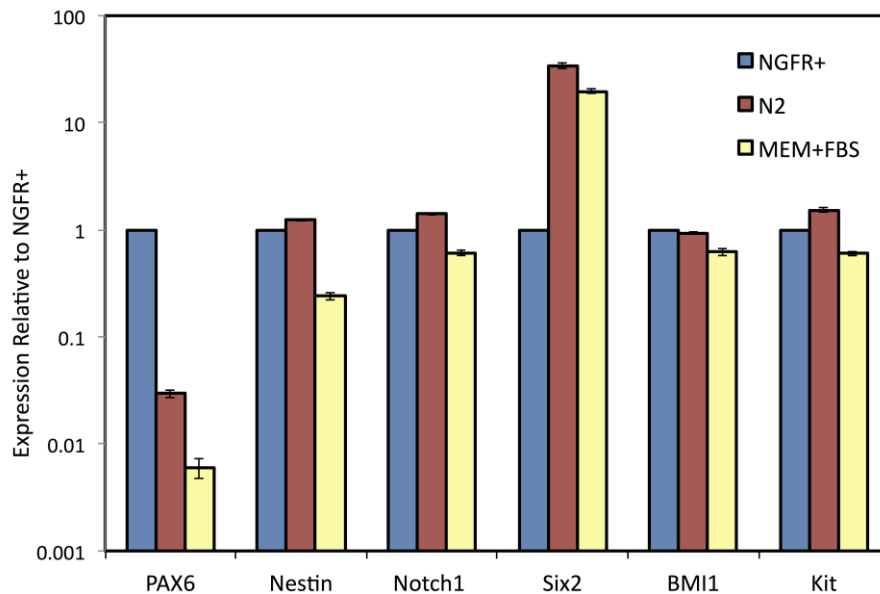


**Figure 11 Expression of Adult Stem Cell Markers After Monolayer Culture**

Expression of genes distinguishing adult corneal stem cells from keratocytes: PAX6, NES, NOTCH1, SIX2, BMI1, and KIT, was examined in the NGFR+ cells and in these cells after culture of the cells one week as monolayers in MEM-FBS or in N2 media as described in [Methods](#). Gene expression was determined by qPCR relative to NGFR+ cells (set = 1). Error bars show S.D. of triplicate analyses. Chan, Hertsberg, et. al. doi:10.1371/journal.pone.0056831.g006

Cells from the N2 and MEM-FBS monolayer cultures were transferred to differentiation medium as pellets (Figure 7D) for two weeks and assayed for expression of six genes that are highly expressed in keratocytes (Figure 12). We saw that aquaporin-1 (AQP1) was increased 24-fold, PTGDS 20-fold, B3GNT7 10-fold, and ALDH3A1 100-fold when compared with the NGFR+ cells. Most notably, expression of keratocan (KERA), a cornea-specific proteoglycan present in stromal extracellular matrix, was increased over 10,000-fold.

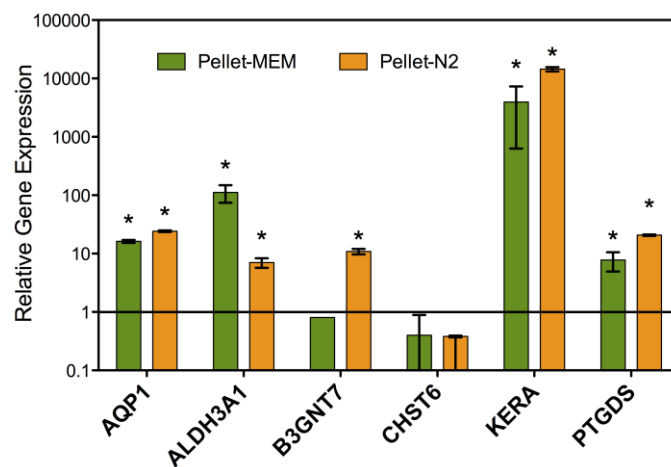


**Figure 12 Upregulation of Keratocyte Specific Gene Expression after Pellet Culture**

Expression of six genes, previously identified as up-regulated during keratocyte differentiation, was determined after 2 weeks in pellet cultures derived from either MEM+FBS or N2 monolayer cultures as described in Methods. Gene expression is calculated relative to the NGFR+ derived hES cells. Error bars represent S.D. of triplicates. All genes were significantly ( $p < 0.05$ ) upregulated in pellets compared to NGFR+ cells except for CHST6. Asterisks show cases in which pellet culture induced a significant ( $p < 0.05$ ) increase in gene expression compared to the monolayers cultures.

Chan, Hertsenberg et. al. doi:10.1371/journal.pone.0056831.g007

The most characteristic molecular identifiers of keratocytes are the keratan sulfate proteoglycans<sup>138</sup>. These are a group of three proteins, one of which being keratocan, modified by highly sulfated keratan sulfate glycosaminoglycan chains. Biosynthesis of corneal keratan sulfate is reported to require two cornea-specific enzymes, beta3-GnT7 (EC 2.4.1), a glycosyltransferase, and corneal N-acetylglucosamine 6-sulfotransferase (EC 2.8.2.17)<sup>139</sup>. Messenger RNA for keratocan (KERA) and for these two enzymes (B3GNT7, CHST6) are all

markedly increased when adult stem cells differentiate to keratocytes<sup>133</sup>, so it seemed curious that the CHST6 showed little upregulation as hES-derived cells began expressing keratocan. To better understand this phenomenon we compared expression of the biosynthetic genes in hES-derived cells with that of human corneal fibroblasts (HCF), cells that do not synthesize keratan sulfate, and with freshly isolated uncultured human keratocytes<sup>89</sup>. Additionally, we found that the NGFR+ cells as well as the monolayer cultures all express high levels of the keratan sulfate sulfotransferase (CHST6) mRNA, almost equivalent to that in uncultured keratocytes and that the glycosyltransferase (B3GNT7) mRNA was also highly abundant compared to the level in corneal fibroblasts (Figure 13). Cells in MEM-FBS had reduced mRNA abundance for these genes, and when cultured as pellets, expressed little more than the HCF. Pellet cultures from cells expanded in N2 medium, however, showed levels of expression almost identical to those in keratocytes. These results suggest that CHST6 and B3GNT7 may not be upregulated in pellet culture because they are already expressed at high levels by the NGFR+ cells.

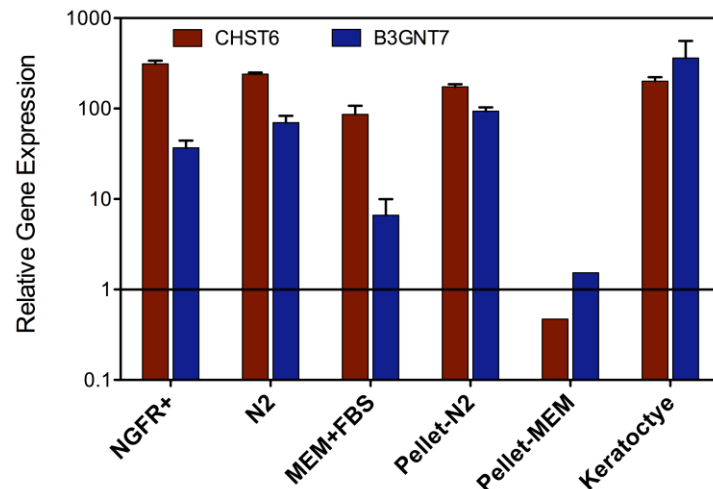


**Figure 13 Expression Levels of CHST6 and B3GNT7**

Expression of CHST6 and B3GNT7 in the hES-derived cells was compared relative to that of human corneal fibroblasts (cells that do not secrete keratan sulfate) and to freshly isolated stromal keratocytes as described in Methods. Levels of both genes are comparable in NGFR+ cells to those in keratocytes but are reduced in the presence of FBS. Cell cultures are those described in Methods. Error bars show S.D. of triplicate analyses.

Chan, Hertsberg, et. al. doi:10.1371/journal.pone.0056831.g008

Secretion of high molecular weight keratan sulfate proteoglycans (KSPG) is a unique phenotypic property of keratocytes and is required for corneal transparency. High expression of KERA, B3GNT7 and CHST6 suggests that these specialized proteoglycans may be produced by the hES-derived pellet cultures. Antibodies to keratocan precipitated a high molecular weight (>100 kDa) heterogeneous protein from pellet-conditioned culture media (Figure 14, lane 3). This material was sensitive to digestion by endo-beta-galactosidase (Figure 14, lane 4), a keratan sulfate-degrading enzyme. Presence of the keratan sulfate in this fraction was confirmed by immune precipitation with anti-keratan sulfate monoclonal antibody J19 and subsequent digestion with endo-beta-galactosidase (Figure 14, Lanes 7 and 8). These results demonstrate secretion in the pellet cultures of molecular components of corneal stroma that represent unique biosynthetic products of differentiated keratocytes.

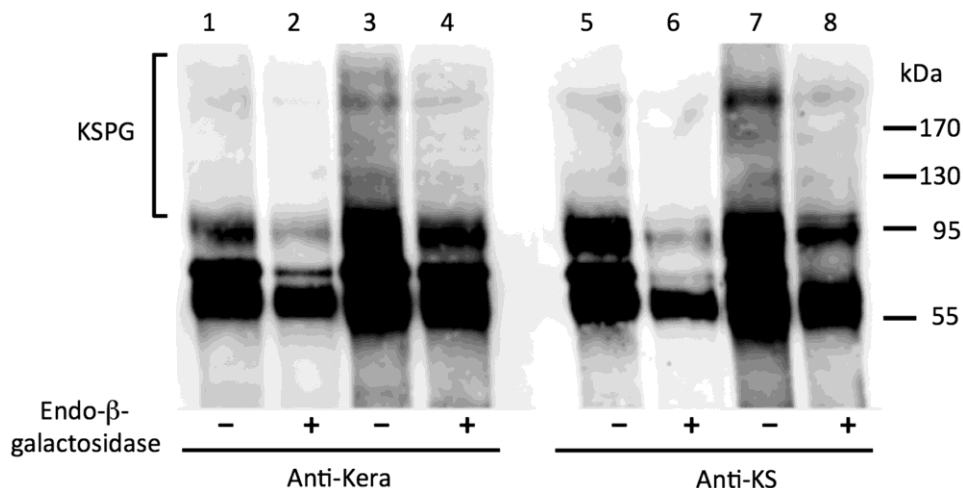


**Figure 14 Secretion of Corneal Keratan Sulfate Proteoglycans In Pellet Culture**

Proteoglycans were isolated from culture medium before (Lanes 1,2,5,6) or after (3,4,7,8) three-week incubation with hES pellets. The proteoglycan fractions were biotin- labeled and immune-precipitated with antibodies against keratocan (anti-Kera) (lanes 1–4) or keratan sulfate glycosaminoglycan (anti-KS) (lanes 5–8). Half of each sample was digested with endo- $\beta$ -galactosidase (as described under Methods) to hydrolyze keratan sulfate, and samples were separated by SDS-PAGE, transferred to PVDF membranes and biotinylated proteins detected with avidin-labeled infrared dye as described in Methods. Presence of biotinylated proteins migrating as a broad, heterogeneous >100 band typical of keratan sulfate proteoglycan (KSPG - bracket on the left) was present in lanes 3 and 7. Sensitivity of this material to digestion with keratan sulfate-specific glycosidase (lanes 4 and 8) demonstrates presence of keratocan-linked keratan sulfate, a unique keratocyte biosynthetic product.

Chan, Hertsberg, et. al. doi:10.1371/journal.pone.0056831.g009

## 2.4 DISCUSSION

In this study, we show that hES-derived cells expressing NC marker genes can be induced to differentiate into cells expressing keratocyte-specific genes and extracellular matrix components. Using a well-established co-culture procedure (Figure 7A) that induces neuronal differentiation in H1-hES cells, we selected a population of NGFR-expressing cells. As previously reported, these cells express several characteristic NC marker genes. The isolated NGFR+ cells were expanded in monolayer cultures during which time they continued expression of several genes we previously identified in adult corneal stromal stem cells <sup>130</sup>. The monolayer cells were then incubated as free-floating pellets, a condition we previously found to induce the keratocyte phenotype in adult stem cells <sup>130</sup>. In the pellets, expression of genes that characterize the phenotype of keratocytes was detected, including KERA, AQP1, ALDH3A1, CHST6, B3GNT7 and PTGDS. To confirm the phenotype we demonstrated the presence of keratan sulfate proteoglycans containing both keratocan and high-molecular weight keratan sulfate in conditioned media from the pellet cultures. These matrix components are tissue-specific biosynthetic products of keratocytes present only in corneal stroma. Previously, keratocan production has been induced in various multipotent stem cells including adult adipose-derived stem cells <sup>131</sup>, corneal stromal stem cells <sup>130</sup>, and bone marrow mesenchymal stem cells <sup>140</sup>. The current results provide convincing evidence that stromal extracellular matrix can also be produced by pluripotent stem cells.

An important aspect of the selection process was the use of NGFR-expressing cells.

Selection of NGFR<sup>+</sup> cells allowed isolation of a population with neural crest phenotype, free of mouse feeder cells. NGFR is a cell surface protein expressed mostly in migrating NC cells in embryos <sup>127</sup>. Stromal keratocytes are derived from NC, and adult human cornea was recently reported to express mRNA for NGFR <sup>141</sup>. The data in Figure 6 confirm previous reports <sup>135,136</sup> that NGFR protein is present on cells in the limbal stromal cells. Furthermore, this figure adds new information that little NGFR protein is present in the central corneal stroma. Our observation that hES-derived cells expressing NGFR have the potential to become keratocytes is consistent with the idea that the NGFR<sup>+</sup> cells in limbal stroma may be keratocyte progenitor cells.

Immobilized anti-NGFR antibodies have been previously used to select NC-like populations from hES cells during neural differentiation <sup>125</sup>. This approach clearly enriched for a NGFR<sup>+</sup> population, but according to Figure 9 the isolated population contained a substantial sub-population of NGFR<sup>-</sup> cells as well. In the future we may obtain a more potent population by multiple rounds of selection or by fluorescence-activated cell sorting (FACS). NC gene expression by these cells suggests the differentiating hES cells were heterogeneous because not all of the NC gene expression segregated equally with the NGFR<sup>+</sup> cells. NGFR mRNA was enriched by at least 6-fold in the NGFR<sup>+</sup> selected cells but other NC markers much less so. One advantage of the selection process was that it completely eliminated mouse PA6 feeder cells (Table 2).

We found the NGFR<sup>+</sup> population unable to differentiate to keratocytes directly and introduced an intermediate monolayer culture of the NGFR<sup>+</sup> cells. During this culture, expression of genes previously found to be expressed in stromal stem cells, particularly that of PAX6, was reduced. Fetal bovine serum and expansion of the cells beyond a single passage

appeared to be detrimental to their ultimate ability to differentiate. Although this culture stage appears to be essential, it seems likely that additional optimization of conditions of this stage of the process might ultimately provide a more efficient differentiation.

The ability of adult cells to differentiate to keratocytes appears to require the presence of soluble ascorbate and culture in an environment allowing formation of a three-dimensional cell construct<sup>130,131,133,142-145</sup>. We originally found that in serum-free medium containing ascorbate-2-phosphate, insulin, and FGF2, primary keratocytes form free-floating spheres that release from the plastic surface, adapting a highly differentiated phenotype<sup>143</sup>. Spherical aggregates of adult stem cells from cornea, adipose, and trabecular meshwork tissues formed by centrifuging the cells into a pellet also express keratocyte genes and organize a cornea-like extracellular matrix<sup>130,131,142</sup>. Based on these studies, we believe that expression of an array of keratocyte-specific genes by hES-derived NGFR+ cells cultured under these same conditions provides a strong argument that these cells have become functional keratocytes.

This argument was bolstered by the detection (in Figure 14) of corneal keratan sulfate proteoglycans secreted by the pellets. These data document secretion of a high molecular weight (>100 kDa) heterogeneous protein that precipitates with antibodies to keratocan and keratan sulfate and is also degraded by a glycosidase that breaks down keratan sulfate. Since this molecular form of proteoglycan is uniquely secreted by keratocytes in vivo, we believe this experiment provides incontrovertible evidence that the hES-derived cells have adopted a function previously only observed in corneal keratocytes.

Production of keratocytes from pluripotent cells has significant implications for cell-based therapy and tissue engineering for treatment of corneal diseases. Based on these results, pluripotent hES cells could represent a consistent, inexhaustible source of tissue for the surgical

treatment of severe corneal opacities. Furthermore, induced pluripotent stem cells derived from adult somatic cells could be used in place of human embryonic stem cells to provide autologous material for bioengineered corneal matrix or for direct cell-based therapy having a decreased risk of rejection and in greater supply than donor tissue.

In summary, this study has developed methodology to induce differentiation of hES cells into cells with a gene-expression phenotype similar to that of adult human keratocytes. This method may prove useful in the ongoing development of cell-based treatment for corneal blindness.

## 2.5 ACKNOWLEDGEMENTS

The authors thank Nancy Zurowski for help with flow cytometry and the support of the University of Pittsburgh Stem Cell Core Facility.

This chapter was modified with permission from:

Differentiation of Human Embryonic Stem Cells into Cells with Corneal Keratocyte Phenotype  
Audrey A. Chan\*, Andrew J. Hertsenbergs\*, Martha L. Funderburgh, Mary M. Mann, Yiqin Du, Katherine A. Davoli,  
Jocelyn Danielle Mich-Basso, Lei Yang, James L. Funderburgh  
PLoS One. 2013; 8(2): e56831. Published online 2013 February 21. doi: 10.1371/journal.pone.0056831  
PMCID: PMC3578879

\*These authors contributed equally to this work.

### **3.0 LIMBAL BIOPSY-DERIVED CORNEAL STROMAL STEM CELLS FOR AUTOLOGOUS TREATMENT OF CORNEAL SCARRING**

#### **3.1 INTRODUCTION**

The cornea is the first tissue through which light enters the eye and serves a critical role in focusing it onto the retina. When the cornea is injured or inflamed, normally quiescent cells of the corneal stroma, the keratocytes, transform into fibroblasts to repair the damage by secreting scar tissue<sup>31,146</sup>. The presence of fibrotic extracellular matrix (ECM) components in stromal scars results in scatter of incident light, causing a deterioration of visual function<sup>147,148</sup>. Visual impairment and blindness owing to corneal scarring affects millions worldwide<sup>3,4</sup> and is the commonest indication for corneal transplantation (penetrating keratoplasty) in the developing world<sup>149</sup>. Penetrating keratoplasty is the most widespread organ grafting procedure and usually highly effective in improving vision<sup>150</sup>; however, global demand for donor corneal tissue vastly exceeds its availability. Moreover, post-operative complications, particularly immune rejection, reduce the functional survival time for corneal allografts<sup>86</sup>, especially in developing countries<sup>151</sup>. For these reasons there is increasing interest in the development of therapeutic alternatives to corneal transplantation, including stem cell therapy, cell-free collagen scaffolds, bioengineered constructs, and corneal prostheses<sup>84,98,152,153</sup>.

The discovery of multipotent stem cells in the corneal stroma <sup>89,130</sup> has opened up the possibility of developing a cell-based approach to treating blinding corneal stromal disorders. In a mouse model of corneal opacity, human stromal stem cells were effective in regenerating normal corneal ECM and repairing collagen fibril defects <sup>106</sup>. The ability of mesenchymal stem cells to restore corneal transparency in lumican-knockout mice was subsequently confirmed using umbilical cord stem cells <sup>154</sup>. The presence of adult stem cells of mesenchymal lineage in human corneal stroma has been the subject of several reports <sup>92,98,155,156</sup>. Mesenchymal stem cells are immune-suppressant and therefore may have a role not only in remodeling but also in preventing inflammation, scarring, and immune rejection of transplanted tissue <sup>157,158</sup>.

The transitional region between optically clear cornea and opaque sclera, known as the limbus, is the location of a population of epithelial stem cells that can be obtained by biopsy and expanded in vitro. Limbal epithelial cells, obtained from surface biopsy, have been used successfully for autologous treatment of limbal stem cell deficiency in clinical trials <sup>78,80,159-161</sup>. Cultures from limbal biopsy procedures also contain a population of mesenchymal cells with properties similar to mesenchymal stem cells from bone marrow <sup>92</sup>. Other studies also have identified mesenchymal stem cells in the limbal region of the corneal stroma <sup>92,155-157</sup>. We have proposed that these reports all describe a single population of cells, the corneal stromal stem cells we have shown to differentiate to keratocytes and to regenerate stromal tissue in vivo <sup>98</sup>. The implication that corneal stromal stem cells may be present in biopsy samples suggests their availability for autologous use.

Our current study addresses the hypothesis that mesenchymal cells obtained from limbal biopsy tissue from human corneas can be expanded in a culture medium containing autologous serum and can differentiate to keratocytes with the potential for use in cell-based therapy. To

demonstrate this property we used a therapeutic model in which human limbal biopsy-derived stromal cells (LBSCs) embedded in fibrin gel were applied to the surface of a healing murine debridement wound. We report that human stromal cells derived from limbal biopsies can not only differentiate to functional keratocytes *in vitro*, but also induce regeneration of damaged stromal tissue *in vivo* resulting in a matrix indistinguishable from that of native cornea.

## 3.2 MATERIALS AND METHODS

### Study Design

The purpose of this study was to determine if mesenchymal cells present in human corneal limbal biopsies (LBSCs) differentiate into corneal keratocytes *in vitro*, and whether they can prevent corneal scarring in a murine model *in vivo*. *In vitro*, stem cell potential was assessed using clonogenic potential, sphere formation, and expression of stem-cell genes. Keratocyte differentiation was examined by gene and protein expression and by secretion of typical stromal ECM. *In vivo*, LBSCs were introduced into mouse corneal debridement wounds and the effect on corneal transparency, fibrotic EMC expression, and ECM ultrastructural organization was assessed. Statistical analyses used two-sided t-tests and two-way analysis of variance (ANOVA). *In vivo* experiments were designed to provide a power of 0.8 based on results from our previous study (23) using animals randomized as to treatment. Collection and analysis of *in vivo* data was carried out with observers blinded as to treatment groups. No adverse events were observed and no data points were excluded from analyses.

## **Limbal biopsy**

Human corneo-scleral rims from donors younger than 60 yo with less than 5 days of preservation were obtained from the Center for Organ Recovery and Education ([www.core.org](http://www.core.org)). Rims were rinsed twice in Dulbecco's modified Eagle's medium (DMEM/F12) containing gentamicin, penicillin, and streptomycin for 10 minutes each. As illustrated in Figure 15, under a dissecting microscope residual conjunctiva was grasped with a toothed forceps and sub-conjunctival dissection was carried out using Vannas scissors towards the anatomical limbus extending 0.5 mm into the clear cornea. Conjunctiva was excised and dissection of anterior limbal tissue was carried out circumferentially in the same plane. An annular ring of tissue consisting of the superficial limbal epithelium and stroma with 0.5 mm of cornea and sclera on either side was excised. This was divided into equal halves and each half was further divided into 4 equal segments (total of 8 segments) ~4.5 mm each.

## **Isolation and culture of stromal cells**

Four limbal segments were incubated in 0.5 mg/ml collagenase (Sigma-Aldrich, type L) overnight at 37°C, without epithelial removal. The remaining 4 segments were first incubated for 40 minutes in Dispase II neutral protease (Zen Bio) at 37°C. Epithelial cells were removed by gentle scraping, and the stripped limbal segments were incubated in collagenase similar to the first four segments. The digests were ticturated, incubated an additional hour, and filtered through a 70- $\mu$ m nylon screen to obtain a single-cell suspension. Cells obtained from each segment were seeded onto FNC-coated wells of a 12-well tissue culture plate in stem cell growth medium <sup>106</sup> containing 2% (v/v) fetal bovine or pooled human serum (Innovative Research). Culture media were changed every other day and cells were sub-cultured by brief digestion with TrypLE Express (Life Technologies) when 90% confluent into 6-well plates, 25 cm<sup>2</sup> T-flasks,

and 175 cm<sup>2</sup> T-flasks at passage 1, 2, and 3 (P1, P2, P3) respectively. Corneal fibroblasts were isolated by collagenase digestion of the peripheral 1-2 mm corneal rim left behind after excising the limbus and the sclera and expanded in DMEM/F12 with 10% FBS and used at passage 4-6<sup>89</sup>.

### **Clonogenic Assay (CFU-f)**

P3 cells were plated at a density of 250 cells in a 10-cm diameter dish (~5 cells/cm<sup>2</sup>) in the same media that were originally used to culture the cells. After 10 days, media were removed and cells were fixed with cold methanol 10 min then stained with 0.1% crystal violet in 20% ethanol for 5 minutes. Colonies of >50 cells were evaluated as to size and number using Fiji (ImageJ) software. Colony counts were determined in duplicate for cell lines derived from 4 donor corneas (n=8). Diameter of colonies in 4 dishes was determined for each condition (n>400).

### **Sphere Formation**

P3 LBSCs were placed in 6-well plates coated with poly(2-hydroxyethyl methacrylate) (polyHEMA)<sup>162</sup> at a density of 3000 cells/well in sphere medium: Advanced DMEM (containing glutaMAX, Gibco 12491), B27 (1:50), 10 ng/mL fibroblast growth factor basic, 20 ng/mL epidermal growth factor, 50 ug/mL gentamicin, 100 ug/mL streptomycin and 100 IU/mL penicillin. The individual spheres were photographed and collected for RNA analysis on day 7.

### **Differentiation to keratocytes**

P3 LBSCs were cultured on collagen gel-coated 12-well plates at a density of 100,000 cells per well. After 24 hours, medium was changed to keratocyte differentiation medium (KDM) consisting of Advanced DMEM (containing glutaMAX, Gibco 12491), ascorbate-2-phosphate (1 mM), FGF2 (10 ng/ml) and TGF-β3 (0.1 ng/ml)<sup>153</sup>. One week later the gel was digested with 0.5

ml of collagenase (2 mg/ml, Sigma-Aldrich, type L). Cells were collected by centrifugation and lysed in RLT buffer (Qiagen) for RNA isolation.

### **Gene expression before and after differentiation**

RNA isolated by Qiagen miniPrep was transcribed into cDNA using SuperScript III (Life Technologies) and analyzed for expression of stem cell (*ABCG2* and *Nestin*) and keratocyte (*ALDH*, *AQPRI*, *CHST6*, *Keratocan* and *PTDGS*) gene markers using procedures and primers previously described<sup>106,130,163</sup>. Assessment of mRNA copy numbers was carried out using standard curves based on linearized plasmids containing the amplified sequences<sup>163</sup>.

### **Production of Stromal Matrix**

P3 cells were plated on 15 mm diameter PLC aligned nanofiber inserts (Nanofiber Solutions #242402) in a 24-well plate at a density of 20,000 cells per well. After 24 hours in stem cell growth medium, cultures were shifted to KDM. The medium was changed every 3 days for one month after which the tissue was fixed in paraformaldehyde and immunostained (as below) for collagen I, f-actin using phalloidin, and nuclear DNA with 4',6-diamidino-2-phenylindole (DAPI)<sup>133,153</sup>. Stained constructs were imaged using a Fluoview 1000 Olympus confocal microscope with a 20X oil immersion objective. Z-stack images captured optical sections throughout the construct and were used to determine construct thickness. Proteoglycans isolated from the culture medium were separated by polyacrylamide gel electrophoresis and detected by immunoblotting using antibody J19 to detect keratan sulfate, as described previously<sup>153</sup>.

### **Immunostaining**

Immunostaining of mouse tissue was carried out on 8  $\mu$ m cryostat sections fixed overnight in 3% paraformaldehyde and blocked using 10% heat-inactivated goat or donkey serum in phosphate buffered saline (PBS). Primary antibody was incubated at 4°C overnight. Primary antibodies

used were: human keratocan (1:150, Gift from Chia-Yang Liu <sup>164</sup>), human-specific collagen I (1:100, Sigma C2456), decorin (1:100, Santa-Cruz Biotechnology, SC-22753), biglycan (1:80, R&D Systems AF2667), fibronectin (1:80, Abcam, ab26245), or tenascin C (10 µg/mL, R&D Systems, MAB 2138). To detect hyaluronan (HA) tissue was fixed in ice-cold 4% paraformaldehyde, 70% ethanol, 5% glacial acetic acid (v/v) for 10 minutes. After washing 3 times in PBS, slides were blocked using an Endogenous Biotin-Blocking Kit (Life Technologies E-21390) and stained with biotinylated HABP (1:100, Millipore 385911) overnight at 4°C. Slides were then washed 3 times in PBS and stained with AlexaFluor 546 conjugated Streptavidin (Life Technologies S-11225) at 1:1000 for 2 hours at room temperature. Slides were subsequently washed 3 times in PBS before staining with secondary antibody and DAPI for 2 hours at room temperature. Slides were imaged using the Olympus Fluoview 1000 confocal microscope with 20X or 40X oil objective.

### **Corneal Debridement**

All animal procedures were done in accordance to The Association for Research in Vision and Ophthalmology (ARVO) Statement for the Use of Animals in Ophthalmic and Vision Research and approved by the Institutional Animal Care and Use Committee (IACUC) of the University of Pittsburgh. Debridement procedures were done as previously described <sup>158</sup>. Briefly, 7-week old female C57Bl/6 in randomized groups of 6-10 were anesthetized by intraperitoneal injection of ketamine (50 mg/kg) and xylazine (5 mg/kg). Our previous study and power analysis determined that at least 6 eyes were required for statistical significance in OCT analysis, and that 2-weeks and 4-weeks provided appropriate time points for analysis of gene expression and fibrosis <sup>158</sup>. One drop of Proparacaine Hydrochloride (0.5%) was added to each eye before debridement. Corneal epithelial debridement was performed by passing an Algerbrush II (The Alger

Company) over the central 2 mm of the mouse cornea. Once the epithelium was removed, a second application of the Algerbrush II was used, this time applying more pressure to remove the basement membrane and 10-15  $\mu\text{m}$  of anterior stromal tissue. See Figure 20 for a schematic of this procedure. Immediately after the procedure mice received 3 mg/kg ketoprofen for analgesia.

### **Fibrin Gel and LBSC Application**

LBSCs expanded in human serum at  $1 \times 10^6$  cells/ml in DMEM/F-12 were stained with 50  $\mu\text{g/ml}$  Vybrant DiO(3,3'-dioctadecyloxacarbocyanine) (Life Technologies) 20 minutes  $37^\circ\text{C}$ . The cells were washed twice with DMEM/F-12 and resuspended in a solution of human fibrinogen, 20 mg/mL in PBS at  $2.5 \times 10^7$  cells/ml. This concentration was determined to be the maximum number of cells that was retained on the corneal surface during healing. The relationship between cell number and biological efficacy was not investigated. After wounding, 0.5  $\mu\text{L}$  thrombin (100 U/mL, Sigma) was added to the wound bed followed immediately by 1  $\mu\text{L}$  of fibrinogen (with or without LBSCs). After 1-2 min, the fibrinogen had gelled, a second round of thrombin and fibrinogen was added. The wound was irrigated with sterile PBS and a drop of gentamycin ophthalmic solution 0.3% was added. The corneal epithelium closed the wound in 24-36 hr. Immunostaining was performed after 4 weeks, as described above. Eyes were examined daily for signs of rejection and infection for 1 week and weekly thereafter.

### **Optical Coherence Tomography (OCT)**

OCT was performed weekly to quantify light scatter, the cause of reduced vision in corneal scars<sup>147,148</sup>. Mice were anesthetized by intraperitoneal injection of ketamine (50 mg/kg) and xylazine (5 mg/kg) and eyes were scanned using a Bioptigen SD-OCT (Bioptigen, Research Triangle Park, NC). Animals were randomized as to order of analysis, and scanning data was collected and analyzed in a masked fashion regarding experimental treatment of the animals. Image

processing and analysis were conducted using ImageJ (NIH) and MetaMorph 7.7.3 (Molecular Devices, Inc). For quantification of corneal light scatter, Imaris (Bitplane USA) was used to isolate the cornea from the lens, iris, and interfering eyelashes. Pixel intensity measurements were taken both of the cornea and background using ImageJ and exported to Excel (Microsoft Corp), where the average background pixel intensity was subtracted from the average corneal pixel intensity. For generating threshold images, corneal epithelium was removed using Metamorph to isolate only the corneal stroma. Control eyes were used to set the threshold, and scar volume beyond the control threshold was displayed graphically.

### **Transmission Electron Microscopy**

Three corneas per group were analyzed by transmission electron microscopy. The corneas were processed as described previously<sup>106,158</sup>. Briefly, tissue was fixed immediately post-mortem in fresh 4% paraformaldehyde, 2.5% glutaraldehyde, 0.1 M sodium cacodylate, pH 7.4, and 8 mM CaCl<sub>2</sub> followed by postfixation with 1% osmium tetroxide. After dehydration in an ethanol series followed by propylene oxide, corneas were infiltrated and embedded in a mixture of EMbed 812, Nadic methyl anhydride, dodecyl succinic anhydride, and DMP-30 (Electron Microscopy Sciences). Thin sections were cut using a Leica Ultracut UCT ultramicrotome equipped with a diamond knife and were stained with 2% aqueous uranyl acetate and 1% phosphotungstic acid, pH 3.2. Anterior and posterior stroma regions of sections from central cornea were captured by investigators masked to the experimental treatment of the eyes. Micrographs were captured at 80 kV using a JEOL 1400 transmission electron microscope (JEOL Ltd) equipped with a Gatan Orius widefield side mount CC Digital camera (Gatan Inc). LBSC-treated eyes were fully sectioned and serially screened to confirm the absence of scarring.

## **Statistical analyses**

LBSCs were isolated from 4 separate donor eyes, so data in Figs. 14, 15, 16, and 17 present mean values of four biological replicates. P values for differences were determined by double-sided non-parametric t-tests or ANOVA with Tukey's post-hoc analysis, as indicated in figure captions, using GraphPad Prism software. Differences were considered significant when  $P < 0.05$ . Error bars show standard deviation of the mean unless otherwise indicated in the figure legend. Determination of differences in vascularization in Figure 24, shown in Table 6 used the chi squared test on a 2 x 2 contingency table to determine 2-tailed  $P$  values.

## **3.3 RESULTS**

### **3.3.1 Culture characteristics of limbal biopsy-derived stromal cells**

Cells were obtained from donated human corneas from which a central button had been taken for penetrating keratoplasty. Tissue samples were excised in a manner simulating limbal biopsies used to obtain epithelial cells from living human patients (Figure 15)<sup>80,159,165,166</sup>. In initial trials, stromal cells were released by collagenase digestion with or without prior removal of epithelial cells using the neutral protease dispase. Previously we found that an initial dispase treatment yielded mesenchymal cell cultures free of epithelial cells<sup>89</sup>. Isolation of cells using only collagenase (omitting dispase) produced primary cultures (Passage 0) cells with both epithelial and mesenchymal morphology (Figure 16A). After expansion (Passage 3) cells with epithelial morphology were lost and cultures consisted of homogenous small mesenchymal cells (Figure 16A). Collagenase-only isolation of cells resulted in significantly faster proliferation of LBSC

than dispase/collagenase isolation (Figure 16B, Table 3).

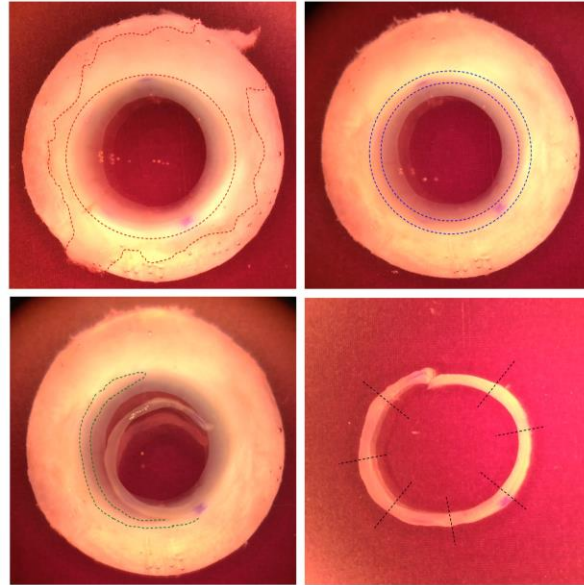


**Figure 15 Ex Vivo Model of Corneal Limbal Biopsy**

Donated human corneas were used in this study after removal of central tissue for transplant. A dissection procedure was designed obtain tissue identical to that of an in vivo surface biopsy. (Top left) The remnants of the conjunctiva and Tenon’s capsule (dashed-line) were excised from the corneo-scleral rim using Vannas scissors. (Top right) The limbal epithelium (blue dashed-line) was left intact. (Bottom left) A 1.5 to 2mm wide strip of superficial limbal tissue, including the epithelium and a sliver of limbal stroma was excised with the same scissors. The area from which the biopsy was obtained is highlighted within the green dashed-lines. (Bottom right) The annular biopsied limbal tissue was cut into 8, 1.5 clock-hour segments (black dashed-lines) each the same size as obtained from a clinical limbal biopsy procedure.

Basu S\*, Hertsenber AJ, et. al. doi: 10.1126/scitranslmed.3009644

Colony Area	FBS	HS
Mean	5.789	7.472
S.D.	3.15	5.121
N	415	549
p value (t-test)	<0.0001	

**Table 3 Area of Colonies Cultured in Different Sera**

Area of colonies from clonogenicity assay (Figure 16) comparing FBS and HS.

Basu S\*, Hertsenber AJ, et. al. doi: 10.1126/scitranslmed.3009644

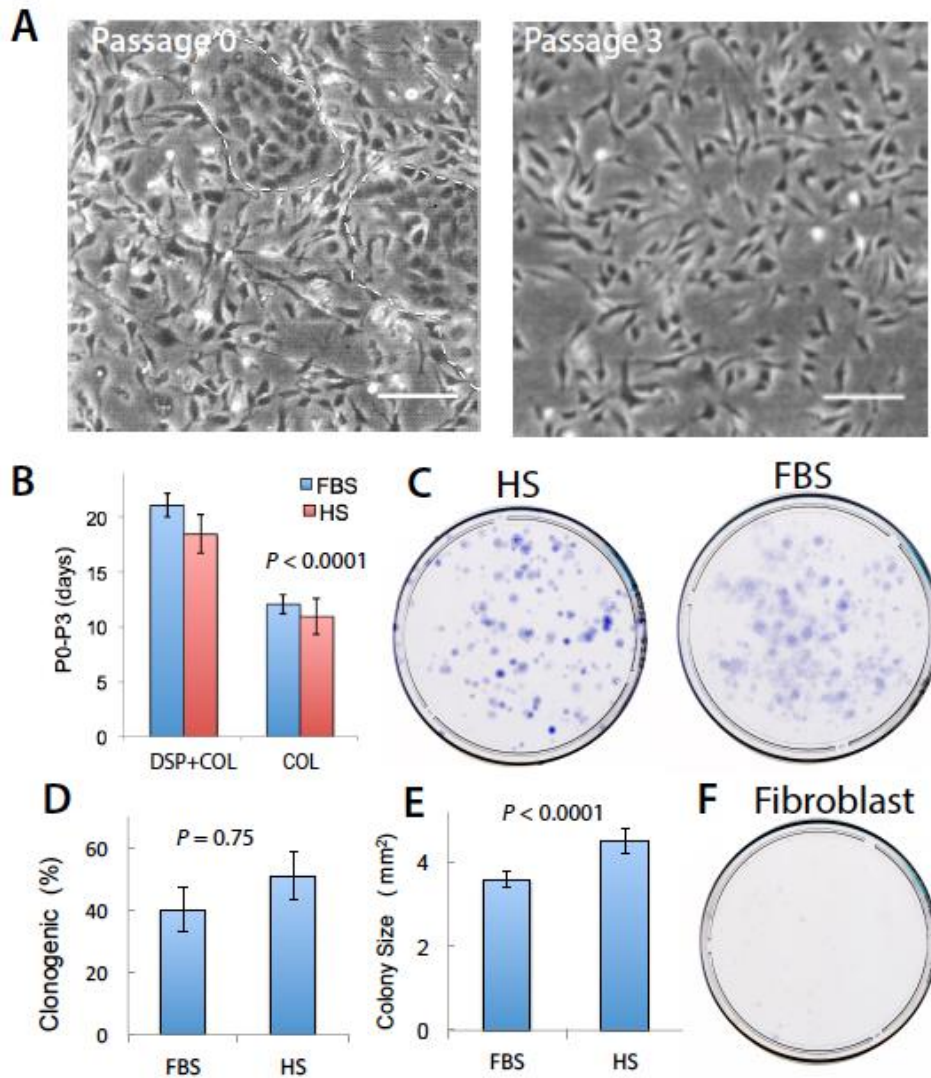


**Figure 16 Ex Vivo Expansion and Clonogenicity of Limbal Biopsy Stromal Stem Cells**

(A) Phase-contrast images of primary cells cultured from limbal biopsy tissue prepared by digestion with collagenase only. In initial plating (P0), red dashed lines mark islands of epithelial cells. Scale bars, 50  $\mu$ m. (B) The length of time (in days) required to expand cells from P0 to P3 was compared to LBSCs prepared with dispase and collagenase (DSP + COL) or collagenase only (COL), expanding cells in either HS or FBS. Data are means  $\pm$  SD (n=4). *P* value determined by two-way analysis of variance (ANOVA). (C) Clonal growth of LBSCs in HS and FBS. (D) Percentage of clonogenic cells in P3 cultures. Data are means  $\pm$  SD (n = 4). (E) Colony size was calculated with Fiji image analysis software. Data are means  $\pm$  SD (n > 400). *P* values in (D) and (E) were determined by a two-sided *t* test. (F) Corneal fibroblasts in FBS did not exhibit clonal growth (n = 4).

Basu S\*, Hertsberg AJ, et. al. doi: 10.1126/scitranslmed.3009644

### 3.3.2 Stem cell-like properties of LBSCs

Mesenchymal cells isolated from limbal biopsies were highly clonogenic irrespective of the culture conditions (Figure 16C). Approximately 40% of passage 3 cells grew as colonies from cells expanded in the presence of fetal bovine serum (FBS) or human serum (HS) (Figure 16D, Table 2). Cells cultured in FBS had significantly smaller colonies compared clones in HS (Figure 16E, Table 5). Stromal fibroblasts, mesenchymal cells from central cornea, did not form colonies under identical conditions (Figure 16F). When cultured in substratum-free conditions, LBSCs organized into free-floating spheres (Figure 17A). Under these conditions LBSCs

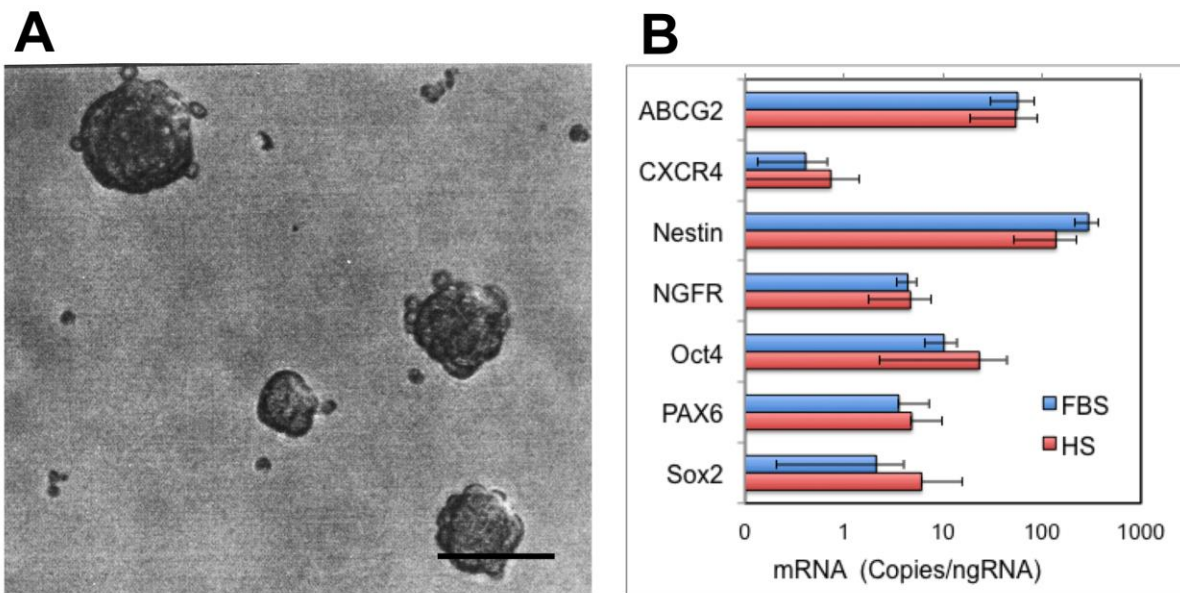


**Figure 17 Sphere Formation and Stem Cell Gene Expression by LBSC**

Passage-3 LBSC were cultured 2 weeks in low-attachment plates in a sphere-forming medium as described in Methods. (A) Cells formed into spheres 100-200  $\mu\text{m}$  in diameter. (B) Gene expression of characteristic of adult and pluripotent stem cells was determined in spheres by qPCR as describe in Methods. Cells expanded in human serum (red bars, HS) and fetal bovine serum (blue bars, FBS) showed no significant differences in expression levels. Values are an average of values obtained from four different cell line cells obtained from separate donor corneas. Error bars represent standard deviation. Scale bar shows 200  $\mu\text{m}$ .

Basu S\*, Hertsberg AJ, et. al. doi: 10.1126/scitranslmed.3009644

upregulated expression of genes associated with both adult and pluripotent stem cells (*ABCG2*, *Nestin*, *OCT4*, *PAX6*, *NGFR* and *SOX2*) (Figure 16B).

### 3.3.3 LBSCs differentiate into keratocytes *in vitro*

LBSCs cultured on a collagen gel substratum in ascorbate-containing, serum-free keratocyte differentiation medium (KDM) exhibited a marked decrease in the expression of the stem cell genes *ABCG2* and *Nestin*, and an increase in expression of genes associated with keratocyte differentiation: *ALDH3A1*, *AQP1*, *KERA* and *PTGDS* (Figure 18)<sup>130,163,167</sup>. When LBSCs were cultured on a substratum of parallel, aligned nanofibers<sup>133,153</sup> in KDM, the cells secreted a thick ECM of fibrillar collagen type I, and keratan sulfate-containing proteoglycans (Figure 19). The cells and collagen fibrils showed strong alignment with the nanofiber substratum, but collagen deposited 30-40  $\mu\text{m}$  above the substratum exhibited an orientation rotated by about 40° with respect to the lower layers (Fig. 19A). This rotation is similar to that of stromal lamellae *in vivo*, demonstrating a lamellar organization similar to that of corneal stroma. After 30 days in culture the collagen construct was 35-40  $\mu\text{m}$  in thickness (Figure 19B), a value independent of the culture medium. Conditioned media pooled from cultures contained high molecular weight (>130 kDa) keratan sulfate-containing proteoglycans, unique components of corneal ECM (Figure 19C).

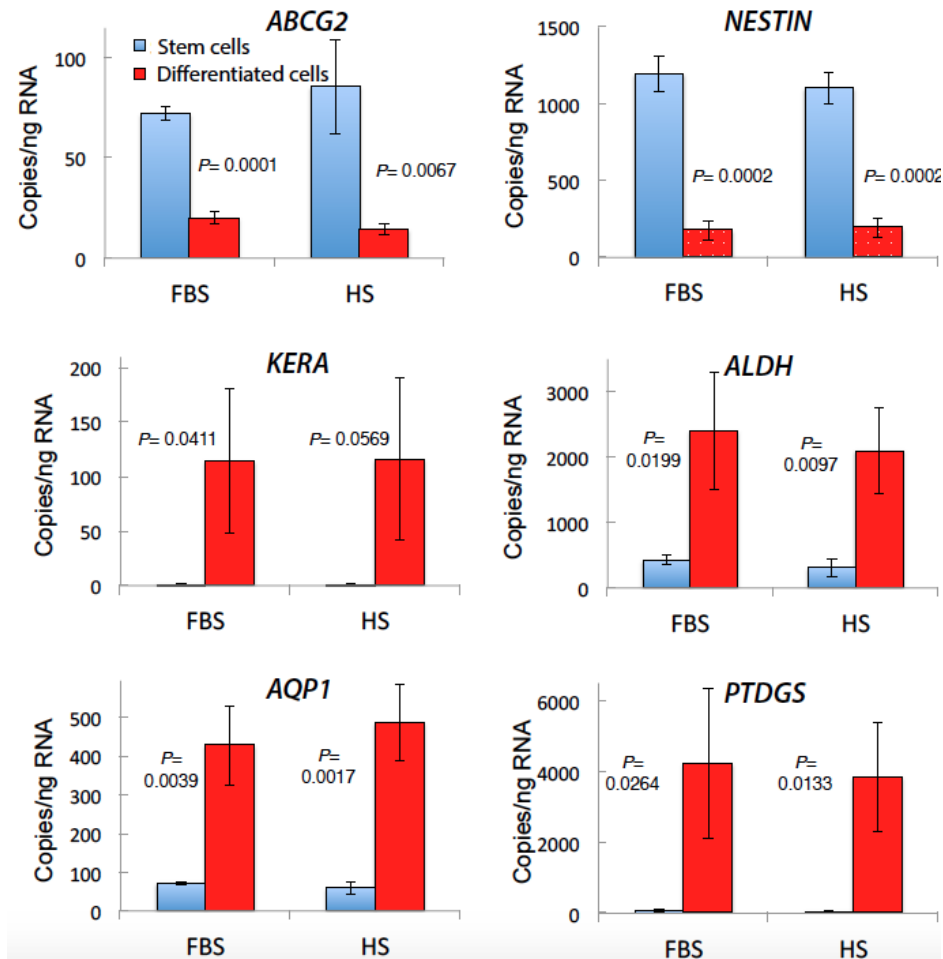


**Figure 18 Gene Expressio During Ex Vivo Differentiation of LBSC**

LBSCs expanded to P3 in FBS or HS were cultured in differentiation conditions on collagen gels for 1 week. mRNA was quantified as copies per nanogram of cellular RNA, determined by quantitative polymerase chain reaction (qPCR). Data are averages  $\pm$  SD from four different cell lines, each obtained from a different donor cornea. P values were determined by two-sided t-test.

Basu S\*, Hertsenber AJ, et. al. doi: 10.1126/scitranslmed.3009644

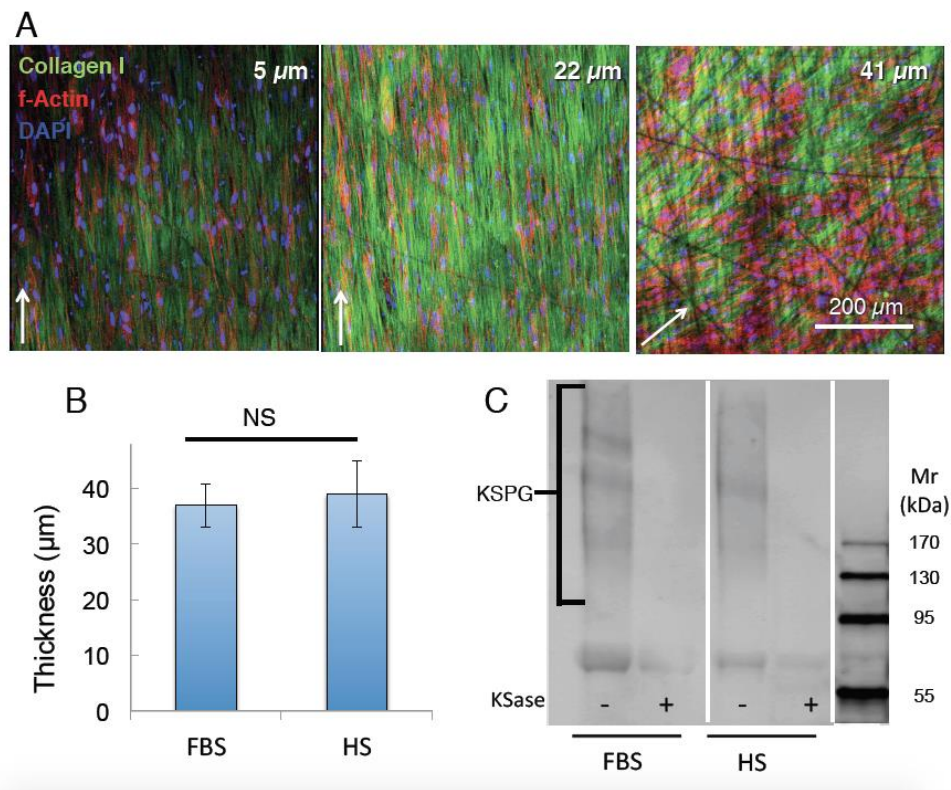


**Figure 19 Generation of Three-Dimensional Stroma-Like Tissue In Vitro**

ECM produced by LBSCs cultured on aligned nanofiber substrate for 4 weeks was imaged by confocal microscopy capturing optical sections at different z levels above the substratum. (A) Type I collagen fibrils (green) and keratocytes (nuclei, blue; F-actin, red) are shown at different depths of the construct. (B) Thickness of collagenous matrix at 4 weeks in HS or FBS was determined from confocal analysis. Data in (B) show averages  $\pm$  SD from cell lines from four different donors. Lack of significance (NS;  $P > 0.05$ ) was determined by a two-sided t test. (C) Cornea-specific keratin sulfate proteoglycan (KSPG) was detected by immunoblotting. Alternate lanes show sensitivity of the heterogeneous KSPG band (130 to 300 kD) to keratanase (KSase).  $M_r$ , relative molecular mass.

Basu S\*, Hertsenberg AJ, et. al. doi: 10.1126/scitranslmed.3009644

### 3.3.4 Human LBSCs engraft in murine cornea *in vivo*

The ability of LBSCs to prevent and/or remediate corneal scarring was examined using a mouse corneal debridement model which induces fibrotic matrix deposition, long-term disruption of the organization of the stromal collagenous ECM structure, and produces visible stromal scars<sup>158</sup>.

At the time of wounding, 50,000 LBSCs were applied to the wound bed in a solution of fibrinogen, which formed a fibrin gel in response to the concomitant addition thrombin. At one week after wounding, 3,3'-dioctadecyloxacarbocyanine (DiO)-labeled LBSCs remained in the cornea distributed throughout the wounded area (Figures 20 and 21A). LBSCs remained in the anterior stroma, for at least four weeks during which time the average number of engrafted cells decreased by about half (data not shown). During that time no inflammation or rejection was observed in response to these cells. Four weeks after wounding, anterior stromal tissue subjacent to the corneal epithelium and near engrafted LBSCs, contained human keratocan and type-I collagen, components of normal transparent stromal ECM (Fig. 21B).

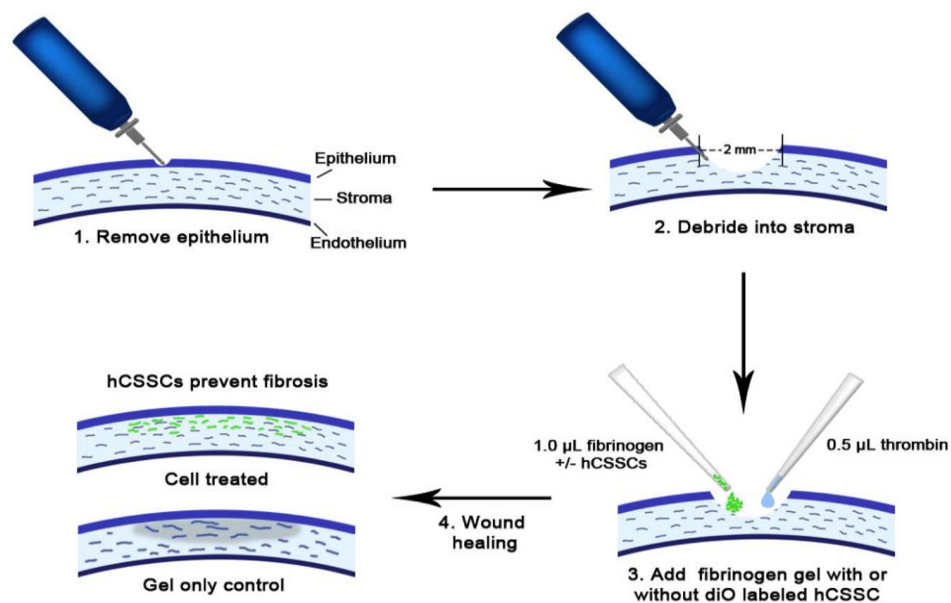


**Figure 20 Murine Corneal Debridement Model**

This cartoon shows debridement of the surface of the mouse cornea using an Algerbrush II motorized burr. The debridement continues through the epithelial basement membrane and into the anterior 10-15  $\mu\text{m}$  of the stroma. Immediately after wounding, 0.5  $\mu\text{l}$  of thrombin solution is added to the wound surface followed by fibrinogen (1  $\mu\text{l}$ ) containing 50,000 LBSC cells. Subsequent analysis shows that the corneal epithelium closes the wound engrafting the fibrin-gel trapped cells in the anterior stroma.

Basu S\*, Hertsenber AJ, et. al. doi: 10.1126/scitranslmed.3009644

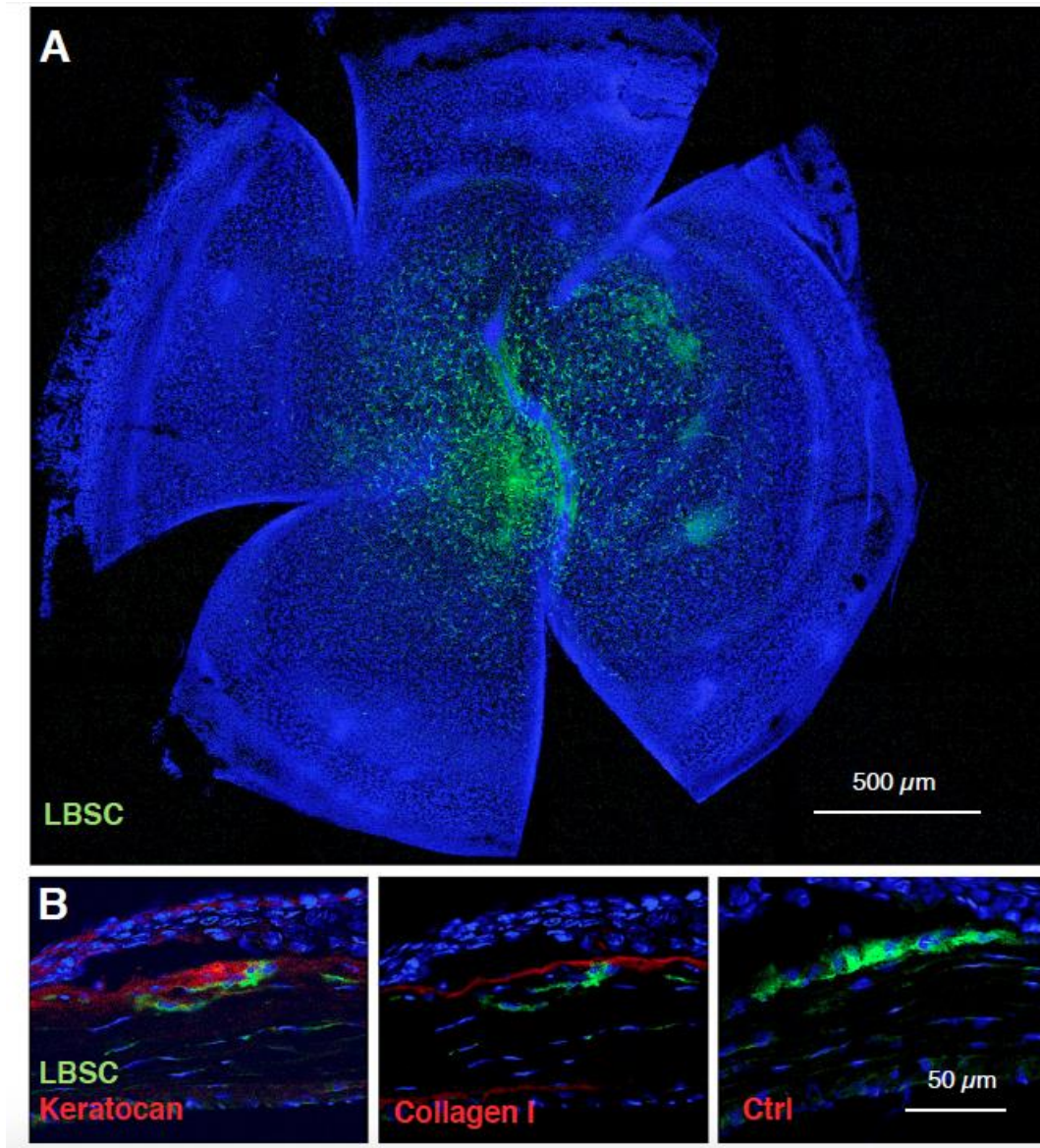


**Figure 21 LBSC Engraftment and Stromal Matrix Synthesis in Mouse Cornea *In Vivo***

Fluorescent DiO-labeled human LBSCs were transferred to a superficially debrided mouse cornea in a fibrin gel as depicted in Figure 18. (A) One week after wounding, whole-mount staining showed persistence of the human LBSCs (green) in the central cornea. (B) At 1 month, histological sections immunostained with human-specific antibodies show human keratocan and collagen type I. Omission of primary antibody controlled nonspecific staining. In all images, nuclei are stained with 4',6-diamidino-2-phenylindole (DAPI) (blue). Anterior of the eye is oriented up in each images in (B), and the corneal epithelium is visible as a dense layer of cells near the top of each image. Ctrl, control.

Basu S\*, Hertsenber AJ, et. al. doi: 10.1126/scitranslmed.3009644

### **3.3.5 LBSCs promote regeneration of stromal tissue during wound repair**

Wound repair in the corneal stroma typically results in the accumulation of a number of ECM components associated with light-scattering scar tissue, absent in normal stroma, including fibronectin, tenascin-c, biglycan, hyaluronan, type III collagen, and SPARC (secreted protein acidic and rich in cysteine)<sup>30,31,168-171</sup>. In wounds allowed to heal without addition of LBSC (Figure 22A, left panels), fibrotic markers hyaluronan, fibronectin, tenascin-c, biglycan, and decorin were abundant in anterior stroma, indicating scar formation. In wounded corneas treated with LBSCs, only the proteoglycan decorin, a component of normal stromal matrix, was detected (Figure 22A). Similarly, mRNAs for mouse type III collagen and SPARC were upregulated two weeks after wounding in debrided corneas; however, the presence of LBSCs significantly reduced the upregulation to levels similar to unwounded controls (Figure 22B).

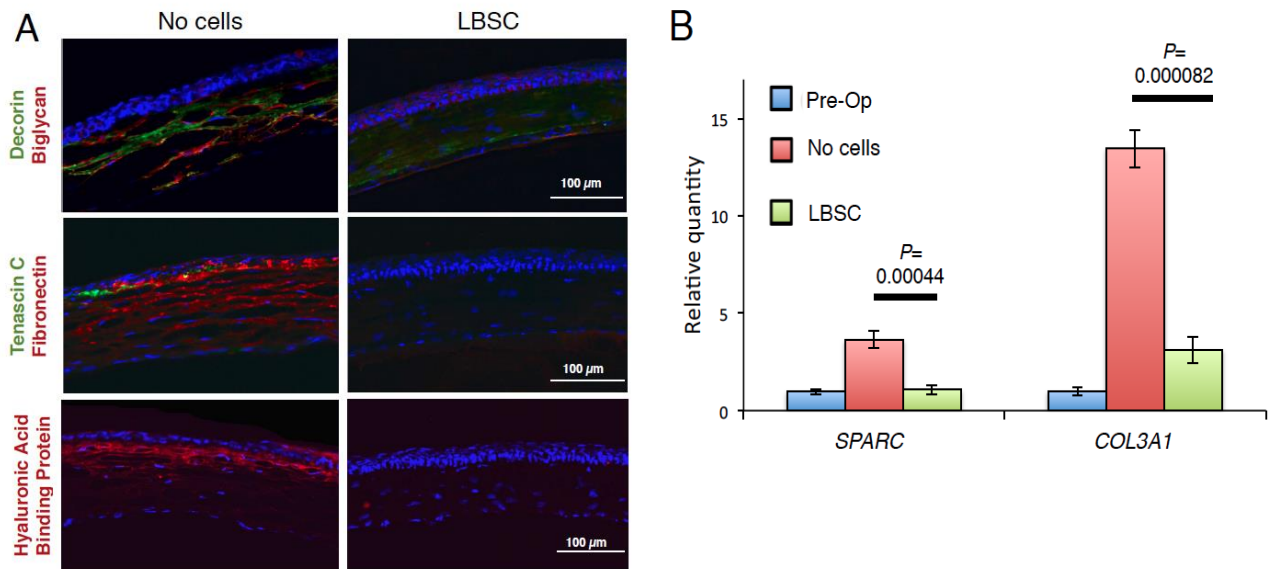


**Figure 22 LBSC Block Deposition of Fibrotic Matrix in Healing Murine Corneas**

(A) Debridement-wounded mouse corneas were treated with fibrin gel only (no cells) or with 50,000 LBSCs in fibrin gel. After 4 weeks of healing, histological sections (epithelium oriented up) were stained for fibrotic markers decorin, biglycan, tenascin C, fibronectin, and hyaluronan. Images are representative of sections from three corneas for each condition. (B) Quantification of SPARC and Type III Collagen (COL3A1) mRNA preoperative (pre-op) and weeks after treatment with LBSCs or no cells. Data are averages  $\pm$  SD. P values determined by two-sided t test.

Basu S\*, Hertsberg AJ, et. al. doi: 10.1126/scitranslmed.3009644

Low-magnification photos of wounded corneas using diffuse lighting revealed the presence of visible scarring in all of the eyes that healed without LBSCs, whereas visible scars were absent in all eyes receiving LBSCs (Figure 23A). Light scatter by corneal scars, a cause of reduced visual acuity, was assessed using spectral domain optical coherence tomography (OCT). Light scatter in individual cross-sectional OCT scans was revealed as bright stromal regions in untreated corneas 2 and 4 weeks after debridement (Figure 23B). Thresholding of these bright pixels in *en face* projections allowed a qualitative assessment of scar area and volume (Figure 23C). Quantification of the thresholded images revealed a significant increase in light scatter in the untreated scars at both 2 weeks and 4 weeks after wounding (Figure 23D). In eyes treated with LBSCs at the time of wounding, however, light scatter was not increased compared to the pre-operative normal corneas (Figure 23D).

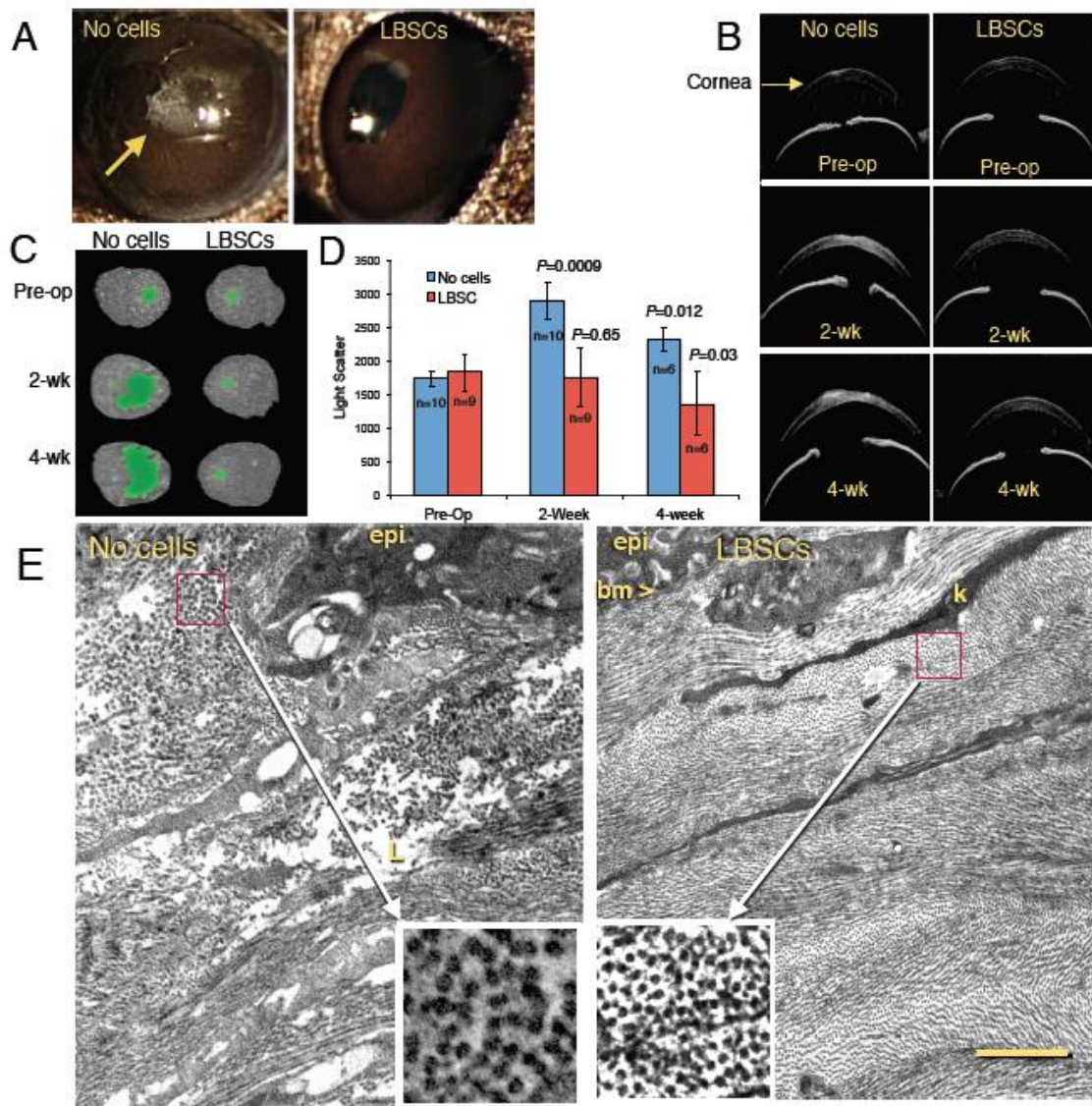


**Figure 23 LBSC Treatment Influences Light Transmission Properties of ECM Deposited after Debridement**

(A) Macroscopic images of mouse eyes in diffuse lighting reveal opaque scars (arrow) in untreated (no cells) eyes but none in LBSC-treated corneas. (B) OCT imaging shows transverse optical sections of preoperative (Pre-op) eyes and those 2 and 4 weeks after debridement, with scarring visible as bright pixels in the corneal stroma. (C) Thresholding of high-intensity pixels in three-dimensional (3D) OCT images of individual corneas defines scarred region (green) at 2 and 4 weeks after debridement. (D) Light scatter in 3D OCT scans at 2 and 4 weeks was compare with the values in preoperative eyes. Data are means  $\pm$  SD. The number of eyes is indicated in the graph. P values were determined with unpaired t tests at each time point compared to respective Pre-op values. (E) Transmission electron micrographs 4 weeks after debridement show the ablated region of the anterior stroma. Epi, epithelial cells; bm, basement membrane; k, keratocyte processes; L, amorphous matrix deposit (lake). Insets show magnification of a box (1 $\mu$ m X 1 $\mu$ m) from the indicated region containing orthogonal views of collagen fibrils. Scale bar, 2  $\mu$ m. Images are representative of n = 3 animals.

Basu S\*, Hertsberg AJ, et. al. doi: 10.1126/scitranslmed.3009644

Corneal transparency relies on a high level of ultrastructural organization of the collagenous ECM of the stroma<sup>26,172</sup>. It was therefore important to assess whether LBSC-treated eyes showed differences in collagen organization compared to wounds that did not receive stem cells. Transmission electron micrography of the healed untreated wounds showed ablated region of the anterior stroma to be reconstituted with ECM typical of that of corneal scars (Figure 23E, left panel). New ECM lacked characteristic lamellae organization. Collagen fibrils were large (inset), typically not tightly packed or in parallel orientation, and the tissue contained amorphous deposits and empty regions known as lakes<sup>173</sup>. In healed corneas treated with LBSCs, collagen organization in the stroma was essentially indistinguishable from that of native tissue (Figure 23E). Collagen was organized into distinct layers (lamellae) containing small, uniform, tightly packed fibrils. Keratocyte processes (k) were seen sandwiched between lamellae. Epithelial cells (epi) had elaborated a continuous basement membrane (bm). Higher magnification of the fibrils (Figure 23E, insets) showed fibril diameters in LBSC-treated tissue to be significantly smaller than those of the untreated scars ( $31.0 \pm 2.9$  nm vs  $50.6 \pm 6.6$  nm, respectively,  $P = 0.001$  using a single sample t-test,  $n = 28$ ).

### **3.3.6 LBSC treatment reduced corneal vascularization in mice**

Adult cornea is a non-vascularized tissue, and neo-vascularization in response to inflammation or trauma can represent a threat to vision. Immunostaining of healed corneas for CD31, a marker of vascular endothelial cells, revealed blood vessels in the central region of all (5 of 5) corneas that healed without addition of LBSCs (Figure 24A). Conversely, 3 out of 5 corneas that healed with LBSC treatment were free of central blood vessels (Figure 24B). Chi-squared analysis of these

results demonstrated a significant reduction in the vascularization in response to LBSC treatment (Figure 24C).

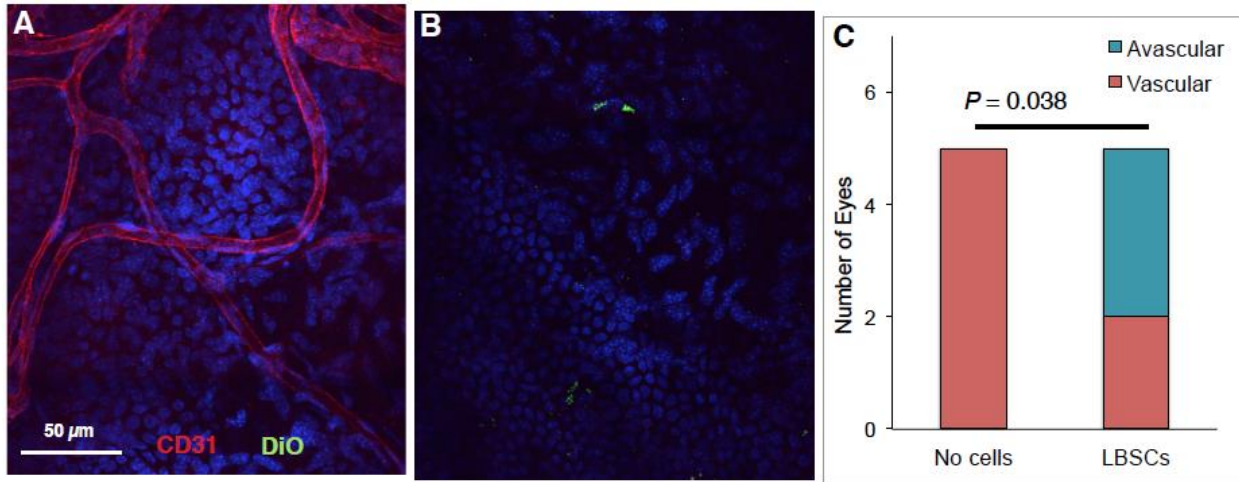


**Figure 24 Vascularization of Debridement Wounds**

One month after wounding, whole-mount corneas were stained with antibody to CD31 (red) to detect ingrowth of blood vessels. Cell nuclei were imaged with DAPI (blue), and added human LBSCs appear green. (A) Vessels in a healed cornea in which no cells were added. (B) DiO-labeled LBSCs are visible (green) but no vessels were present in the central LBSC-treated wound. (C) A stacked bar graph shows the proportion of vascularized corneas in human LBSC-treated (n=5) and untreated (n=5) mouse eyes analyzed by staining as in (A). P value was obtained from a two tailed chi-squared test with a 2 X 2 contingency table.

Basu S\*, Hertszenberg AJ, et. al. doi: 10.1126/scitranslmed.3009644

### 3.4 DISCUSSION

Over the past decade we have characterized multipotent mesenchymal stem cells in human corneal stroma which differentiate to keratocytes and elaborate a multilamellar collagenous ECM resembling that of cornea stroma<sup>89,106,130,133,153,163</sup>. In vivo, these cells restore transparency to lumican knockout mice, which have hazy stromas and disorganized stromal collagen<sup>106</sup>. The current study reveals two new properties of these cells. First, these cells can be obtained in a biopsy procedure that will permit autologous use. Second, we show that in an actively healing

wound, these cells suppress accumulation of fibrotic scar tissue and promote regeneration of new native, transparent corneal ECM. Together these findings present an argument for investigating clinical use of LBSCs to treat corneal scarring.

Our data demonstrate that corneal stromal stem cells can be obtained from a small surface ocular biopsy. In the current study we emulated a biopsy procedure, but clinical use of such biopsies to obtain limbal epithelial stem cells is well established <sup>80,159,165</sup>. The presence of mesenchymal cells in limbal biopsy tissue has been described <sup>92</sup>. The current study confirms that mesenchymal stem cells obtained from limbal biopsies are functionally equivalent to corneal stromal stem cells we have previously described, based on sphere-forming ability (Figure 17), gene expression patterns (Figure 18), and the ability to organize stromal ECM in vitro (Figure 19). The importance of this finding is that we are now able to use a clinically established procedure to obtain autologous stem cells with regenerative potential. These cells also grow rapidly in human serum, thus allowing production of a fully autologous, xenobiotic-free cell-based reagent.

Recent reports have described mesenchymal stromal cells proximal to the epithelial basement membrane in limbal regions near epithelial stem cells. These mesenchymal ‘niche cells’ are thought to help maintain the phenotype of limbal epithelial stem cells in vivo <sup>101,174,175</sup>. Niche cells can form spheres in vitro and express stem cell genes including *ABCG2*, *SOX2*, *Nanog*, *OCT4* and *Nestin* <sup>90,156,175,176</sup>. LBSCs isolated in this study from human limbal biopsies closely resembled niche cells. They grew more rapidly when only collagenase was used in their isolation and they were highly clonogenic, formed spheres and expressed genes characteristic of both adult and pluripotent cells. By these criteria, LBSCs, corneal stromal stem cells, and limbal

niche cells appear indistinguishable and probably represent the same population of neural crest-derived mesenchymal stem cells.

An important advance contributed by this study is observation that LBSCs induce deposition of a native stromal tissue rather than scar tissue in healing wounds. Previous *in vivo* studies have used lumican-null mice, which develop stromal haze owing to abnormal collagen fibrillogenesis<sup>106,154</sup>. Although the disruption of stromal matrix in these mice resembles that in scars, it is not evident that restoration of transparency to lumican null corneas is fully analogous to remediation of corneal scars. In the current study we found that human LBSCs in the healing wound allowed regeneration of a fully transparent native stromal tissue. The new tissue had no expression of fibrotic mRNA or proteins, had no change in light scatter, and had highly organized stromal ECM indistinguishable from that of normal mouse cornea. Few mammalian tissues heal by regenerating native tissue. Scarring provides a strong and rapid structural repair, but tissue functionality can be impaired by scar tissue. This is particularly true for cornea in which collagen fibril diameter, parallel alignment, packing, and lamellar organization are essential for vision. Traumatic damage to stroma typically heals leaving scar tissue with disorganized collagen that scatters light and produces long-term disruption of vision. The ability of LBSCs to induce the replacement of ablated tissue with transparent ECM containing native components with collagen organization indistinguishable from that of normal stroma is an exciting finding that points to the clear potential for use of these cells in clinical applications to treat human corneal scars.

In this study, LBSCs were engrafted only in the most anterior portion of the stroma and were in low abundance in comparison to the mouse stromal cells. Amelioration of fibrotic matrix, light scatter, and disruption of the stromal organization occurred both where LBSCs were

located, and also in more posterior regions of the stoma. The lack of co-localization of LBSCs and scarring suggests that LBSCs exert their effects indirectly. Rather than simply replacing mouse stromal ECM with that produced by the differentiated LBSC, these cells are likely exerting a paracrine influence on the mouse stromal cells repopulating the wounded region. The mechanism of this regenerative effect is unknown. The ability of the stem cells to work at a distance may be an advantage in cell-based therapy of existing scars, in that it may not be necessary to saturate scar tissue with stem cells but rather only to deliver them proximal to the region needing to be regeneration. Whether existing scars can be treated with these cells remains an open question.

Much work over the previous decade has focused on corneal limbal epithelial stem cells for treatment of limbal stem cell deficiency, a potentially blinding, but rare condition. Autologous limbal epithelial stem cells have been successfully used to correct this condition in several human trials <sup>78,80,159-161,177</sup>. Corneal epithelium and stroma are structurally and functionally distinct tissues, and epithelial stem cells are not suitable for stromal therapy. However, the positive results of pioneering clinical trials with epithelial stem cells, and the data presented in our current study strongly support the idea that autologous mesenchymal stem cells (LBSCs) may be successful in treating stromal scarring, the major cause of corneal blindness in the world. Because these cells can be obtained and cultured in an autologous, xenobiotic-free fashion, and because fibrinogen-based adhesives are currently approved for ocular applications, barriers to bringing this treatment to clinical trial may be modest.

In summary, we have found a population of mesenchymal cells expanded from human limbal biopsy tissue with the potential to differentiate into keratocytes, to generate stromal tissue in vitro, to block corneal scarring, and to stimulate regeneration of transparent stromal tissue in

murine healing wounds in vivo. The ability to obtain cells from clinically reliable biopsies and to expand them in human serum presents the opportunity to use these cells clinically to remediate cornea wounds and scars.

### 3.5 ACKNOWLEDGEMENTS

We thank Erin K. Steer for assistance in creating schematics used in this publication, Moira Geary for assistance with animal work, Katherine Davoli for assistance with histology, and Dr. Gadi Wollstein for assistance with OCT imaging.

This chapter was modified with permission from:

Human limbal biopsy-derived stromal stem cells prevent corneal scarring.  
Basu S\*, Hertszenberg AJ\*, Funderburgh ML, Burrow MK, Mann MM, Du Y, Lathrop KL, Syed-Picard FN, Adams SM, Birk DE, Funderburgh JL.  
Sci Transl Med. 2014 Dec 10;6(266):266ra172. doi: 10.1126/scitranslmed.3009644.

\*These authors contributed equally to this work.

## **4.0 NEUTROPHIL REDUCTION PREVENTS CORNEAL LIGHT SCATTER: A POTENTIAL MECHANISM FOR LBSC IN WOUND HEALING**

### **4.1 INTRODUCTION**

Vision impairment and blindness are devastating conditions affecting millions of people worldwide. Corneal blindness – the result of scarring that occurs after ocular trauma or infection – affects 7-10 million people globally<sup>178</sup>. Currently the only treatment option for these patients is corneal transplant (penetrating keratoplasty), a procedure complicated by tissue rejection and limited by the supply of donor tissue<sup>179</sup>. As such, there is an increasingly important need to develop alternative therapies for these patients.

Alternatives to cadaveric transplant for penetrating keratoplasty, including prostheses, cell therapy, and bioengineered tissues are currently being studied with the hope of becoming standard of care for corneal scars. Indeed, collagen based prosthetics for corneal transplants are being developed and have been successful as corneal grafts in animals<sup>180-182</sup>. Stem cells are also being investigated for use as cell therapy as well as for the engineering of biosynthetic graft tissue. Human corneal stromal stem cells (hCSSC) are of particular interest as the natural progenitor for the cells that make up the corneal stroma. hCSSC have successfully been isolated and from human limbal tissue, were demonstrated to produce stroma-like tissue, and shown to restore transparency in a genetic model of corneal haze in mice<sup>89,106,130</sup>. These same cells have

also been used to generate organized, collagenous matrices that mimic corneal tissue that may be useful as a biosynthetic prosthetic for transplant <sup>133,153,183</sup>. More recently, we have shown that limbal biopsy-derived hCSSC prevent fibrotic wound healing that causes scarring and promote regeneration in a mouse model of corneal wounding <sup>107</sup>. This finding may lead to the use of hCSSC in an autologous manner to repair damaged corneal tissue in a way that avoids the use of donor tissue. Key to moving forward with hCSSC cell therapy is to elucidate the mechanism by which they prevent fibrosis and scarring.

Stem cells offer the ability to regenerate damaged tissue with both function and integrity. A multitude of studies have revealed these characteristics in multiple wound models <sup>184-187</sup>. It is becoming increasingly apparent that immunomodulation by stem cells is largely responsible for anti-fibrotic/pro-regenerative wound healing where they are applied <sup>188-190</sup>. While many secreted molecules are being investigated for immunosuppressive properties, notable among them is tumor necrosis factor alpha stimulated gene 6 (TSG-6) <sup>191-193</sup>. TSG-6 is a matrikine known to bind hyaluronan and other glycosaminoglycans, and is expressed by several cell types in response to inflammation <sup>194</sup>. More specifically, it directly inhibits neutrophil migration by binding the chemokine Interleukin-8, a neutrophil chemotactic factor <sup>195</sup>. As neutrophils are the first responders to wound sites and function in part by recruiting other inflammatory cells, it stands to reason that preventing their infiltration at the site of injury may prevent tissue-damaging effects of later arriving cells such as macrophages. Indeed, TSG-6 added topically or via secretion by bone marrow derived mesenchymal stem cells has been shown to modulate wound healing by preventing the acute phase of inflammation <sup>196-198</sup>.

In the present study, we investigated the mechanism by which hCSSC derived from limbal biopsies (termed LBSC) prevent fibrosis in a mouse model of corneal wounding described

in previous studies<sup>107,158</sup>. We hypothesize that LBSC, like other mesenchymal stem cells, have immunomodulatory properties that abrogate fibrotic wound healing. We show for the first time that LBSC produce TSG-6, that the expression of this protein reduces neutrophil infiltration to the corneal stroma after wounding, and that this leads to the reduction of light scatter observed in LBSC treated wounds. In contrast to previous studies that examined short-lived stromal haze in acute wounds shortly after injury, the present study follows wounds for four weeks to assess light scatter as a result of clinically relevant fibrotic scarring. Our results add to the collection of literature demonstrating the importance of TSG-6 in immunomodulation while further demonstrating the wound healing capacity of LBSC.

## **4.2 MATERIALS AND METHODS**

### **Limbal biopsy and cell culture**

Human corneo-scleral rims from donors younger than 60 years with less than 5 days of preservation were obtained from the Center for Organ Recovery and Education ([www.core.org](http://www.core.org)). Research followed the tenets of the Declaration of Helsinki, de-identified living donors approved tissue for research purposes, and the research approved by the institutional review board (IRB). Limbal biopsies were performed as described previously<sup>107</sup>. Briefly, rims were rinsed in Dulbecco's modified Eagle's medium (DMEM/F12) with antibiotics. Corneal conjunctiva was grasped with a toothed forceps and subconjunctival dissection was carried out with Vannas scissors toward the anatomical limbus 0.5 mm into the cornea. Conjunctiva was excised, and dissection of anterior limbal tissue was carried out circumferentially in the same plane. An annular ring of tissue consisting of the superficial limbal epithelium and stroma was excised.

Excised limbal segments were incubated in collagenase (0.5 mg/ml) (Sigma-Aldrich, type L) overnight at 37°C. The next day, digests were triturated, incubated for an additional hour, and filtered through a 70- $\mu$ m, nylon filter to obtain a single-cell suspension. Cells obtained from each segment were seeded onto FNC (AthenaES)-coated wells of a 12-well tissue culture plate in stem cell growth medium<sup>106</sup> (“SGM”) containing 2% (v/v) pooled human serum (Innovative Research). Culture medium was changed every other day and cells were passaged by brief digestion with TrypLE Express (Life Technologies) when 80% confluent into six-well plates, 25-cm<sup>2</sup> T-flasks, and 175-cm<sup>2</sup> T-flasks at P1, P2, and P3, respectively. For *tsg-6* expression studies, LBSC were cultured in SGM with 15 ng/mL TNF $\alpha$  for up to 72 hours. Differentiation conditions were as described previously<sup>153</sup> in keratocyte differentiation medium (“KDM”) composed of advanced DMEM (containing GlutaMAX, Gibco, 12491), ascorbate-2-phosphate (1 mM), fibroblast growth factor-2 (10 ng/ml), and transforming growth factor- $\beta$ 3 (0.1 ng/ml).

### **siRNA Knockdown**

Five hundred pmoles of TSG-6 siRNA (Santa Cruz Biotechnologies) in 50  $\mu$ l serum and antibiotic free OptiMEM (Life Technologies) was mixed with 100  $\mu$ l of OptiMEM containing 4  $\mu$ l Lipofectamine 2000 (Life Technologies) pre-incubated 20 min at room temperature.  $5 \times 10^5$  LBSC in 0.4 ml of antibiotic-free Advanced-MEM (Life Technologies) were added to the siRNA and incubated for 3 hr on a rocking platform at 37 °C. The cell suspension was washed 3 times to remove lipofectamine and plated in SGM. As a control, cells were transfected with scrambled siRNA. Cells were cultured at 37 °C with 5% CO<sub>2</sub> for 48 hours before being suspended in fibrinogen as described next.

### **Fibrin gel and LBSC application**

Five hundred thousand LBSC were suspended in a solution of human fibrinogen, 20 mg/ml in PBS at  $2.5 \times 10^7$  cells/ml. After wounding, 0.5  $\mu$ l of thrombin (100 U/ml, Sigma) was added to the wound bed, followed immediately by 1  $\mu$ l of fibrinogen (with or without LBSC treated with siSCR or siTSG-6). After 1 to 2 min, a fibrin gel formed, and a second round of thrombin and fibrinogen was applied. The wound was irrigated with sterile PBS, and a drop of gentamicin ophthalmic solution (0.3%) was added. The corneal epithelium reformed over the wound in 24 to 36 hours. Immunostaining was performed after 4 weeks, as described above. Eyes were examined daily for signs of rejection and infection for 1 week and weekly thereafter.

### **Corneal debridement**

All animal procedures were done in accordance with The Association for Research in Vision and Ophthalmology Statement for the Use of Animals in Ophthalmic and Vision Research and approved by the Institutional Animal Care and Use Committee of the University of Pittsburgh. Debridement procedures were done as previously described<sup>107,158</sup>. Briefly, 7-week-old female C57BL/6 mice in groups of 5 were anesthetized by intraperitoneal injection of ketamine (50 mg/kg) and xylazine (5 mg/kg). Our previous study and power analysis determined that at least six eyes were required for statistical significance in optical coherence tomography (OCT) analysis and that 2 and 4 weeks provided appropriate time points for analysis of gene expression and fibrosis<sup>107,158</sup>. One drop of proparacaine hydrochloride (0.5%) was added to each eye before debridement for topical anesthesia. Corneal epithelial debridement was performed by passing an AlgerBrush II (The Alger Company) over the central 2 mm of the mouse cornea. Once the epithelium was removed, a second application of the AlgerBrush II was used, this time applying more pressure to remove the basement membrane and 10 to 15  $\mu$ m of anterior stromal tissue.

Immediately after the procedure mice received Ketoprofen (3 mg/kg) for analgesia.

### **Neutralizing Antibody**

Three female C57Bl/6 mice at 8 weeks of age were used per group (with or without antibody). 24 hours prior to debridement, 0.5 mg of the anti-Ly6G (clone 1A8) neutropenia-inducing antibody was given via intraperitoneal injection. A second dose was given at the time of debridement. Corneas were wounded as described above with no cells added.

### **Flow Cytometry for Neutrophil Quantification**

24 hours after wounding, mice were sacrificed and both eyes were enucleated and the corneas dissected. Corneas were cut into quarters and digested in Collagenase Type 1 (Sigma) 820 U/mL in DMEM/F12 + 10% fetal bovine serum (FBS) at 37°C for 1 hour, vortexing every 20 minutes to break up tissue. Digests were then triturated until tissue was completely broken up and digested for 20 minutes longer if necessary. Digests were then filtered through 70- $\mu$ m nylon filter to remove debris. Cell suspensions were then pelleted by spinning at 340 x g for 10 minutes and pellets resuspended in 50 $\mu$ L staining buffer: phosphate buffered saline, 1% FBS, and 0.1% sodium azide. Keeping the cells on ice, Fc-Block, CD45-PerCP, Gr-1-PE (clone RB6-8C5), and CD11B-AF647 (all BD Biosciences) were added at 1:50 and incubated for 30 minutes on ice in the dark. Cells were then washed in 1mL of staining buffer and resuspended in 300 $\mu$ L 1% PFA in staining buffer before being run on a FACS Aria III Flow Cytometer (BD Biosciences). Data were analyzed using FlowJo 8.7 (FlowJo) and statistical analysis calculated using Prism 6 (GraphPad).

### **Real Time Polymerase Chain Reaction (RT-qPCR)**

RNA isolated by Qiagen Miniprep was transcribed to cDNA using SuperScript III (Life Technologies). cDNA and target primers (Table 4) were combined with SYBR Green Real-Time

Master Mix (Life Technologies) and real-time polymerase chain reaction run and data analyzed using the StepOnePlus Real-Time PCR System (Applied Biosystems).

Gene Symbol (Accession Number)	Direction	Sequence
KERA (NM_007035.3)	Forward	ATCTGCAGCACCTTCACCTT
	Reverse	CATTGGAATTGGTGGTTTGA
TSG-6 (NM_007115.3)	Forward	AAGCACGGTCTGGCAAATACAAGC
	Reverse	ATCCATCCAGCAGCACAGACATGA
18S rRNA (NR_003286.2)	Forward	CCCTGTAATTGGAATGAGTCCAC
	Reverse	GCTGGAATTACCGCGGCT

**Table 4 Target Primers Used for qPCR**

### Immunostaining

Immunostaining of mouse tissue was carried out on 8- $\mu$ m cryostat sections fixed in ice-cold 4% paraformaldehyde, 70% ethanol, and 5% glacial acetic acid (v/v) for 10 minutes and blocked with 10% heat-inactivated goat or donkey serum in phosphate-buffered saline (PBS). A human specific antibody to TSG-6 (1:150, Santa Cruz Biotechnology) was incubated on the sections at 4°C overnight. Slides were then washed three times in PBS and stained with AlexaFluor 546–conjugated anti-rat secondary antibody (Life Technologies) at 1:1000 for 2 hours at room temperature. Slides were subsequently washed three times in PBS before staining with DAPI for 15 minutes at room temperature. Slides were imaged with an Olympus FluoView 1000 confocal microscope with a 20X or 40X oil objective.

### Spectral Domain Optical coherence tomography

OCT and analysis were performed as described previously<sup>107,158</sup>. Briefly, OCT was used 4 weeks after injury to quantify light scatter, the cause of reduced vision in corneal scars<sup>147,148</sup>. Mice were

anesthetized by intraperitoneal injection of ketamine (50 mg/kg) and xylazine (5 mg/kg), and eyes were scanned with a Bioptigen SD-OCT (Bioptigen). Animals were randomized as to order of analysis, and scanning data were collected and analyzed in a masked fashion regarding experimental treatment of the animals. Image processing and analysis were conducted with ImageJ [National Institutes of Health (NIH)] and MetaMorph 7.7.3 (Molecular Devices Inc.). For quantification of corneal light scatter, Imaris (Bitplane USA) was used to isolate the cornea from the lens, iris, and interfering eyelashes. Pixel intensity measurements were taken both of the cornea and of the background with ImageJ and exported to Excel (Microsoft Corp.), where the average background pixel intensity was subtracted from the average corneal pixel intensity.

### 4.3 RESULTS

#### 4.3.1 LBSC express *tsg-6* after TNF $\alpha$ stimulation and during differentiation.

TSG-6 is a hyaluronan binding protein whose expression is induced by tumor necrosis factor alpha (TNF $\alpha$ )<sup>199</sup>. It is expressed by a multitude of cell types, notably stem cells. As it has not yet been shown to be expressed by corneal stromal stem cells, we first tested if LBSC did indeed express *Tsg-6*. After treatment with TNF $\alpha$ , LBSC increased expression of *Tsg-6* nearly 3-fold after both 24 and 72 hours in culture as measured by quantitative PCR (Figure 25A). While it is an important finding that LBSC express *Tsg-6* after TNF $\alpha$  stimulation, we also wanted to examine whether *tsg-6* expression would increase as the cells differentiate. After 72 hours in differentiation medium (with no exogenous TNF $\alpha$  added), *Tsg-6* expression is upregulated nearly 50-fold compared to undifferentiated cells (Figure 25B). To be sure the

cells were differentiating, we also looked at the expression of Keratocan, a marker of hCSCC differentiation<sup>200,201</sup>. Indeed, Keratocan expression was significantly upregulated compared to control cells. These results demonstrate that human corneal stromal stem cells express *tsg-6* both after TNF $\alpha$  stimulation as well as during the differentiation process.

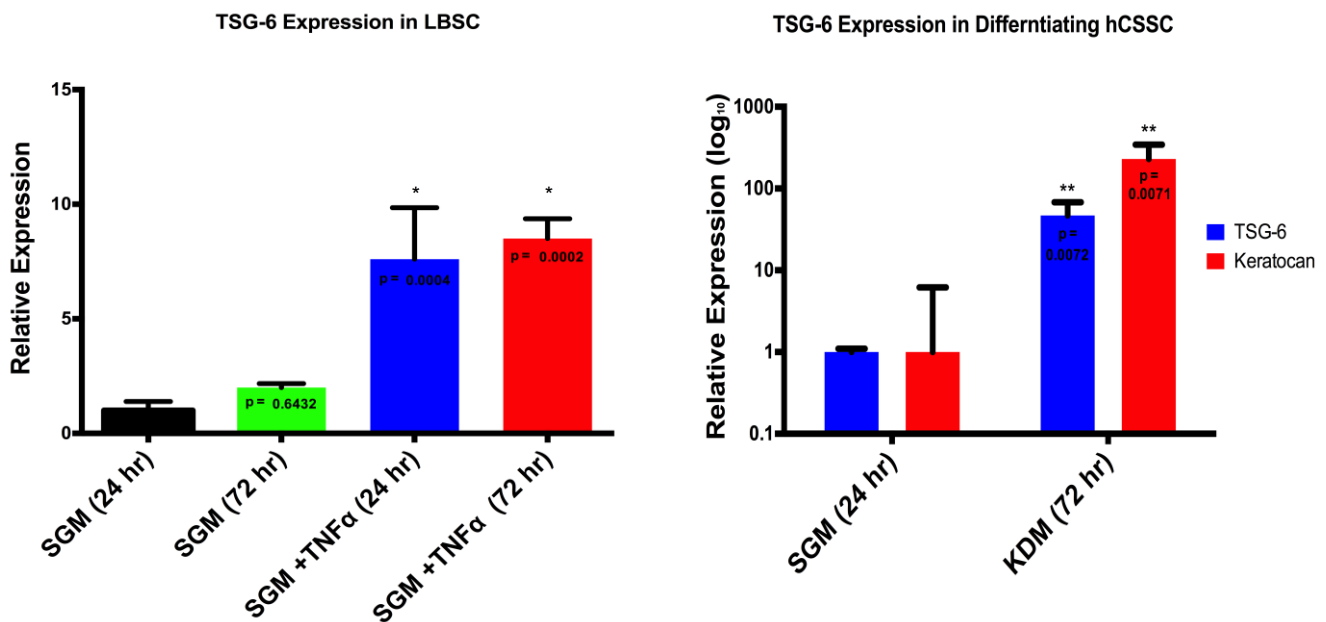


**Figure 25 LBSC Express *Tsg-6* upon TNF-alpha Stimulation and During Differentiation**

- A) *Tsg-6* expression is significantly upregulated 24 and 72 hours after culture with TNF $\alpha$ .
- B) *Tsg-6* expression is significantly upregulated ( $p < 0.001$ ) 72 hours after culture in keratocyte differentiation medium (KDM). *Kera* was used as a positive control for differentiation and expression was significantly upregulated ( $P < 0.01$ ), confirming differentiation. ANOVA with Dunnett's post-test.

### 4.3.2 LBSC produce TSG-6 in mouse corneal stromal wounds.

Our previous study examining the ability of LBSC to prevent fibrosis in mouse corneal wounds demonstrated a model wherein successful engraftment of LBSC in the corneal stroma is achieved after epithelial and partial debridement<sup>107</sup>. After showing that LBSC express *tsg-6* *in vitro*, we looked at TSG-6 expression *in vivo*. Four weeks after wounding, mouse corneal sections were stained for TSG-6 using a human specific antibody as described in methods. Immunohistochemistry shows that TSG-6 expression in corneas treated with LBSC but no expression in controls (Figure 26).

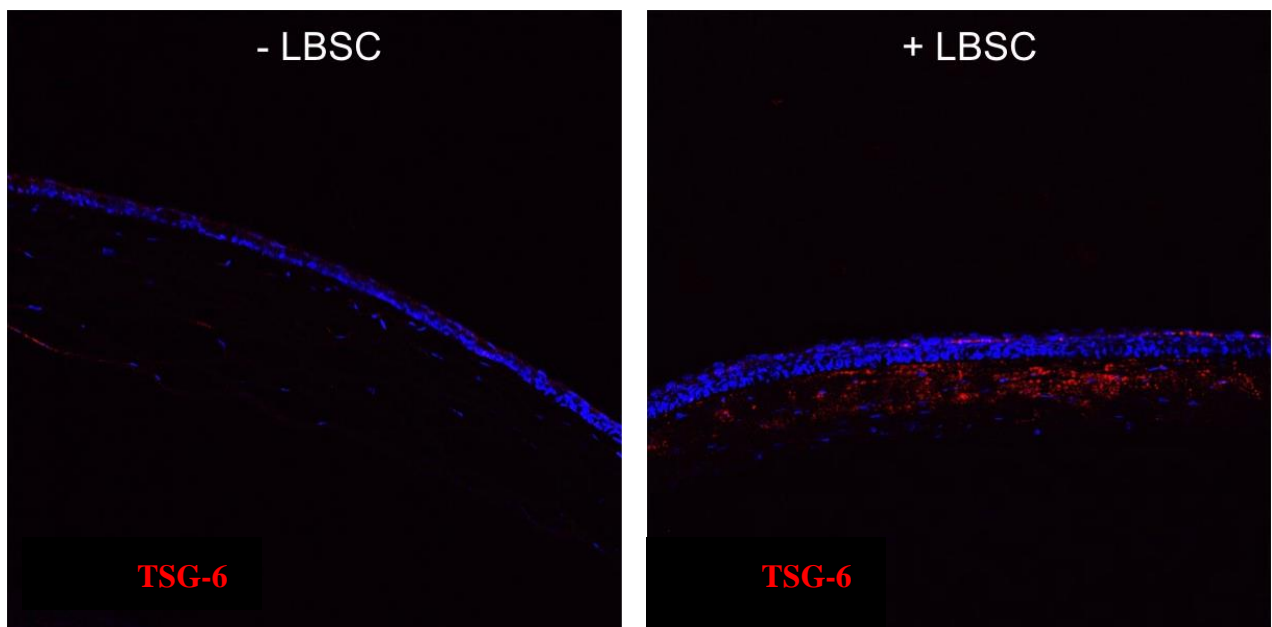


**Figure 26 LBSC Express TSG-6 In Vivo**

4 weeks after wounding, LBSC treated wounds (+LBSC) show TSG-6 expression while untreated wounds (-LBSC) do not.

### 4.3.3 LBSC significantly reduce neutrophil infiltration at the wound site via TSG-6.

TSG-6 has recently been shown *in vitro* to inhibit neutrophil migration via its interaction with Interleukin 8<sup>195</sup>. After demonstrating that LBSC produce TSG-6 *in vivo*, we tested the effect of LBSC treated with and without siRNA to *tsg-6* on neutrophil infiltration at the cornea 24 hours after wounding. siRNA to *Tsg-6* significantly reduced expression when compared to LBSC treated with scrambled siRNA (Figure 27A). LBSC treated with the scrambled siRNA had significantly fewer neutrophils present at the wound while LBSC treated with siRNA to *Tsg-6* had nearly the same number of neutrophils as the gel-only control (Figure 27B).

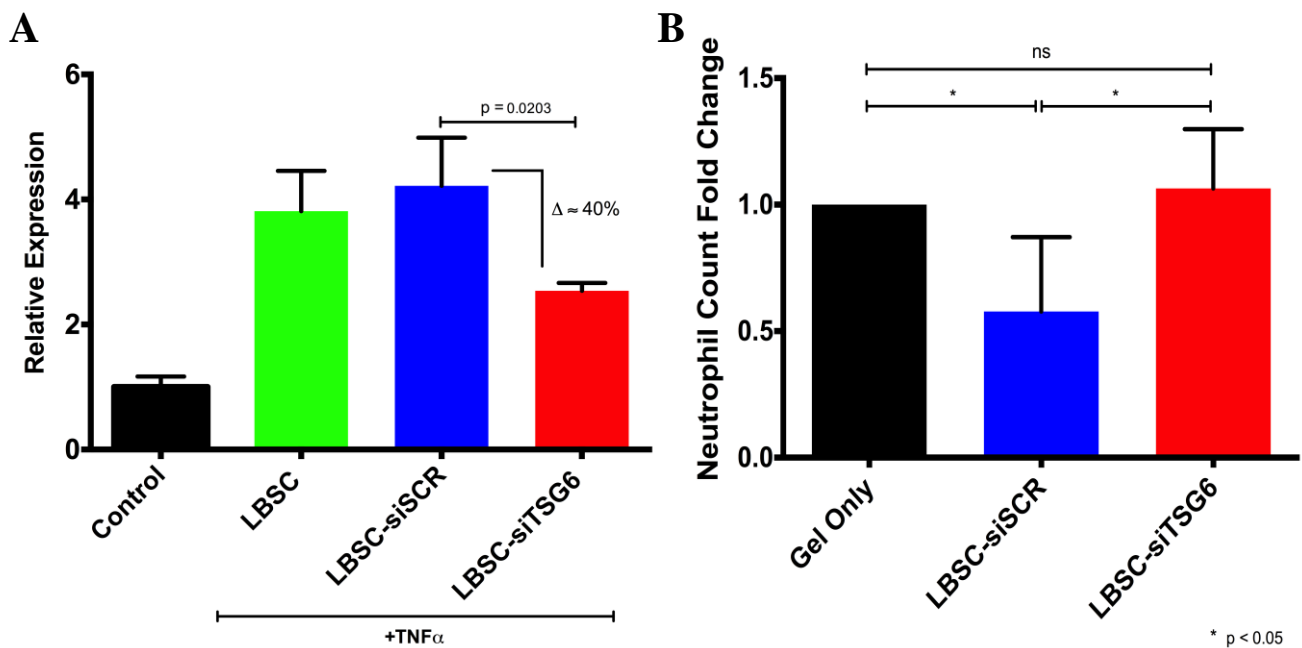


**Figure 27 *Tsg-6* Expression by LBSC Reduces Neutrophil Infiltration to Corneal Wounds**

- A) *TSG-6* expression is significantly reduced in LBSC treated with siRNA to *TSG-6* (siTSG6) when compared to LBSC treated with scrambled siRNA (siSCR).
- B) *TSG-6* expression by LBSC (siSCR) reduces neutrophil infiltration to the cornea 4 weeks after wounding. Statistical analysis using ANOVA with Tukey's correction for multiple comparisons.

#### **4.3.4 LBSC Reduce Corneal Light Scatter After Wounding via TSG-6 Production.**

The clinical outcome of corneal scarring is vision impairing light scatter that results from the scar. When fibrotic matrix replaces the normal, functional matrix of the cornea, light is unable to focus properly onto the retina, resulting in vision impairment <sup>26</sup>. We assessed light scatter by optical coherence tomography (OCT) as in previous studies <sup>107,158</sup>. We found that, in corneas treated with fibrin gel alone or siRNA to *Tsg-6*, light scatter as measured by pixel intensity was significantly greater than the unwounded mouse; corneas treated with scrambled siRNA did not show significantly greater light scatter when compared to the unwounded control (Figure 28).

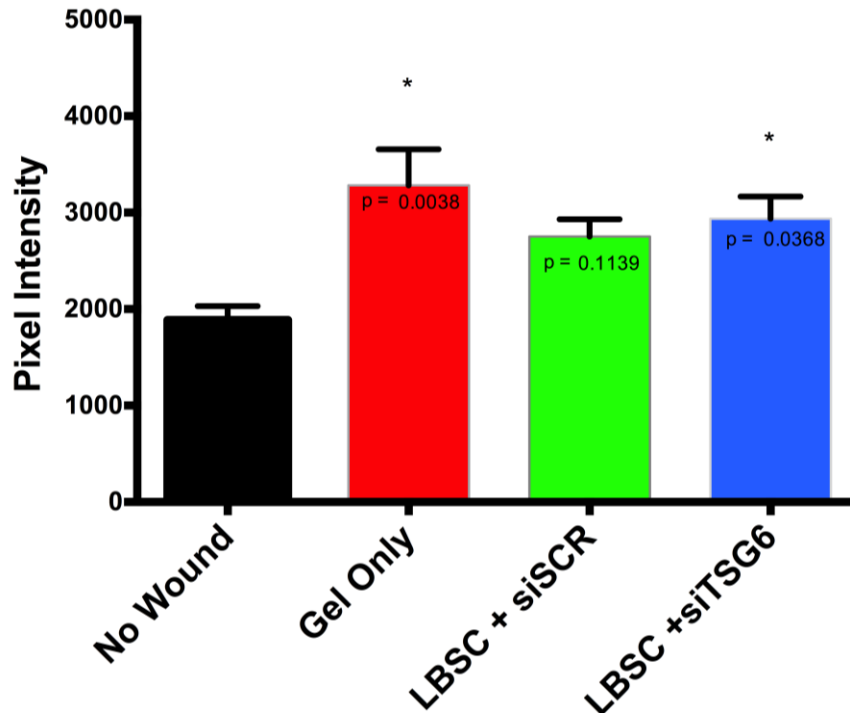


**Figure 28 *Tsg-6* Knockdown in LBSC Results in Significantly Greater Light Scatter as Measured by OCT Imaging Compared to Unwounded Animals**

Compared to the unwounded eye, only gel-treated and LBSC+siTSG6 treated corneas show significantly increased light scatter 4 weeks after wounding. Statistical Analysis was performed using ANOVA with Dunnett's post-test.

#### **4.3.5 Induction of Neutropenia at the Time of Wounding Prevents Light Scatter 4 Weeks After Wounding.**

Because our knockdown of *Tsg-6* was relatively inefficient (~40%, Figure 27A) and the dose-response for TSG-6 on *in vivo* neutrophil infiltration is unknown, we used a mouse model of neutropenia to study the effect that complete abrogation of neutrophils would have on light scatter. We used the well-documented neutralizing antibody to Ly6G (clone 1A8) to induce acute neutropenia in mice that were wounded<sup>202-205</sup>. Flow analysis revealed that the antibody reduced the neutrophil population (GR-1<sup>+</sup>CD11b<sup>+</sup>) in the cornea 24 hours after wounding from 11.3% to roughly 0.25% of the total cell population (Figure 29A). Interestingly, light scatter analysis revealed a significant increase in the gel only group when compared to the unwounded mouse

while the antibody treated mouse showed only slightly greater light scatter (but not significantly) when compared to the unwounded mouse (Figure 29B). These data support the hypothesis that neutrophil involvement in corneal wounds is indeed important to the clinical outcome associated with corneal scarring.

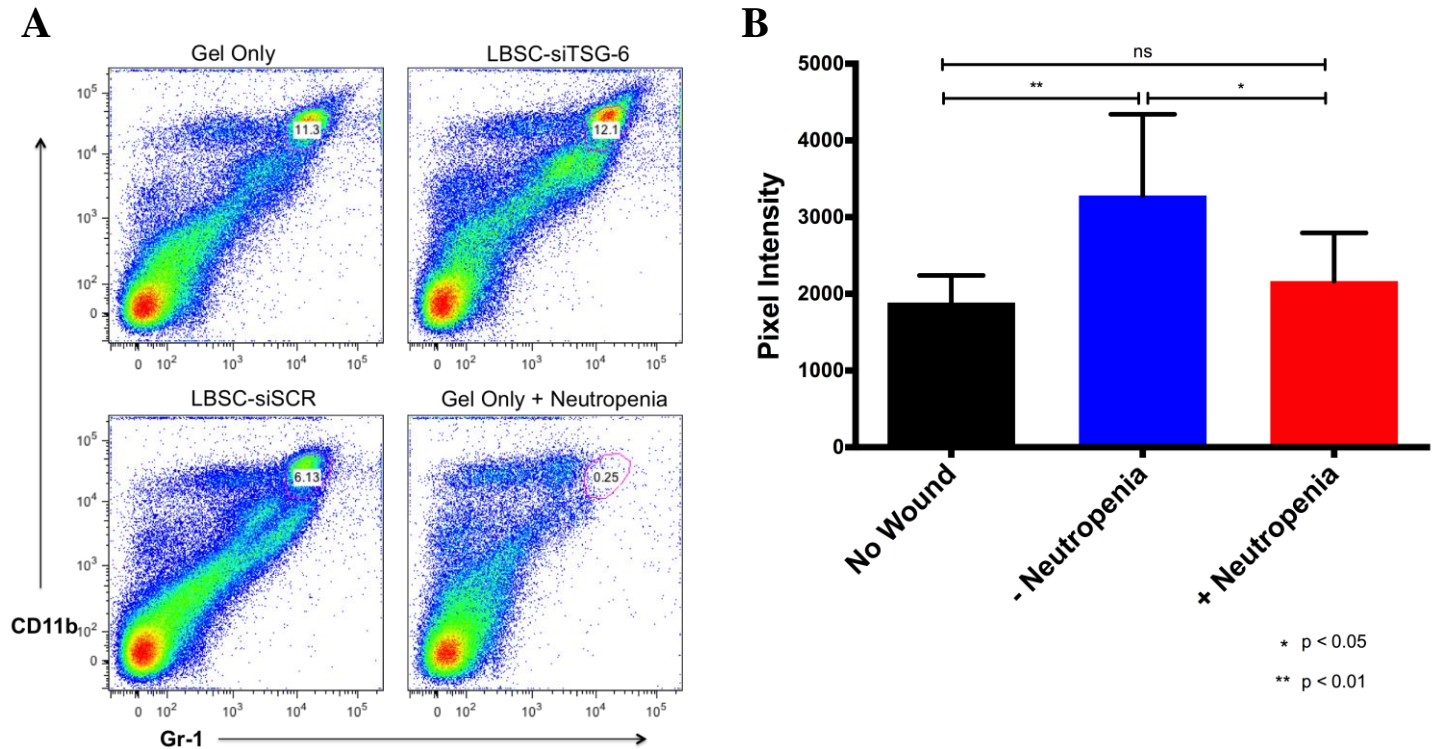


**Figure 29 Neutrophil Depletion Prevents Light Scatter After Corneal Wounding**

- (A) Flow Cytometry demonstrating neutrophil depletion in the cornea 24 hours after wounding and treatment with a neutropenia inducing antibody (as described in the Methods section). Antibody clones used for treatment and flow cytometry were different.
- (B) OCT analysis 4 weeks after wounding and neutropenic-antibody treatment shows that early induction of temporary neutropenia prevents the development of corneal light scatter. Statistical analysis: ANOVA with Dunnett's post-test.

## 4.4 DISCUSSION

Corneal wounds that result in scarring has caused life-changing vision impairment and even blindness in millions of individuals around the world. Due to the lack of available donor tissue and complications that arise from transplant therapy, new alternatives are being developed to restore vision or prevent scarring in those who suffer corneal blindness. Stem cell therapy offers enormous potential in achieving this goal, but the mechanism by which they act is still being investigated.

The present study investigates the mechanism of limbal biopsy-derived corneal stromal stem cells as it relates to the expression of TSG-6, a known mediator of neutrophil migration. As inflammation at the site of injury often leads to fibrosis, it stands to reason that a dampening of the acute response might prevent the fibrotic response. This study demonstrates for the first time the LBSC express *Tsg-6* upon TNF $\alpha$  stimulation as well as during differentiation – suggesting a role for this protein in corneal physiology. That LBSC produce TSG-6 during differentiation suggests that as mature keratocytes they may express the protein if stimulated *in vivo*, a study that will be carried out in the future. Additionally, LBSC were shown to produce TSG-6 at the site of wounding in a mouse model of corneal fibrosis. That the protein is present at the site of injury when LBSC are present suggests that neutrophil infiltration into the stroma may be inhibited in these animals, preventing a large, pro-fibrotic inflammatory response to injury.

*In vivo* studies in this study demonstrate the importance of TSG-6 production by LBSC at the site of injury in the corneal stroma. siRNA knockdown of *Tsg-6* of only 40% resulted in the significant reduction of neutrophils in the stroma 24 hours after wounding. Future studies with complete TSG-6 knockdown or even knockout will be completed to assess whether or not there is a dose response with varying levels of expression. When light scatter was analyzed among the treatment groups in this study, it was demonstrated that the gel only controls and wounds treated with LBSC + siTSG6 showed significantly greater light scatter compared to the unwounded mouse. That the knockdown efficiency was ~40%, and that TSG-6 is known to prevent neutrophil chemotaxis, suggests that complete abrogation of the neutrophil response at the site of injury may prevent wound healing that results in stromal light scatter. To demonstrate this, the neutropenia-inducing antibody to Ly6G was administered to the mouse at the time of wounding, light scatter was nearly identical to that of the unwounded animal.

Interestingly, and in contrast with our previous study examining LBSC <sup>107</sup>, the light scatter in mouse corneas treated with scrambled siRNA (i.e. LBSC with normal *Tsg-6* expression) was elevated (though not significant when compared to the unwounded eye). We believe this is due to the well-documented heterogeneity between donors in isolated stem cell populations. This supports the idea that not all donors are equal and stem cells from different donors must be characterized – whether it be by stem cell markers, differentiation ability, immunomodulatory properties, et cetera - to identify ideal donor candidates. While we are currently undertaking this process for LBSC, other groups have already started the process in bone marrow derived mesenchymal stem cells <sup>206</sup>.

Though this study demonstrates that TSG-6 and neutrophils are playing an important role in the outcome of corneal wound healing, future studies will examine other inflammatory cells,

notably macrophages, for the interaction they may have with stem cells during the wound healing process. Stem cells clearly show promise as an alternative treatment to corneal transplant for the treatment of corneal scarring. Future studies that further elucidate the mechanism by which they function *in vivo* are needed to further demonstrate their efficacy and justify clinical trials for this alternative therapy that may restore vision to millions of people around the world.

#### **4.5 ACKNOWLEDGEMENTS**

We thank Moira Geary for her assistance with animal work, Nancy Zurowski for her assistance with flow cytometry, and Dr. Kristine-Ann Buela for her advice on immunological assays.

This chapter is in preparation for submission.

Neutrophil Reduction After Wounding Prevents Corneal Light Scatter: A Potential Therapeutic Mechanism for Corneal Stromal Stem Cells in Wound Healing.  
Hertsenberg AJ, Funderburgh JL

## 5.0 SUMMARY AND FUTURE DIRECTIONS

The goal of the work presented here is to expand the treatment options available to the millions of people worldwide suffering from corneal blindness. While corneal transplant is a generally successful procedure used to treat this condition, immunological rejection and donor tissue shortages necessitate therapeutic alternatives. I have presented data in the preceding chapters that lay the groundwork for therapies that may circumvent these complications of corneal transplant.

The data presented here expands what is known about human embryonic stem cells and their differentiation capabilities. Until now, it has not been shown that embryonic stem cells are capable of differentiating to keratocytes and these results suggest that there may be a cell source for corneal tissue engineering and perhaps cell therapy. The demonstration that corneal stromal stem cells can be isolated as a biopsy and used to prevent fibrosis has expanded our current knowledge of this stem cell population and provided a clinical method for the use of the cells in patients in the near future. Finally, studies examining the role of TSG-6 at the site of injury upon stem cell treatment and the effect of neutrophil ablation during wound healing expand our knowledge of immunomodulation and the role of the immune system after wounding in the corneal stroma.

Human Embryonic Stem Cells (hESC) represent a virtually unlimited source of stem cells with the capability to differentiate into corneal keratocytes. In Chapter 2 I describe a two-step

method for the differentiation of hESC to keratocytes via a neural crest stem cell intermediate. As hESC can be expanded for 100+ passages while retaining stem cell phenotype, they have the potential to bridge the gap between supply and demand that exists between patients in need of transplant and available donor grafts. Though hESC are not an autologous source of tissue and therefore may result in immunological rejection, numerous studies have suggested their immunomodulatory properties may prevent such an outcome<sup>207-209</sup>.

Future studies in the lab are aimed at using these cells in mouse models of corneal wounding, much like what was presented in Chapter 3. Ideally it will be shown that they act similarly or better than the autologous stem cells that were used in that study, supporting the hypothesis that these cells are a readily expandable source of cells for therapy.

Limbal Biopsy-Derived Corneal Stromal Stem Cells (LBSC) are a potential source of autologous progenitor cells to corneal keratocytes that actually prevent scar formation in mouse corneal wounds, as shown in Chapter 3. In this study we demonstrate that LBSC effectively prevent fibrotic wound healing in a mouse model of corneal fibrosis. Though this is a preventative measure, as opposed to a treatment for existing scars, the data collected from this study will undoubtedly lead to better understanding of these cells which may result in the development of therapies via tissue engineering or cell-based tissue replacement. Currently, Drs. Virender Sangwan and Sayan Basu of the L V Prasad Eye Institute (Hyderabad, India) are conducting a Phase I clinical trial based on this study to assess the safety of these cells as an autologous therapy for the treatment of existing scars.

Finally, in Chapter 4, I present data that supports the hypothesis that immunomodulation by way of blocking neutrophil infiltration to the wound bed may prevent fibrosis after corneal wounding. We investigated the protein TNF $\alpha$ -stimulated-gene-6 (TSG-6) for it's

immunomodulatory properties – specifically it’s ability to prevent neutrophil migration to the site of wounding <sup>195</sup>. Numerous other authors studying mesenchymal stem cells in wound healing have also begun investigating this protein and its immunomodulatory and anti-fibrotic action <sup>191,210-212</sup>. We found that LBSC inhibit neutrophil infiltration to the wound site via in the cornea via TSG-6 expression after wounding and that a reduction in neutrophil infiltration to the site of injury prevents light scatter four weeks after wounding. As such, TSG-6 may be a mechanism by which LBSC prevent fibrotic wound healing after injury and, therefore, may be a novel therapeutic for the treatment of inflammation after injury.

Interestingly, and an important aside to mention, in this study we discovered that there exist differences between donors in their ability to promote regeneration of corneal tissue after wounding. Multiple experiments using LBSC derived from different donors showed enormous variability in the ability of these cells to prevent light scatter after wounding. In Figure 28, LBSC (treated with scrambled siRNA) fail to prevent light scatter to the same degree that was seen in Figure 23 – the only difference between the studies being the patients from whom these donor cells were derived. This discovery has resulted in a study wherein different donors are being screened via qPCR and neutrophil migration assays to select the donors most likely to suppress neutrophil migration and, presumably, reduce light scatter after wounding. While this finding was a setback in our study, this knowledge is beneficial to any lab studying cells derived from a variety of donors – one donor is not equal to the next. With enough samples, we expect we may eventually find a combination of factors (e.g. age, gender, body mass index, underlying illnesses, antigen exposure, ad infinitum...) that, together, identify “good” from “bad” donors.

Stem cell biology is an important field of biomedical research from which numerous therapies may one day be derived – expanding the ever-growing field of “personalized”

medicine. The data presented in this dissertation add to an expanding body of work in ophthalmology, wound healing, and regenerative medicine that aim to provide therapeutic alternatives for the treatment of corneal blindness and vision impairment. Progress toward this goal will improve the quality of life of millions of people around the globe while what is learned during this endeavor informs and improves research in regenerative medicine across all medical disciplines.

## APPENDIX A

<b>Acronym</b>	<b>Definition</b>
<b>ABCB5</b>	<b>ATP-Binding Casette Sub-Family B Member 5</b>
<b>ABCG2</b>	<b>ATP-Binding Casette Sub-Family G Member 2</b>
<b>ALDH3A1</b>	<b>aldehyde dehydrogenase 3 family, member A1</b>
<b>AQP1</b>	<b>Aquaporin 1</b>
<b>ATP</b>	<b>Adenosine Triphosphate</b>
<b>B3GNT7</b>	<b>Beta-1,3-N-Acetylglucosaminyltransferase 7</b>
<b>BM</b>	<b>Bowman's Membrane</b>
<b>BMI1</b>	<b>Polycomb group RING finger protein 4 (a.k.a. PCGF4)</b>
<b>C-EBP-Delta</b>	<b>CCAAT/enhancer-binding protein delta</b>
<b>CD271</b>	<b>Cluster of Differentiation 271 (a.k.a. NGFR, p75NTR)</b>
<b>cDNA</b>	<b>Complimentary DNA</b>
<b>CHST6</b>	<b>Carbohydrate sulfotransferase 6</b>
<b>CK</b>	<b>Cytokeratin</b>
<b>cKit</b>	<b>tyrosine-protein kinase Kit</b>
<b>DiO</b>	<b>3,3'-Diocetadecyloxacarbocyanine</b>
<b>DM</b>	<b>Descemet's Membrane</b>
<b>DNA</b>	<b>Deoxyribonucleic Acid</b>
<b>ECM</b>	<b>Extracellular Matrix</b>

<b>FACS</b>	<b>Fluorescence-Activated Cell Sorting</b>
<b>FBS</b>	<b>Fetal Bovine Serum</b>
<b>FOXC2</b>	<b>Forkhead box protein C2</b>
<b>GAPDH</b>	<b>Glyceraldehyde 3-phosphate dehydrogenase</b>
<b>GR-1</b>	<b>Granulocyte Differentiation Antigen 1</b>
<b>HABP</b>	<b>Hyaluronic Acid Binding Protein</b>
<b>hCSSC</b>	<b>Human Corneal Stromal Stem Cell</b>
<b>hESC</b>	<b>Human Embryonic Stem Cell</b>
<b>HS</b>	<b>Pooled Human Serum</b>
<b>KDM</b>	<b>Keratocyte Differentiation Medium</b>
<b>KERA</b>	<b>Keratoan</b>
<b>KS</b>	<b>Keratan Sulfate</b>
<b>KSPG</b>	<b>Keratan Sulfate Proteoglycan</b>
<b>LBSC</b>	<b>Limbal Biopsy-Derived Corneal Stromal Stem Cell</b>
<b>LESC</b>	<b>Limbal Epithelial Stem Cell</b>
<b>LGR5</b>	<b>Leucine-rich repeat-containing G-protein coupled receptor 5</b>
<b>LSCD</b>	<b>Limbal Epithelial Stem Cell Deficiency</b>
<b>Ly6G</b>	<b>lymphocyte antigen 6 complex, locus G</b>
<b>MACS</b>	<b>Magnetic Activated Cell Sorting</b>
<b>mRNA</b>	<b>Messenger Ribonucleic Acid</b>
<b>MSX1</b>	<b>Msh homeobox 1</b>
<b>NC</b>	<b>Neural Crest</b>
<b>NGFR</b>	<b>Nerve Growth Factor Receptor (a.k.a. p75NTR, CD271)</b>
<b>NTRK3</b>	<b>Neurotrophic tyrosine kinase, receptor, type 3</b>
<b>OCT</b>	<b>Optical Coherence Tomography</b>

<b>Pax6</b>	<b>Paired box protein Pax-6</b>
<b>PTGDS</b>	<b>prostaglandin D2 synthase</b>
<b>qPCR</b>	<b>Real-Time Quantitative Reverse Transcription Polymerase Chain Reaction</b>
<b>SGM</b>	<b>Stem Cell Growth Medium</b>
<b>siRNA</b>	<b>Small Interfering RNA</b>
<b>Six2</b>	<b>SIX homeobox 2</b>
<b>SNAI1</b>	<b>Snail Family Zinc Finger 1</b>
<b>SOX9</b>	<b>Transcription factor SOX-9</b>
<b>SPARC</b>	<b>Secreted Protein Acidic and Rich in Cysteine (a.k.a Osteonectin)</b>
<b>βGal</b>	<b>Beta-Galactosidase</b>
<b>TBP1</b>	<b>TATA-box-binding protein 1</b>
<b>TEM</b>	<b>Transmission Electron Microscopy</b>
<b>TSG-6</b>	<b>Tumor necrosis factor stimulated gene 6 protein</b>

## BIBLIOGRAPHY

1. Ambekar R, Toussaint KC, Jr., Wagoner Johnson A. The effect of keratoconus on the structural, mechanical, and optical properties of the cornea. *Journal of the mechanical behavior of biomedical materials*. Apr 2011;4(3):223-236.
2. Lewis PN, Pinali C, Young RD, Meek KM, Quantock AJ, Knupp C. Structural interactions between collagen and proteoglycans are elucidated by three-dimensional electron tomography of bovine cornea. *Structure*. Feb 10 2010;18(2):239-245.
3. Pascolini D, Mariotti SP, Pokharel GP, et al. 2002 global update of available data on visual impairment: a compilation of population-based prevalence studies. *Ophthalmic epidemiology*. Apr 2004;11(2):67-115.
4. Whitcher JP, Srinivasan M, Upadhyay MP. Corneal blindness: a global perspective. *Bulletin of the World Health Organization*. 2001;79(3):214-221.
5. Davies SB, Chui J, Madigan MC, Provis JM, Wakefield D, Di Girolamo N. Stem cell activity in the developing human cornea. *Stem cells*. Nov 2009;27(11):2781-2792.
6. Chow RL, Lang RA. Early eye development in vertebrates. *Annual review of cell and developmental biology*. 2001;17:255-296.
7. Lwigale PY, Bronner-Fraser M. Semaphorin3A/neuropilin-1 signaling acts as a molecular switch regulating neural crest migration during cornea development. *Developmental biology*. Dec 15 2009;336(2):257-265.
8. Hay ED. Development of the vertebrate cornea. *International review of cytology*. 1980;63:263-322.
9. Hay ED, Revel JP. Fine structure of the developing avian cornea. *Monographs in developmental biology*. 1969;1:1-144.
10. Jester JV, Lee YG, Huang J, et al. Postnatal corneal transparency, keratocyte cell cycle exit and expression of ALDH1A1. *Investigative ophthalmology & visual science*. Sep 2007;48(9):4061-4069.
11. Zinn KM, Mockel-Pohl S. Fine structure of the developing cornea. *International ophthalmology clinics*. Spring 1975;15(1):19-37.
12. Buck RC. Cell migration in repair of mouse corneal epithelium. *Investigative ophthalmology & visual science*. Aug 1979;18(8):767-784.
13. Collinson JM, Morris L, Reid AI, et al. Clonal analysis of patterns of growth, stem cell activity, and cell movement during the development and maintenance of the murine corneal epithelium. *Developmental dynamics : an official publication of the American Association of Anatomists*. Aug 2002;224(4):432-440.
14. Davanger M, Evensen A. Role of the pericorneal papillary structure in renewal of corneal epithelium. *Nature*. Feb 19 1971;229(5286):560-561.

15. Nagasaki T, Zhao J. Centripetal movement of corneal epithelial cells in the normal adult mouse. *Investigative ophthalmology & visual science*. Feb 2003;44(2):558-566.
16. Dohlman CH. The function of the corneal epithelium in health and disease. The Jonas S. Friedenwald Memorial Lecture. *Investigative ophthalmology*. Jun 1971;10(6):383-407.
17. Perez-Merino P, Martinez-Garcia MC, Mar-Sardana S, et al. Corneal light transmission and roughness after refractive surgery. *Optometry and vision science : official publication of the American Academy of Optometry*. Jul 2010;87(7):E469-474.
18. DelMonte DW, Kim T. Anatomy and physiology of the cornea. *Journal of cataract and refractive surgery*. Mar 2011;37(3):588-598.
19. Wilson SE, Hong JW. Bowman's layer structure and function: critical or dispensable to corneal function? A hypothesis. *Cornea*. Jul 2000;19(4):417-420.
20. Lagali N, Germundsson J, Fagerholm P. The role of Bowman's layer in corneal regeneration after phototherapeutic keratectomy: a prospective study using in vivo confocal microscopy. *Investigative ophthalmology & visual science*. Sep 2009;50(9):4192-4198.
21. Cameron JD. *Cornea*. 2 ed. Philadelphia, PA: Elsevier Mosby; 2005.
22. Knupp C, Pinali C, Lewis PN, et al. The architecture of the cornea and structural basis of its transparency. *Advances in protein chemistry and structural biology*. 2009;78:25-49.
23. Nakayasu K, Tanaka M, Konomi H, Hayashi T. Distribution of types I, II, III, IV and V collagen in normal and keratoconus corneas. *Ophthalmic research*. 1986;18(1):1-10.
24. Farrell RA, McCally RL, Tatham PE. Wave-length dependencies of light scattering in normal and cold swollen rabbit corneas and their structural implications. *The Journal of physiology*. Sep 1973;233(3):589-612.
25. Maurice DM. The structure and transparency of the cornea. *The Journal of physiology*. Apr 30 1957;136(2):263-286.
26. Hassell JR, Birk DE. The molecular basis of corneal transparency. *Experimental eye research*. Sep 2010;91(3):326-335.
27. Chakravarti S, Magnuson T, Lass JH, Jepsen KJ, LaMantia C, Carroll H. Lumican regulates collagen fibril assembly: skin fragility and corneal opacity in the absence of lumican. *The Journal of cell biology*. Jun 1 1998;141(5):1277-1286.
28. Chen S, Young MF, Chakravarti S, Birk DE. Interclass small leucine-rich repeat proteoglycan interactions regulate collagen fibrillogenesis and corneal stromal assembly. *Matrix biology : journal of the International Society for Matrix Biology*. Apr 2014;35:103-111.
29. Rada JA, Cornuet PK, Hassell JR. Regulation of corneal collagen fibrillogenesis in vitro by corneal proteoglycan (lumican and decorin) core proteins. *Experimental eye research*. Jun 1993;56(6):635-648.
30. Funderburgh JL, Funderburgh ML, Mann MM, Corpuz L, Roth MR. Proteoglycan expression during transforming growth factor beta -induced keratocyte-myofibroblast transdifferentiation. *The Journal of biological chemistry*. 2001;276(47):44173-44178.
31. Funderburgh JL, Mann MM, Funderburgh ML. Keratocyte phenotype mediates proteoglycan structure: a role for fibroblasts in corneal fibrosis. *The Journal of biological chemistry*. 2003;278(46):45629-45637.
32. Fini ME. Keratocyte and fibroblast phenotypes in the repairing cornea. *Progress in retinal and eye research*. Jul 1999;18(4):529-551.

33. Cintron C, Schneider H, Kublin C. Corneal scar formation. *Experimental eye research*. Nov 11 1973;17(3):251-259.
34. Fini ME, Girard MT, Matsubara M. Collagenolytic/gelatinolytic enzymes in corneal wound healing. *Acta ophthalmologica. Supplement*. 1992(202):26-33.
35. Ljubimov AV, Alba SA, Burgeson RE, et al. Extracellular matrix changes in human corneas after radial keratotomy. *Experimental eye research*. Sep 1998;67(3):265-272.
36. Cionni RJ, Katakami C, Lavrich JB, Kao WW. Collagen metabolism following corneal laceration in rabbits. *Current eye research*. Aug 1986;5(8):549-558.
37. Cintron C, Hassinger LC, Kublin CL, Cannon DJ. Biochemical and ultrastructural changes in collagen during corneal wound healing. *Journal of ultrastructure research*. Oct 1978;65(1):13-22.
38. Cintron C, Kublin CL. Regeneration of corneal tissue. *Developmental biology*. Dec 1977;61(2):346-357.
39. Benya PD. EC collagen: biosynthesis by corneal endothelial cells and separation from type IV without pepsin treatment or denaturation. *Renal physiology*. 1980;3(1-6):30-35.
40. Fitch JM, Birk DE, Linsenmayer C, Linsenmayer TF. The spatial organization of Descemet's membrane-associated type IV collagen in the avian cornea. *The Journal of cell biology*. Apr 1990;110(4):1457-1468.
41. Schlötzer-Schrehardt U, Kruse FE. Identification and characterization of limbal stem cells. *Experimental eye research*. 2005;81(3):247-264.
42. Cotsarelis G, Cheng SZ, Dong G, Sun TT, Lavker RM. Existence of slow-cycling limbal epithelial basal cells that can be preferentially stimulated to proliferate: implications on epithelial stem cells. *Cell*. 1989;57(2):201-209.
43. Schermer A, Galvin S, Sun TT. Differentiation-related expression of a major 64K corneal keratin in vivo and in culture suggests limbal location of corneal epithelial stem cells. *The Journal of cell biology*. Jul 1986;103(1):49-62.
44. Rodrigues M, Ben-Zvi A, Krachmer J, Schermer A, Sun TT. Suprabasal expression of a 64-kilodalton keratin (no. 3) in developing human corneal epithelium. *Differentiation; research in biological diversity*. 1987;34(1):60-67.
45. Vassar R, Rosenberg M, Ross S, Tyner A, Fuchs E. Tissue-specific and differentiation-specific expression of a human K14 keratin gene in transgenic mice. *Proceedings of the National Academy of Sciences of the United States of America*. Mar 1989;86(5):1563-1567.
46. Fuchs E, Green H. Changes in keratin gene expression during terminal differentiation of the keratinocyte. *Cell*. Apr 1980;19(4):1033-1042.
47. Coulombe PA, Kopan R, Fuchs E. Expression of keratin K14 in the epidermis and hair follicle: insights into complex programs of differentiation. *The Journal of cell biology*. Nov 1989;109(5):2295-2312.
48. Bose A, Teh MT, Mackenzie IC, Waseem A. Keratin k15 as a biomarker of epidermal stem cells. *International journal of molecular sciences*. 2013;14(10):19385-19398.
49. Lavker RM, Tseng SC, Sun TT. Corneal epithelial stem cells at the limbus: looking at some old problems from a new angle. *Experimental eye research*. Mar 2004;78(3):433-446.
50. Lehrer MS, Sun TT, Lavker RM. Strategies of epithelial repair: modulation of stem cell and transit amplifying cell proliferation. *Journal of cell science*. Oct 1998;111 ( Pt 19):2867-2875.

51. Chen Z, de Paiva CS, Luo L, Kretzer FL, Pflugfelder SC, Li DQ. Characterization of putative stem cell phenotype in human limbal epithelia. *Stem cells*. 2004;22(3):355-366.
52. de Paiva CS, Chen Z, Corrales RM, Pflugfelder SC, Li DQ. ABCG2 transporter identifies a population of clonogenic human limbal epithelial cells. *Stem cells*. 2005;23(1):63-73.
53. Ksander BR, Kolovou PE, Wilson BJ, et al. ABCB5 is a limbal stem cell gene required for corneal development and repair. *Nature*. Jul 17 2014;511(7509):353-357.
54. Barbaro V, Testa A, Di Iorio E, Mavilio F, Pellegrini G, De Luca M. C/EBPdelta regulates cell cycle and self-renewal of human limbal stem cells. *The Journal of cell biology*. Jun 18 2007;177(6):1037-1049.
55. Thomas PB, Liu YH, Zhuang FF, et al. Identification of Notch-1 expression in the limbal basal epithelium. *Molecular vision*. 2007;13:337-344.
56. Barker N. Adult intestinal stem cells: critical drivers of epithelial homeostasis and regeneration. *Nature reviews. Molecular cell biology*. Jan 2014;15(1):19-33.
57. Spradling A, Drummond-Barbosa D, Kai T. Stem cells find their niche. *Nature*. Nov 1 2001;414(6859):98-104.
58. Tadeu AM, Horsley V. Epithelial stem cells in adult skin. *Current topics in developmental biology*. 2014;107:109-131.
59. Chen JJ, Tseng SC. Corneal epithelial wound healing in partial limbal deficiency. *Investigative ophthalmology & visual science*. Jul 1990;31(7):1301-1314.
60. Huang AJ, Tseng SC. Corneal epithelial wound healing in the absence of limbal epithelium. *Investigative ophthalmology & visual science*. Jan 1991;32(1):96-105.
61. Kruse FE, Chen JJ, Tsai RJ, Tseng SC. Conjunctival transdifferentiation is due to the incomplete removal of limbal basal epithelium. *Investigative ophthalmology & visual science*. Sep 1990;31(9):1903-1913.
62. Ahmad S. Concise review: limbal stem cell deficiency, dysfunction, and distress. *Stem Cells Transl Med*. 2012;1(2):110-115.
63. Sangwan VS. Limbal stem cells in health and disease. *Biosci Rep*. 2001;21(4):385-405.
64. Goldstein RS, Pomp O, Brokhman I, Ziegler L. Generation of neural crest cells and peripheral sensory neurons from human embryonic stem cells. *Methods in molecular biology*. 2010;584:283-300.
65. Zhang W, Zhao J, Chen L, Urbanowicz MM, Nagasaki T. Abnormal epithelial homeostasis in the cornea of mice with a destrin deletion. *Molecular vision*. 2008;14:1929-1939.
66. Dua HS, Miri A, Alomar T, Yeung AM, Said DG. The role of limbal stem cells in corneal epithelial maintenance: testing the dogma. *Ophthalmology*. 2009;116(5):856-863.
67. Majo F, Rochat A, Nicolas M, Jaoude GA, Barrandon Y. Oligopotent stem cells are distributed throughout the mammalian ocular surface. *Nature*. Nov 13 2008;456(7219):250-254.
68. Chang C-YA, McGhee JJ, Green CR, Sherwin T. Comparison of stem cell properties in cell populations isolated from human central and limbal corneal epithelium. *Cornea*. 2011;30(10):1155-1162.
69. Di Girolamo N, Bobba S, Raviraj V, et al. Tracing the fate of limbal epithelial progenitor cells in the murine cornea. *Stem cells*. 2015;33(1):157-169.
70. Dua HS, Gomes JA, Singh A. Corneal epithelial wound healing. *The British journal of ophthalmology*. May 1994;78(5):401-408.

71. Reinhard T, Spelsberg H, Henke L, et al. Long-term results of allogeneic penetrating limbo-keratoplasty in total limbal stem cell deficiency. *Ophthalmology*. 2004;111(4):775-782.
72. Miri A, Al-Deiri B, Dua HS. Long-term outcomes of autolimbal and allolimbal transplants. *Ophthalmology*. 2010;117(6):1207-1213.
73. Eberwein P, Böhringer D, Schwartzkopff J, Birnbaum F, Reinhard T. Allogenic limbo-keratoplasty with conjunctivoplasty, mitomycin C, and amniotic membrane for bilateral limbal stem cell deficiency. *Ophthalmology*. 2012;119(5):930-937.
74. Pellegrini G, Traverso CE, Franzi AT, Zingirian M, Cancedda R, De Luca M. Long-term restoration of damaged corneal surfaces with autologous cultivated corneal epithelium. *Lancet*. Apr 5 1997;349(9057):990-993.
75. Tsai RJ, Tseng SC. Human allograft limbal transplantation for corneal surface reconstruction. *Cornea*. Sep 1994;13(5):389-400.
76. Koizumi N, Inatomi T, Suzuki T, Sotozono C, Kinoshita S. Cultivated corneal epithelial stem cell transplantation in ocular surface disorders. *Ophthalmology*. Sep 2001;108(9):1569-1574.
77. Sangwan VS, Jain R, Basu S, et al. Transforming ocular surface stem cell research into successful clinical practice. *Indian J Ophthalmol*. 2014;62(1):29-40.
78. Rama P, Matuska S, Paganoni G, Spinelli A, De Luca M, Pellegrini G. Limbal stem-cell therapy and long-term corneal regeneration. *The New England journal of medicine*. Jul 8 2010;363(2):147-155.
79. Shortt AJ, Bunce C, Levis HJ, et al. Three-year outcomes of cultured limbal epithelial allografts in aniridia and Stevens-Johnson syndrome evaluated using the Clinical Outcome Assessment in Surgical Trials assessment tool. *Stem Cells Transl Med*. 2014;3(2):265-275.
80. Basu S, Fernandez MM, Das S, Gaddipati S, Vemuganti GK, Sangwan VS. Clinical outcomes of xeno-free allogeneic cultivated limbal epithelial transplantation for bilateral limbal stem cell deficiency. *The British journal of ophthalmology*. 2012;96(12):1504-1509.
81. Oliva MS, Schottman T, Gulati M. Turning the tide of corneal blindness. *Indian J Ophthalmol*. 2012;60(5):423-427.
82. Shortt AJ, Tuft SJ, Daniels JT. Ex vivo cultured limbal epithelial transplantation. A clinical perspective. *The ocular surface*. Apr 2010;8(2):80-90.
83. Ontario HQ. Limbal stem cell transplantation: an evidence-based analysis. *Ont Health Technol Assess Ser*. 2008;8(7):1-58.
84. Tan DTH, Dart JKG, Holland EJ, Kinoshita S. Corneal transplantation. *Lancet*. 2012;379(9827):1749-1761.
85. Lagali N, Fagerholm P, Griffith M. Biosynthetic corneas: prospects for supplementing the human donor cornea supply. *Expert review of medical devices*. Mar 2011;8(2):127-130.
86. Coster DJ, Williams KA. The impact of corneal allograft rejection on the long-term outcome of corneal transplantation. *American journal of ophthalmology*. Dec 2005;140(6):1112-1122.
87. Funderburgh ML, Du Y, Mann MM, SundarRaj N, Funderburgh JL. PAX6 expression identifies progenitor cells for corneal keratocytes. *FASEB journal : official publication of*

- the Federation of American Societies for Experimental Biology*. Aug 2005;19(10):1371-1373.
88. Golebiewska A, Brons NH, Bjerkvig R, Niclou SP. Critical appraisal of the side population assay in stem cell and cancer stem cell research. *Cell stem cell*. Feb 4 2011;8(2):136-147.
  89. Du Y, Funderburgh ML, Mann MM, SundarRaj N, Funderburgh JL. Multipotent stem cells in human corneal stroma. *Stem cells*. Oct 2005;23(9):1266-1275.
  90. Yoshida S, Shimmura S, Nagoshi N, et al. Isolation of multipotent neural crest-derived stem cells from the adult mouse cornea. *Stem cells*. 2006;24(12):2714-2722.
  91. Amano S, Yamagami S, Mimura T, Uchida S, Yokoo S. Corneal stromal and endothelial cell precursors. *Cornea*. Dec 2006;25(10 Suppl 1):S73-77.
  92. Polisetty N, Fatima A, Madhira SL, Sangwan VS, Vemuganti GK. Mesenchymal cells from limbal stroma of human eye. *Molecular vision*. 2008;14:431-442.
  93. Lu J-M, Zhou Z-Y, Zhang X-R, Li X-L, Wang H-F, Song X-J. A preliminary study of mesenchymal stem cell-like cells derived from murine corneal stroma. *Graefe's archive for clinical and experimental ophthalmology = Albrecht von Graefes Archiv fur klinische und experimentelle Ophthalmologie*. 2010;248(9):1279-1285.
  94. Xie H-T, Chen S-Y, Li G-G, Tseng SCG. Isolation and expansion of human limbal stromal niche cells. *Investigative ophthalmology & visual science*. 2012;53(1):279-286.
  95. Branch MJ, Hashmani K, Dhillon P, Jones DRE, Dua HS, Hopkinson A. Mesenchymal stem cells in the human corneal limbal stroma. *Investigative ophthalmology & visual science*. 2012;53(9):5109-5116.
  96. Li G-G, Zhu Y-T, Xie H-T, Chen S-Y, Tseng SCG. Mesenchymal stem cells derived from human limbal niche cells. *Investigative ophthalmology & visual science*. 2012;53(9):5686-5697.
  97. Garfias Y, Nieves-Hernandez J, Garcia-Mejia M, Estrada-Reyes C, Jimenez-Martinez MC. Stem cells isolated from the human stromal limbus possess immunosuppressant properties. *Molecular vision*. 2012;18:2087-2095.
  98. Pinnamaneni N, Funderburgh JL. Concise review: Stem cells in the corneal stroma. *Stem cells*. Jun 2012;30(6):1059-1063.
  99. Chen S-Y, Hayashida Y, Chen M-Y, Xie HT, Tseng SCG. A new isolation method of human limbal progenitor cells by maintaining close association with their niche cells. *Tissue Eng Part C Methods*. 2011;17(5):537-548.
  100. Hayashi R, Yamato M, Sugiyama H, et al. N-Cadherin is expressed by putative stem/progenitor cells and melanocytes in the human limbal epithelial stem cell niche. *Stem cells*. 2007;25(2):289-296.
  101. Higa K, Kato N, Yoshida S, et al. Aquaporin 1-positive stromal niche-like cells directly interact with N-cadherin-positive clusters in the basal limbal epithelium. *Stem Cell Res*. Mar 2013;10(2):147-155.
  102. Massie I, Dziasko M, Kureshi A, et al. Advanced imaging and tissue engineering of the human limbal epithelial stem cell niche. *Methods in molecular biology*. 2015;1235:179-202.
  103. Dziasko MA, Armer HE, Levis HJ, Shortt AJ, Tuft S, Daniels JT. Localisation of epithelial cells capable of holoclone formation in vitro and direct interaction with stromal cells in the native human limbal crypt. *PLoS one*. 2014;9(4):e94283.

104. Higa K, Shimmura S, Miyashita H, et al. N-cadherin in the maintenance of human corneal limbal epithelial progenitor cells in vitro. *Investigative ophthalmology & visual science*. 2009;50(10):4640-4645.
105. Omoto M, Miyashita H, Shimmura S, et al. The use of human mesenchymal stem cell-derived feeder cells for the cultivation of transplantable epithelial sheets. *Investigative ophthalmology & visual science*. 2009;50(5):2109-2115.
106. Du Y, Carlson EC, Funderburgh ML, et al. Stem cell therapy restores transparency to defective murine corneas. *Stem cells*. Jul 2009;27(7):1635-1642.
107. Basu S, Hertszenberg AJ, Funderburgh ML, et al. Human limbal biopsy-derived stromal stem cells prevent corneal scarring. *Science translational medicine*. Dec 10 2014;6(266):266ra172.
108. Mishima S. Clinical investigations on the corneal endothelium. *Ophthalmology*. Jun 1982;89(6):525-530.
109. Yokoo S, Yamagami S, Yanagi Y, et al. Human corneal endothelial cell precursors isolated by sphere-forming assay. *Investigative ophthalmology & visual science*. May 2005;46(5):1626-1631.
110. Coles BL, Angenieux B, Inoue T, et al. Facile isolation and the characterization of human retinal stem cells. *Proceedings of the National Academy of Sciences of the United States of America*. Nov 2 2004;101(44):15772-15777.
111. Tropepe V, Coles BL, Chiasson BJ, et al. Retinal stem cells in the adult mammalian eye. *Science*. Mar 17 2000;287(5460):2032-2036.
112. Mimura T, Yamagami S, Yokoo S, Araie M, Amano S. Comparison of rabbit corneal endothelial cell precursors in the central and peripheral cornea. *Investigative ophthalmology & visual science*. Oct 2005;46(10):3645-3648.
113. Yamagami S, Yokoo S, Mimura T, Takato T, Araie M, Amano S. Distribution of precursors in human corneal stromal cells and endothelial cells. *Ophthalmology*. Mar 2007;114(3):433-439.
114. Hirata-Tominaga K, Nakamura T, Okumura N, et al. Corneal endothelial cell fate is maintained by LGR5 through the regulation of hedgehog and Wnt pathway. *Stem cells*. Jul 2013;31(7):1396-1407.
115. Hara S, Hayashi R, Soma T, et al. Identification and potential application of human corneal endothelial progenitor cells. *Stem cells and development*. Sep 15 2014;23(18):2190-2201.
116. Satake Y, Yamaguchi T, Hirayama M, et al. Ocular surface reconstruction by cultivated epithelial sheet transplantation. *Cornea*. Nov 2014;33 Suppl 11:S42-46.
117. Morishige N, Takagi Y, Chikama T, Takahara A, Nishida T. Three-dimensional analysis of collagen lamellae in the anterior stroma of the human cornea visualized by second harmonic generation imaging microscopy. *Investigative ophthalmology & visual science*. Feb 2011;52(2):911-915.
118. Vrana NE, Builles N, Justin V, et al. Development of a reconstructed cornea from collagen-chondroitin sulfate foams and human cell cultures. *Investigative ophthalmology & visual science*. Dec 2008;49(12):5325-5331.
119. Torbet J, Malbouyres M, Builles N, et al. Tissue engineering of the cornea: orthogonal scaffold of magnetically aligned collagen lamellae for corneal stroma reconstruction. *Conference proceedings : ... Annual International Conference of the IEEE Engineering in*

- Medicine and Biology Society. IEEE Engineering in Medicine and Biology Society. Annual Conference. 2007;2007:6400.*
120. Doillon CJ, Watsky MA, Hakim M, et al. A collagen-based scaffold for a tissue engineered human cornea: physical and physiological properties. *The International journal of artificial organs.* Aug 2003;26(8):764-773.
  121. Long CJ, Roth MR, Tasheva ES, et al. Fibroblast growth factor-2 promotes keratan sulfate proteoglycan expression by keratocytes in vitro. *The Journal of biological chemistry.* May 5 2000;275(18):13918-13923.
  122. Pomp O, Brokhman I, Ben-Dor I, Reubinoff B, Goldstein RS. Generation of peripheral sensory and sympathetic neurons and neural crest cells from human embryonic stem cells. *Stem cells.* Aug 2005;23(7):923-930.
  123. Lee G, Chambers SM, Tomishima MJ, Studer L. Derivation of neural crest cells from human pluripotent stem cells. *Nature protocols.* Apr 2010;5(4):688-701.
  124. Lee G, Kim H, Elkabetz Y, et al. Isolation and directed differentiation of neural crest stem cells derived from human embryonic stem cells. *Nature biotechnology.* Dec 2007;25(12):1468-1475.
  125. Jiang X, Gwye Y, McKeown SJ, Bronner-Fraser M, Lutzko C, Lawlor ER. Isolation and characterization of neural crest stem cells derived from in vitro-differentiated human embryonic stem cells. *Stem cells and development.* Sep 2009;18(7):1059-1070.
  126. Vaculik C, Schuster C, Bauer W, et al. Human dermis harbors distinct mesenchymal stromal cell subsets. *The Journal of investigative dermatology.* Mar 2012;132(3 Pt 1):563-574.
  127. Betters E, Liu Y, Kjaeldgaard A, Sundstrom E, Garcia-Castro MI. Analysis of early human neural crest development. *Developmental biology.* Aug 15 2010;344(2):578-592.
  128. Abe S, Hamada K, Miura M, Yamaguchi S. Neural crest stem cell property of apical pulp cells derived from human developing tooth. *Cell biology international.* Oct 1 2012;36(10):927-936.
  129. Ludwig TE, Bergendahl V, Levenstein ME, Yu J, Probasco MD, Thomson JA. Feeder-independent culture of human embryonic stem cells. *Nature methods.* Aug 2006;3(8):637-646.
  130. Du Y, Sundarraj N, Funderburgh ML, Harvey SA, Birk DE, Funderburgh JL. Secretion and organization of a cornea-like tissue in vitro by stem cells from human corneal stroma. *Investigative ophthalmology & visual science.* Nov 2007;48(11):5038-5045.
  131. Du Y, Roh DS, Funderburgh ML, et al. Adipose-derived stem cells differentiate to keratocytes in vitro. *Molecular vision.* 2010;16:2680-2689.
  132. Roh DS, Funderburgh JL. Rapid changes in connexin-43 in response to genotoxic stress stabilize cell-cell communication in corneal endothelium. *Investigative ophthalmology & visual science.* Jul 2011;52(8):5174-5182.
  133. Wu J, Du Y, Watkins SC, Funderburgh JL, Wagner WR. The engineering of organized human corneal tissue through the spatial guidance of corneal stromal stem cells. *Biomaterials.* Feb 2012;33(5):1343-1352.
  134. Cox G, Boxall SA, Giannoudis PV, et al. High abundance of CD271(+) multipotential stromal cells (MSCs) in intramedullary cavities of long bones. *Bone.* Feb 2012;50(2):510-517.
  135. Qi H, Chuang EY, Yoon KC, et al. Patterned expression of neurotrophic factors and receptors in human limbal and corneal regions. *Molecular vision.* 2007;13:1934-1941.

136. Qi H, Li DQ, Shine HD, et al. Nerve growth factor and its receptor TrkA serve as potential markers for human corneal epithelial progenitor cells. *Experimental eye research*. Jan 2008;86(1):34-40.
137. Ren S, Zhang F, Li C, et al. Selection of housekeeping genes for use in quantitative reverse transcription PCR assays on the murine cornea. *Molecular vision*. 2010;16:1076-1086.
138. Funderburgh JL. Keratan sulfate: structure, biosynthesis, and function. *Glycobiology*. Oct 2000;10(10):951-958.
139. Kitayama K, Hayashida Y, Nishida K, Akama TO. Enzymes responsible for synthesis of corneal keratan sulfate glycosaminoglycans. *The Journal of biological chemistry*. Oct 12 2007;282(41):30085-30096.
140. Liu H, Zhang J, Liu CY, Hayashi Y, Kao WW. Bone marrow mesenchymal stem cells can differentiate and assume corneal keratocyte phenotype. *Journal of cellular and molecular medicine*. May 2012;16(5):1114-1124.
141. Lambiase A, Merlo D, Mollinari C, et al. Molecular basis for keratoconus: lack of TrkA expression and its transcriptional repression by Sp3. *Proceedings of the National Academy of Sciences of the United States of America*. Nov 15 2005;102(46):16795-16800.
142. Du Y, Roh DS, Mann MM, Funderburgh ML, Funderburgh JL, Schuman JS. Multipotent stem cells from trabecular meshwork become phagocytic TM cells. *Investigative ophthalmology & visual science*. Mar 2012;53(3):1566-1575.
143. Funderburgh ML, Mann MM, Funderburgh JL. Keratocyte phenotype is enhanced in the absence of attachment to the substratum. *Molecular vision*. 2008;14:308-317.
144. Guo N, Kanter D, Funderburgh ML, Mann MM, Du Y, Funderburgh JL. A rapid transient increase in hyaluronan synthase-2 mRNA initiates secretion of hyaluronan by corneal keratocytes in response to transforming growth factor beta. *The Journal of biological chemistry*. Apr 27 2007;282(17):12475-12483.
145. Karamichos D, Guo XQ, Hutcheon AE, Zieske JD. Human corneal fibrosis: an in vitro model. *Investigative ophthalmology & visual science*. Mar 2010;51(3):1382-1388.
146. Jester JV, Barry-Lane PA, Cavanagh HD, Petroll WM. Induction of alpha-smooth muscle actin expression and myofibroblast transformation in cultured corneal keratocytes. *Cornea*. Sep 1996;15(5):505-516.
147. Koh S, Maeda N, Nakagawa T, Nishida K. Quality of vision in eyes after selective lamellar keratoplasty. *Cornea*. Nov 2012;31 Suppl 1:S45-49.
148. Patel SV, McLaren JW, Hodge DO, Baratz KH. Scattered light and visual function in a randomized trial of deep lamellar endothelial keratoplasty and penetrating keratoplasty. *American journal of ophthalmology*. 2008;145(1):97-105.
149. Dandona L, Ragu K, Janarthanan M, Naduvilath TJ, Shenoy R, Rao GN. Indications for penetrating keratoplasty in India. *Indian journal of ophthalmology*. Sep 1997;45(3):163-168.
150. Williams KA, Esterman AJ, Bartlett C, Holland H, Hornsby NB, Coster DJ. How effective is penetrating corneal transplantation? Factors influencing long-term outcome in multivariate analysis. *Transplantation*. Mar 27 2006;81(6):896-901.
151. Dandona L, Naduvilath TJ, Janarthanan M, Ragu K, Rao GN. Survival analysis and visual outcome in a large series of corneal transplants in India. *The British journal of ophthalmology*. Sep 1997;81(9):726-731.

152. Poliseti N, Islam MM, Griffith M. The artificial cornea. *Methods in molecular biology*. 2013;1014:45-52.
153. Wu J, Du Y, Mann MM, Yang E, Funderburgh JL, Wagner WR. Bioengineering organized, multilamellar human corneal stromal tissue by growth factor supplementation on highly aligned synthetic substrates. *Tissue engineering. Part A*. Sep 2013;19(17-18):2063-2075.
154. Liu H, Zhang J, Liu CY, et al. Cell therapy of congenital corneal diseases with umbilical mesenchymal stem cells: lumican null mice. *PloS one*. 2010;5(5):e10707.
155. Branch MJ, Hashmani K, Dhillon P, Jones DR, Dua HS, Hopkinson A. Mesenchymal stem cells in the human corneal limbal stroma. *Investigative ophthalmology & visual science*. Aug 2012;53(9):5109-5116.
156. Li GG, Zhu YT, Xie HT, Chen SY, Tseng SC. Mesenchymal stem cells derived from human limbal niche cells. *Investigative ophthalmology & visual science*. Aug 2012;53(9):5686-5697.
157. Bray LJ, Heazlewood CF, Munster DJ, Hutmacher DW, Atkinson K, Harkin DG. Immunosuppressive properties of mesenchymal stromal cell cultures derived from the limbus of human and rabbit corneas. *Cytotherapy*. Jan 2014;16(1):64-73.
158. Boote C, Du Y, Morgan S, et al. Quantitative assessment of ultrastructure and light scatter in mouse corneal debridement wounds. *Investigative ophthalmology & visual science*. May 2012;53(6):2786-2795.
159. Sangwan VS, Basu S, Vemuganti GK, et al. Clinical outcomes of xeno-free autologous cultivated limbal epithelial transplantation: a 10-year study. *The British journal of ophthalmology*. Nov 2011;95(11):1525-1529.
160. O'Callaghan AR, Daniels JT. Concise review: limbal epithelial stem cell therapy: controversies and challenges. *Stem cells*. Dec 2011;29(12):1923-1932.
161. Menzel-Severing J, Kruse FE, Schlotzer-Schrehardt U. Stem cell-based therapy for corneal epithelial reconstruction: present and future. *Canadian journal of ophthalmology. Journal canadien d'ophtalmologie*. Feb 2013;48(1):13-21.
162. Folkman J, Moscona A. Role of cell shape in growth control. *Nature*. Jun 1 1978;273(5661):345-349.
163. Karamichos D, Funderburgh ML, Hutcheon AE, et al. A role for topographic cues in the organization of collagenous matrix by corneal fibroblasts and stem cells. *PloS one*. 2014;9(1):e86260.
164. Espana EM, He H, Kawakita T, et al. Human keratocytes cultured on amniotic membrane stroma preserve morphology and express keratocan. *Investigative ophthalmology & visual science*. Dec 2003;44(12):5136-5141.
165. Basu S, Ali H, Sangwan VS. Clinical outcomes of repeat autologous cultivated limbal epithelial transplantation for ocular surface burns. *American journal of ophthalmology*. Apr 2012;153(4):643-650, 650 e641-642.
166. Lal I, Panchal BU, Basu S, Sangwan VS. In-vivo expansion of autologous limbal stem cell using simple limbal epithelial transplantation for treatment of limbal stem cell deficiency. *BMJ case reports*. 2013;2013.
167. Chan AA, Hertsensberg AJ, Funderburgh ML, et al. Differentiation of human embryonic stem cells into cells with corneal keratocyte phenotype. *PloS one*. 2013;8(2):e56831.

168. Fitzsimmons TD, Fagerholm P, Harfstrand A, Schenholm M. Hyaluronic acid in the rabbit cornea after excimer laser superficial keratectomy. *Investigative ophthalmology & visual science*. Oct 1992;33(11):3011-3016.
169. Latvala T, Puolakkainen P, Vesaluoma M, Tervo T. Distribution of SPARC protein (osteonectin) in normal and wounded feline cornea. *Experimental eye research*. Nov 1996;63(5):579-584.
170. Maseruka H, Bonshek RE, Tullo AB. Tenascin-C expression in normal, inflamed, and scarred human corneas. *The British journal of ophthalmology*. Aug 1997;81(8):677-682.
171. Funderburgh JL, Hevelone ND, Roth MR, et al. Decorin and biglycan of normal and pathologic human corneas. *Investigative ophthalmology & visual science*. Sep 1998;39(10):1957-1964.
172. Cox JL, Farrell RA, Hart RW, Langham ME. The transparency of the mammalian cornea. *J Physiol*. 1970;210(3):601-616.
173. Meek KM, Leonard DW, Connon CJ, Dennis S, Khan S. Transparency, swelling and scarring in the corneal stroma. *Eye*. 2003;17(8):927-936.
174. Chen SY, Hayashida Y, Chen MY, Xie HT, Tseng SC. A new isolation method of human limbal progenitor cells by maintaining close association with their niche cells. *Tissue engineering. Part C, Methods*. May 2011;17(5):537-548.
175. Xie HT, Chen SY, Li GG, Tseng SC. Limbal epithelial stem/progenitor cells attract stromal niche cells by SDF-1/CXCR4 signaling to prevent differentiation. *Stem cells*. Nov 2011;29(11):1874-1885.
176. Xie HT, Chen SY, Li GG, Tseng SC. Isolation and expansion of human limbal stromal niche cells. *Investigative ophthalmology & visual science*. Jan 2012;53(1):279-286.
177. Zakaria N, Possemiers T, Dhubhghaill SN, et al. Results of a phase I/II clinical trial: standardized, non-xenogenic, cultivated limbal stem cell transplantation. *J Transl Med*. 2014;12:58.
178. Mariotti SP. Global Data on Visual Impairments 2010. *World Health Organization* <http://www.who.int/blindness/>.
179. Thompson RW, Jr., Price MO, Bowers PJ, Price FW, Jr. Long-term graft survival after penetrating keratoplasty. *Ophthalmology*. Jul 2003;110(7):1396-1402.
180. Griffith M, Jackson WB, Lagali N, Merrett K, Li F, Fagerholm P. Artificial corneas: a regenerative medicine approach. *Eye*. Oct 2009;23(10):1985-1989.
181. Hackett JM, Lagali N, Merrett K, et al. Biosynthetic corneal implants for replacement of pathologic corneal tissue: performance in a controlled rabbit alkali burn model. *Investigative ophthalmology & visual science*. Feb 2011;52(2):651-657.
182. Liu W, Merrett K, Griffith M, et al. Recombinant human collagen for tissue engineered corneal substitutes. *Biomaterials*. Mar 2008;29(9):1147-1158.
183. Wu J, Rnjak-Kovacina J, Du Y, Funderburgh ML, Kaplan DL, Funderburgh JL. Corneal stromal bioequivalents secreted on patterned silk substrates. *Biomaterials*. Apr 2014;35(12):3744-3755.
184. Hassan WU, Greiser U, Wang W. Role of adipose-derived stem cells in wound healing. *Wound repair and regeneration : official publication of the Wound Healing Society [and] the European Tissue Repair Society*. May-Jun 2014;22(3):313-325.
185. Knight MN, Hankenson KD. Mesenchymal Stem Cells in Bone Regeneration. *Advances in wound care*. Jul 2013;2(6):306-316.

186. Li F, Zhao SZ. Mesenchymal stem cells: Potential role in corneal wound repair and transplantation. *World journal of stem cells*. Jul 26 2014;6(3):296-304.
187. Petrof G, Abdul-Wahab A, McGrath JA. Cell therapy in dermatology. *Cold Spring Harbor perspectives in medicine*. Jun 2014;4(6).
188. Forbes SJ, Rosenthal N. Preparing the ground for tissue regeneration: from mechanism to therapy. *Nature medicine*. Aug 2014;20(8):857-869.
189. Glenn JD, Whartenby KA. Mesenchymal stem cells: Emerging mechanisms of immunomodulation and therapy. *World journal of stem cells*. Nov 26 2014;6(5):526-539.
190. Wang Y, Chen X, Cao W, Shi Y. Plasticity of mesenchymal stem cells in immunomodulation: pathological and therapeutic implications. *Nature immunology*. Nov 2014;15(11):1009-1016.
191. Beltran SR, Svoboda KK, Kerns DG, Sheth A, Prockop DJ. Anti-inflammatory protein tumor necrosis factor-alpha-stimulated protein 6 (TSG-6) promotes early gingival wound healing: an in vivo study. *Journal of periodontology*. Jan 2015;86(1):62-71.
192. Liu L, Yu Y, Hou Y, et al. Human umbilical cord mesenchymal stem cells transplantation promotes cutaneous wound healing of severe burned rats. *PloS one*. 2014;9(2):e88348.
193. Wang H, Chen Z, Li XJ, Ma L, Tang YL. Anti-inflammatory cytokine TSG-6 inhibits hypertrophic scar formation in a rabbit ear model. *European journal of pharmacology*. Feb 3 2015;751C:42-49.
194. Milner CM, Day AJ. TSG-6: a multifunctional protein associated with inflammation. *Journal of cell science*. May 15 2003;116(Pt 10):1863-1873.
195. Dyer DP, Thomson JM, Hermant A, et al. TSG-6 inhibits neutrophil migration via direct interaction with the chemokine CXCL8. *Journal of immunology*. Mar 1 2014;192(5):2177-2185.
196. Oh JY, Lee RH, Yu JM, et al. Intravenous mesenchymal stem cells prevented rejection of allogeneic corneal transplants by aborting the early inflammatory response. *Molecular therapy : the journal of the American Society of Gene Therapy*. Nov 2012;20(11):2143-2152.
197. Oh JY, Roddy GW, Choi H, et al. Anti-inflammatory protein TSG-6 reduces inflammatory damage to the cornea following chemical and mechanical injury. *Proceedings of the National Academy of Sciences of the United States of America*. Sep 28 2010;107(39):16875-16880.
198. Qi Y, Jiang D, Sindrilaru A, et al. TSG-6 released from intradermally injected mesenchymal stem cells accelerates wound healing and reduces tissue fibrosis in murine full-thickness skin wounds. *The Journal of investigative dermatology*. Feb 2014;134(2):526-537.
199. Lee TH, Wisniewski HG, Vilcek J. A novel secretory tumor necrosis factor-inducible protein (TSG-6) is a member of the family of hyaluronate binding proteins, closely related to the adhesion receptor CD44. *The Journal of cell biology*. Jan 1992;116(2):545-557.
200. Carlson EC, Liu CY, Chikama T, et al. Keratocan, a cornea-specific keratan sulfate proteoglycan, is regulated by lumican. *The Journal of biological chemistry*. Jul 8 2005;280(27):25541-25547.
201. Tasheva ES, Funderburgh JL, Corpuz LM, Conrad GW. Cloning, characterization and tissue-specific expression of the gene encoding bovine keratocan, a corneal keratan sulfate proteoglycan. *Gene*. Sep 18 1998;218(1-2):63-68.

202. Han Y, Cutler JE. Assessment of a mouse model of neutropenia and the effect of an anti-candidiasis monoclonal antibody in these animals. *The Journal of infectious diseases*. May 1997;175(5):1169-1175.
203. Norman KE, Cotter MJ, Stewart JB, et al. Combined anticoagulant and antiselectin treatments prevent lethal intravascular coagulation. *Blood*. Feb 1 2003;101(3):921-928.
204. Tate MD, Brooks AG, Reading PC, Mintern JD. Neutrophils sustain effective CD8(+) T-cell responses in the respiratory tract following influenza infection. *Immunology and cell biology*. Feb 2012;90(2):197-205.
205. Tateda K, Moore TA, Deng JC, et al. Early recruitment of neutrophils determines subsequent T1/T2 host responses in a murine model of Legionella pneumophila pneumonia. *Journal of immunology*. Mar 1 2001;166(5):3355-3361.
206. Lee RH, Yu JM, Foskett AM, et al. TSG-6 as a biomarker to predict efficacy of human mesenchymal stem/progenitor cells (hMSCs) in modulating sterile inflammation in vivo. *Proceedings of the National Academy of Sciences of the United States of America*. Nov 25 2014;111(47):16766-16771.
207. Tena A, Sachs DH. Stem cells: Immunology and immunomodulation. *Developments in ophthalmology*. 2014;53:122-132.
208. Kim H, Walczak P, Kerr C, et al. Immunomodulation by transplanted human embryonic stem cell-derived oligodendroglial progenitors in experimental autoimmune encephalomyelitis. *Stem cells*. Dec 2012;30(12):2820-2829.
209. Imberti B, Casiraghi F, Cugini D, et al. Embryonic stem cells, derived either after in vitro fertilization or nuclear transfer, prolong survival of semiallogeneic heart transplants. *Journal of immunology*. Apr 1 2011;186(7):4164-4174.
210. Ylostalo JH, Bartosh TJ, Tiblow A, Prockop DJ. Unique characteristics of human mesenchymal stromal/progenitor cells pre-activated in 3-dimensional cultures under different conditions. *Cytotherapy*. Nov 2014;16(11):1486-1500.
211. Xie J, Broxmeyer HE, Feng D, et al. Human adipose-derived stem cells ameliorate cigarette smoke-induced murine myelosuppression via secretion of TSG-6. *Stem cells*. Feb 2015;33(2):468-478.
212. Kim H, Darwish I, Monroy MF, Prockop DJ, Liles WC, Kain KC. Mesenchymal stromal (stem) cells suppress pro-inflammatory cytokine production but fail to improve survival in experimental staphylococcal toxic shock syndrome. *BMC immunology*. 2014;15:1.